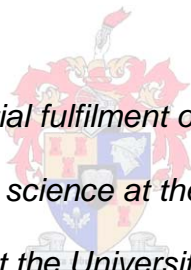


**Approaches for the study of leaf
carbohydrate metabolic compartmentation
in *Arabidopsis thaliana***

by

Richard Derek Fly



*Thesis presented in partial fulfilment of the requirements for the
degree Master of science at the Institute for Plant
Biotechnology at the University of Stellenbosch*

Supervisor: Dr James Lloyd

Co-supervisor Dr Margretha Johanna van der Merwe

Faculty of Genetics

Institute for Plant Biotechnology

December 2010

Declaration

By submitting this thesis/dissertation electronically, I declare that the entirety of the work contained therein is my own, original work, and that I have not previously in its entirety or in part submitted it for obtaining any qualification.

December 2010

Signed

Date

Copyright © 2010 University of Stellenbosch

All rights reserved

Abstract

The study of plants on a sub-cellular level is an important, yet challenging area and its application allows for novel insight into the understanding of metabolism and its regulation. In this study I describe the development of a reverse phase liquid chromatography mass spectrometry (RPLC-MS) technique in which 29 phosphorylated and nucleotide sugars could be detected and quantified. The method was validated with the use of authentic standards and the system displayed very good linearity ($R^2 > 0.95$), while the recovery of the standards added to the plant material before extraction was between 65 and 125%. Further, *Arabidopsis thaliana* wild type (Col-0) and adenylate kinase (*adk1*) mutant leaf discs were fed ^{13}C labeled glucose over a period of 24 hours and harvested at defined time intervals. Non aqueous fractionation, and metabolite profiling *via* the above mentioned rpLC-MS method in conjunction with gas chromatography mass spectrometry (GC-MS) allowed for the detection and quantification of primary metabolites on a sub-cellular level as well as the determination of their relative isotopic label enrichments through primary carbon metabolism. Finally, a yeast complementation system was designed for the identification of tonoplast bound sucrose import proteins. The screening system identified 22 unique sequences from an *Arabidopsis thaliana* cDNA library. Four unknown sequences were identified, one of which displayed tonoplast membrane association upon *in silico* analysis. Three ATP-binding proteins were also identified as well as a sub-unit from the exocyst gene family. Further studies will include the functional characterization of the latter, as well as the development of additional cDNA libraries more suited for screening of sequences that encode sucrose importer proteins.

Opsomming

Die studie van plante op a sub-sellulere vlak is 'n belangrike maar uitdagende navorsingsarea en die toepassing daarvan dra by tot unieke insig tot 'n beter begrip van metabolise regulasie. In die studie bespreek ek die ontwikkeling van 'n teenoorgestelde fase vloeistof kromatografie massa spektrometrie (RPLC-MS) tegniek waarin 29 gefosforileerde en nukleotied suikers gevind en gekwantifiseer kon word. Geldigverklaring van die metode is bewerkstelling met die gebruik van oorspronklike standaarde and die sisteem het baie goeie liniariteit ($R^2 > 0.95$) getoon, terwyl die herstelbaarheid van standaarde wat bygevoeg is by die plant material voor ekstraksie tussen 65% en 125% was. *Arabidopsis thaliana* wilde tipe (Col-O) en die adeniliet kinase (*adk1*) mutant blaar dele is met ^{13}C gemerkte glukose gevoed oor 'n tydperk van 24 uur en geoes by spesifieke tydstippe. Nie-vloeibare fraksionering en metaboliet uitleg is vermag vanaf die genoemde RPLC-MS metode met behulp van gas kromatografie massa spektrometrie (GC-MS) wat die bepaling en kwantifikasie van primere metaboliete op n sub-sellulere vlak sowel as die bepaling van hul relatiewe isotropiese merker verrykers deur primere metabolisme toelaat. Verder is n gis komplementere sisteem ontwerp vir die identifikasie van tonoplas gebinde sukrose invoer proteine. Die verkenningssisteem het 22 unieke volgordes opgelewer vanaf 'n *Arabidopsis thaliana* kDNA biblioteek. Vier onbekende volgordes is geidentifiseer, een wat tonoplas membraan assosiasie toon met *in silico* analise. Drie ATP-bindings proteine is ook geidentifiseer asook 'n sub-eenheid van die eksosyst geen familie. Verdere studies sal die funksionele karakterisering van die laaste proteien insluit, asook die ontwikkeling van addisionele kDNA biblioteke meer gepas vir verkenning sodiende identifiseer van volgordes wat sukrose invoer proteine vertaal.

Aknowledgements

I would like to Dr James Lloyd for all his guidance and assistance with this study, Dr Marna van der Merwe for hours of help, advice and support and Prof Jens Kossmann for the opportunity to study this degree

I would especially like to thank Dr Marietjie Stander and Fletcher Hitten of the central analytical facility for offering their knowledge and help over the duration of this project. I also thank Dr Mike Bester for offering time and assistance with the yeast work.

Thanks go to the students and staff of the IPB for support and encouragement during my time here. And to the National Research Foundation for funding, with out which this project would not have been possible.

Finally I would like to thank my family and friends for the love and support offered over the last two years.

List of contents

ABSTRACT	iii
OPSOMMING	iv
AKNOWLEDGEMENTS	v
LIST OF CONTENTS	vi
LIST OF TABLES AND FIGURES	x
LIST OF ABBREVIATIONS	xii
CHAPTER 1: GENERAL INTRODUCTION	1
CHAPTER 2: CUTTING THROUGH THE GORDIAN KNOT OF COMPARTMENTATION: AN EVALUATION OF THE SPATIAL AND TEMPORAL REGULATION OF PRIMARY CARBOHYDRATE METABOLISM.	5
2.1 Introduction	5
2.2 The biochemistry of primary carbohydrate metabolism	6
2.3 Transporters and compartmentation	17
2.4 Technologies available for studying plant compartmentation	18
2.4.1 Sub-cellular proteomics	19
2.4.2. Sub-cellular metabolomics	20
2.4.3 Fluorescence resonance energy transfer (FRET) technology	21
2.4.4 Micro laser dissection	23
2.5 Layout of thesis	23
CHAPTER 3: DEVELOPMENT OF A REVERSE PHASE LIQUID CHROMATOGRAPHY-MASS SPECTROMETRY METHOD FOR DETECTION AND QUANTIFICATION OF	

NUCLEOTIDE AND PHOSPHORYLATED INTERMEDIATES OF PRIMARY METABOLISM	25
3.1 Introduction	25
3.2 Results and discussion	27
3.2.1 Evaluation of buffer and ion-pair composition on separation and detection of authentic phosphorylated and nucleotide standards	27
3.2.2 Evaluation of linearity and reproducibility of Waters LC MS system	30
3.3. Materials and methods	34
3.3.1 Chemicals	34
3.3.2 Plant material and growth conditions	34
3.3.3 Metabolite extraction	35
3.3.4 LC-MS Analysis	35
3.3.4.1 Instrumentation details	35
3.3.4.2 Octylammonium acetate/acetonitrile (OAAN) buffer composition and elution conditions	36
3.3.4.3 Tributylamine/methanol (TBAM) buffer composition and elution Conditions	36
3.3.5 Data acquisition and analysis	37
CHAPTER 4: Sub-cellular distribution of non-steady state metabolite levels and fluxes of a plastidial adenylate kinase mutant impaired in primary carbon metabolism in <i>Arabidopsis thaliana</i>	38
4.1 Introduction	38
4.2 Results	41
4.2.1 Evaluation of marker enzyme distribution and fractionation efficiency	41
4.2.2 Comparison of metabolic signatures between genotypes and time variation upon glucose feeding	46

4.2.3 Analysis of primary metabolite levels in total fractionated leaf material	49
4.2.4 ¹³ C label incorporation	55
4.2.5 Sub-cellular metabolite levels and enrichments of primary metabolism in Col-0 and <i>adk1</i> rosette leaves	56
4.3 Discussion	63
4.4 Materials and Methods	68
4.4.1 Chemicals	68
4.4.2 Plant material and growth conditions	69
4.4.3 ¹³ C isotopic labeling	70
4.4.4 Non aqueous fractionation	70
4.4.5 Protein extraction and enzyme activity measurements	71
4.4.6 Primary metabolite profiling	72
4.4.7 Phosphorylated and nucleotide profiling	73
4.4.8 ¹³ C enrichment calculations	74
4.3.9 Starch measurements and ¹³ C glucose incorporation	74
4.4.10 Statistical analyses	74
Chapter 5: The development of a yeast functional complementation system to identify tonoplast-localized sucrose transport proteins from <i>Arabidopsis thaliana</i>	79
5.1 Introduction	79
5.2 Results	82
5.3 Discussion	85
5.4 Experimental procedures	91
5.4.1 Chemicals, enzymes and plasmids	91
5.3.2 Vector construction	91

5.3.3 Yeast transformation	91
5.3.4 Transformation with an <i>A. thaliana</i> cDNA library	92
5.3.5 DNA isolation from complemented yeast colonies	92
5.3.6 Insert sequencing	93
5.3.7 <i>In silico</i> analysis	94
Chapter 6 : General conclusion	94

List of figures and tables

Figures

2.1 Simplistic schematic representation of starch and sucrose biosynthesis in autotrophic C3 plant organs	6
3.1 Elution pattern of metabolite standards on OAA gradient	29
4.1 Assessment of marker enzyme activity variation in total protein extracts	42
4.2 Linear correlation analysis of marker enzyme activities of plastidial and vacuolar enriched fractions	44
4.3 Plastidial AGPase and vacuolar α-mannosidase marker enzyme Distribution	46
4.4 Canonical correlation analysis of mass spectral tags (MSTs) extracted from total plant extracts	47
4.5 Amino acid concentrations in <i>Arabidopsis</i> leaf tissue	50
4.6 Sugar and starch concentrations in <i>Arabidopsis</i> leaf tissue	52
4.7 Organic acid concentrations in <i>Arabidopsis</i> leaf tissue	53
4.8 Fractional carbon enrichment in <i>Arabidopsis</i> carbohydrate Metabolism	56
4.9 Amino acid concentrations in fractionated <i>Arabidopsis</i> leaf tissue	60
4.10 Sugar and polyol concentrations in fractionated <i>Arabidopsis</i> leaf tissue	61
4.11 Organic acid concentrations in fractionated <i>Arabidopsis</i> leaf Tissue	62
4.12 Supplemental figure, General biosynthetic scheme of metabolites selected for the targeted metabolome analyses	76
4.13 Supplemental figure, Fractionation of nucleotide and	

phosphorylated sugars at T0, in <i>Arabidopsis</i> leaf tissue	77
5.1 Schematic representation of the yeast complementation system	88
Tables	
2.1 Summary of enzymes and transporters involved in carbohydrate catabolism and starch transport.	16
3.1 Metabolite levels in <i>Arabidopsis</i> leaf tissue harvested at midday of a 12h photoperiod.	32
4.1 Primary metabolite levels of physiologically grown <i>Arabidopsis</i> leaf rosette tissue.	54
4.2 supplemental table, complete list of marker enzyme activities over 4 time points	78
5.1 The family of sucrose transporters identified in <i>Arabidopsis thaliana</i>.	81
5.2 Sequence identities of positive colonies from a yeast complementation screen for tonoplast localized sucrose transporters	84

List of abbreviations

Acid invertase	AI
Adenosine diphosphate	ADP
ADP-glucose	ADP-glc
ADP-glucose pyrophosphorylase	AGPase
Adenosine monophosphate	AMP
Adenosine triphosphate	ATP
Carbon dioxide	CO ₂
Cyan fluorescent protein	CFP
Disproportionating enzyme	DPE
Fluorescence resonance energy transfer	FRET
Fructose 1-phosphate	F1P
Fructose 6-phosphate	F6P
Fructose 1,6-Bisphosphatase	FBPase
Fructose 2,6-bisphosphate	F2,6BP
Fructose 2,6-bisphosphate/kinase	F2KP
Gas chromatography mass spectrometry	GC-MS
Glucose 1,6-bisphosphate	G1,6BP
Glucan water dikinase	GWD
Glucose 1-phosphate	G1P
Glucose 6-phosphate	G6P
Glycerate 3-phosphate	3-PGA
Green fusion protein	GFP
Guanosine diphosphate	GDP
Guanosine triphosphate	GTP

Hexokinase	HXK
High performance liquid chromatography	HPLC
Inositol 1,4,5 triphosphate	Ins1,4,5TP
Laser capture microdissection	LCMD
Light harvesting complexes	LHC
Liquid chromatography mass spectrometry	LC-MS
Non aqueous fractionation	NAQF
Nuclear magnetic resonance	NMR
Octyl ammonium acetate/acetonitrile	OAAN
Orthophosphate	P _i
Phosphofructokinase	PFK
Phosphoglucan water dikinase	PWD
Phosphoglucoisomerase	PGI
Phosphoglucomutase	PGM
Plastocyanin	PC
Pyrophosphate	PP _i
Pyrophosphate-dependant 6-phosphofructokinase	PFP
Reverse phase liquid chromatography mass spectrometry	RPLC-MS
Ribulose 1,5-bisphosphate	R1,5BP
Ribulose 1,5-bisphosphate carboxylase/oxygenase	RuBisCo
Starch branching enzyme	SBE
Starch synthase	SS
Sucrose phosphate phosphatase	SPP
Sucrose phosphate synthase	SPS
Sucrose synthase	SuSy
Thiamine diphosphate	TDP

Thiamine monophosphate	TMP
Thiamine triphosphate	TTP
Thin layer chromatography	TLC
Trehalose 6-phosphate	T6P
Tributylamine/methanol	TBAM
Triose phosphate	Triose-P
Triose phosphatase transporter	TPT
Uridine diphosphate	UDP
UDP-glucose	UDP-glc
UDP-glucose pyrophosphorylase	UGPase
Uridine monophosphate	UMP
Uridine triphosphate	UTP
Vacuolar H ⁺ -translocating ATPase	V-ATPase
Vacuolar H ⁺ -translocating inorganic pyrophosphatase	V-PPase
Yellow fluorescent protein	YFP

Chapter 1

General introduction

Plants use the process of photosynthesis to convert light energy into carbohydrates which, in turn, serve as energy and structural resources to either maintain or attenuate plant growth and development. Despite many years of research on these processes, recent studies have highlighted our limited knowledge about the regulation and complexity of primary carbon metabolism (Kolbe et al., 2005; Sparla et al., 2005; Lunn et al., 2006; Marri et al., 2009). While numerous post-translational modulators are implicated in the regulation of carbohydrate metabolism, it still remains unclear how and when many of these compounds exert their regulatory effect(s) in their defined micro-environments.

Plant cells are divided into different sub-cellular compartments which include the apoplast, plastid, mitochondria, vacuole and cytosol. The most widely accepted hypothesis for the origin of the plastidial and mitochondrial compartments involves the engulfing of cyanobacteria and proteobacteria (in particular, *Rickettsiales* or close relatives), respectively (Margulis, 1975; Blanchard and Lynch, 2000); and the persistence of both organisms in an endosymbiotic manner. These organelles retain a certain degree of autonomy and actively transcribe and translate a small amount of genetic material; however, most genes encoding mitochondrial and chloroplast proteins reside in the nucleus of the host cell. The gene products are in turn transported back to the two compartments (Blanchard and Lynch, 2000; Jarvis, 2001). The mode of action, significance and dynamic nature of this gene transfer and cross-talk between the nuclei and organellar transcriptional and translational machinery remain an active area in current plant research.

Apart from the different organelles present within a particular cell type, it has also become apparent that the same type of compartment within a cell might have multiple functions. In this regard, it has been shown that different types of vacuoles are present within the plant cell, their functions range between active and passive storage (of metabolites such as sucrose, malate, citrate or Na^+) and active lysis (for example proteolysis degradation products) which may also be subject to variation according to developmental stage, tissue - or cell type (Paris et al., 1996). In a similar manner, plastids can be classified into several sub-types testifying to the diversity in their functions. Chloroplasts are primarily responsible for photosynthesis due to the presence of chlorophyll in the light harvesting complexes (LHC) (Pyke, 1997; Lopez-Juez and Pyke, 2005), while xanthophylls, isoprenoids and carotenoids give rise to the characteristic colors of the chromoplasts (Weston and Pyke, 1999; Lopez-Juez and Pyke, 2005). On the other hand, leucoplasts lack pigments and differentiate into amyloplasts, elaioplasts, or proteinoplasts storing starch, lipids or proteins, respectively. Leucoplasts do not only have a storage function, and may also participate in a wide range of biosynthetic functions, including fatty acid, amino acid and tetrapyrrole synthesis. Taken together it is clear that the organelle type, its distribution, and the subsequent regulation that it infers, play a contributing role in the complexity encountered in plant metabolism.

Further complications within primary carbon metabolism may occur as several distinct biochemical pathways share numerous overlapping enzymes (or isoforms) in their individual sub-cellular compartments. Cytosolic glucose (derived from plastidial photosynthesis; as reviewed in (Cruz et al., 2008)) is hydrolyzed to pyruvate during glycolysis, providing carbon skeletons for mitochondrial respiration. However, in the corresponding plastidial-localized Calvin cycle, the majority of these glycolytic

enzymes are also present and functional. While this raises several questions concerning evolutionary traits and the duplication of endosymbiotic events, it also poses a much more basic question concerning the functional role of these enzymes; with regard to plasticity and redundancy within and between the different organelle-targeted isoforms. The isolation and characterization of the plastidial phosphoglucomutase (*pgm*) mutant in *Arabidopsis thaliana* (Lin et al., 1988) shed further light on the intricacies involved in these over-lapping pathways. PGM catalyzes the interconversion of glucose 6-phosphate (G6P) to glucose 1-phosphate (G1P), and both cytosolic and plastidial isoforms exist (Caspar et al., 1985). The plastidial *pgm* mutant is starchless and is characterized by elevated levels of soluble sugars, sucrose phosphate synthase (SPS) and acid invertase (AI) activities, as well as altered growth kinetics (Caspar et al., 1985). Transgenic approaches in potato plants have subsequently illustrated that a reduction in plastidial PGM leads to a reduced photosynthetic rate, decreased starch levels and a minor reduction in sucrose levels in leaves, although no observable phenotype was noted (Tauberger et al., 2000; Fernie et al., 2002). The same biochemical response could also be achieved by repression of the cytosolic isoform in the leaves (Lytovchenko et al., 2002). However, this antisense repression additionally leads to drastic reductions in aerial growth, tuber number and size and decreased photosynthesis rates (Lytovchenko et al., 2002; Fernie et al., 2002). Furthermore, the heterologous expression of *E. coli* PGM in the potato cytosol led to enhanced sucrose and decreased maltose/isomaltose, galactose and arabinose levels without affecting photosynthesis (Lytovchenko et al., 2005). While several plausible explanations could be afforded to account for pleiotropic, primary or organ-specific effects relating to these studies, it is apparent that the different compartments confer some degree of

redundancy and cross-talk, albeit the extent of cross-talk and the unique roles within each compartment is far from being clearly defined.

One of the contributing factors in elucidating the roles of different isoforms would be to characterize and understand the sub-cellular environment more clearly. Metabolite profiling in plant cells describes the biochemical state of the cell at a given time point, and has become one of the methods of choice to understand metabolism and its regulation (Tohge and Fernie, 2010). However, most metabolite profiling studies have relayed information based on whole tissue, and only limited information is available on both the temporal and spatial variation which would provide a more comprehensive representation of metabolite levels (Looger et al., 2005). This project aims to develop and validate screening and profiling tools in order to identify and study compartmentation of metabolism. Two main parallel approaches have been followed. Firstly, the development and assessment of non-aqueous fractionation (NAQF) to study *Arabidopsis* primary carbon metabolism through both metabolomic and fluxomic approaches (Chapter 4). These include the optimization of reverse phase liquid chromatography mass spectrometry (RPLC-MS) methods to examine steady state levels of phosphorylated- and nucleotide sugars (or intermediates) (Chapter 3). Secondly the construction of a yeast complementation system to identify putative sucrose import proteins on the tonoplast membrane of *A. thaliana* was achieved and has been implemented to identify candidate genes mediating this process (Chapter 5). The advantages and limitations of these approaches are discussed within the rest of this thesis.

Chapter 2

Cutting through the Gordian knot of compartmentation: an evaluation of the spatial and temporal regulation of primary carbohydrate metabolism

2.1 Introduction

Despite intense research efforts over the last 50 years, knowledge about when and how sucrose and starch metabolism is coordinately regulated in autotrophic metabolism is incomplete. While the biochemical processes involved in the synthesis and degradation of these two pools have been well-documented over a 24h period or when grown under alternating light conditions, the cross-talk between them is less well understood. Furthermore, with the completion of the *Arabidopsis* genome sequencing project (*Arabidopsis* genome initiative, 2000) the limit of our existing knowledge and the potential relating to gene annotation and biological function assignment has been further realized. In particular, the identification of several unknown transport proteins encountered on the variety of organellar membranes serves as a testament to the large scope of exploration in the sub-cellular domain of plant compartmentation. This chapter highlights what is currently known and understood about autotrophic carbohydrate metabolism and its regulation as studied using either mutagenic- or transgenic approaches. In addition it identifies and compares several key methodologies that are currently employed to study and understand plant (primary) compartmentation; and highlights the need to optimize and cross-validate several strategies to aid in both targeted and untargeted genetic approaches to study cross-talk in plant metabolism.

are less clearly defined. The reactions involved in cytosolic sucrose synthesis are catalyzed by (A) aldolase, (B) fructose 1,6-bisphosphatase (FBPase), (C) phosphoglucoisomerase (PGI), (D) phosphoglucomutase (PGM), (E) UDP-glucose pyrophosphorylase (UGPase), (F) sucrose phosphate synthase (SPS), (G) sucrose phosphate phosphatase (SPP) and (H) invertase. The levels of sucrose might be attenuated by (I) fructose 2,6 bisphosphate kinase (F2KP) leading to enhanced F2,6BP which allosterically activates phospho-fructokinase (PFK) or pyrophosphate-dependent 6-phosphofructokinase (PFP) (not shown). Furthermore, sucrose might also be sequestered in the vacuole (presumably by a putative sucrose importer (designated by (2)) and hydrolyzed to monosaccharides by (J) vacuolar invertase. On the other hand, corresponding isoforms of (K) aldolase, (L) fructose 1,6-bisphosphatase (FBPase), (M) phosphoglucoisomerase (PGI), (N) phosphoglucomutase (PGM), in combination with (N) ADP-glucose pyrophosphorylase (AGPase) (O) starch synthase (SS) and (P) starch branching enzyme (SBE) are involved in plastidial starch synthesis. Transport between plastidial and cytosolic compartments is facilitated by the (1) triose phosphate transporter (3) maltose exporter and (4) (putative) glucose exporter (see text for further details, and Table 2.1 on more details on enzymes involved in starch and sucrose catabolism).

Triose-P's form pivotal components in both sucrose and starch metabolism as they can either be exported into the cytosol and converted to sucrose, or be further metabolized within the plastid to form starch (Fig. 2.1). At the start of the light period 3-PGA is exported from the chloroplast to the cytosol in exchange for cytosolic orthophosphate (Pi) *via* a membrane bound triose phosphate transporter (TPT) (Huber and Huber, 1992). It is apparent that, without compensatory mechanisms,

sub-optimal TPT exchange would lead to either triose-P being withdrawn too fast from the plastid and leading to a depletion in Calvin cycle intermediates, or, if transport is too slow, that phosphorylated intermediates would build up in the stroma, resulting in an exhaustion of stromal Pi and phosphate limitation of photosynthesis (Edwards and Walker, 1983). Surprisingly, *Arabidopsis* TPT mutant studies and tobacco and potato antisense constructs have illustrated that reduced or little TPT activity does not significantly affect either photosynthesis or growth under ambient conditions (Riesmeier et al., 1993; Barnes et al., 1994; Dieter Heineke et al., 1994; Häusler et al., 1998; Häusler et al., 2000a; Häusler et al., 2000b; Schneider et al., 2002). Under normal circumstances, the inhibition of photosynthesis due to Pi limitation is alleviated by activation of AGPase (Sowokinos, 1981; Sowokinos and Preiss, 1982), leading to an increase in the rate of starch synthesis and a resulting release of Pi (see later for further discussion on starch synthesis). The pattern of carbohydrate synthesis in the antisense and mutant plants suggest that they metabolically compensate for the reduced levels of TPT by diverting assimilate into starch, releasing the Pi required for continued photosynthesis (Walters et al., 2004; Weise et al., 2004). Characterization of another insertional TPT mutant in *Arabidopsis* (*ape2*) shows that, under high light conditions, photosynthesis is severely impaired (~50%), while starch levels are increased; this can be attributed to enhanced starch turnover observed during the day in order to maintain the phosphate homeostasis (Walters et al., 2004). The metabolic signals that lead to this diversion have received some attention but seem poorly understood and integrated in our view of carbohydrate metabolism. In tobacco, the disaccharide, sucrose and polyol, mannitol have been implicated in the down- and up-regulation, respectively, of TPT activity (Knight and Gray, 1994). Furthermore, in wheat, TPT activity is modulated by glucose *via* a hexokinase-dependent pathway (Sun et al., 2006).

However, TPT regulation appears to be complex and differs considerably in different species and their respective organs. For instance, in potato, wheat and rice, TPT expression is high in photosynthetic tissues while no expression is detected in roots, stolons, developing tubers or seeds (Schulz et al., 1993; Wang et al., 2002; Wang et al., 2002). In contrast, tomato shows constitutive TPT expression in leaves, roots and red fruits (Schünemann et al., 1996). Additionally, in tobacco, the expression of TPT is light-independent (Knight and Gray, 1994) whereas in potato, its expression is tightly regulated by light (Schulz et al., 1993). The scope of this perturbation might also have wider metabolic consequences since TPT antisense lines were also characterized by enhanced flux into amino acids and decreased malate levels (Häusler et al., 1998). While TPT activity significantly alters plastidial starch metabolism to maintain photosynthetic homeostasis (by affecting the stromal redox status and altering the triose-P:Pi ratio), there exists some discrepancy regarding the corresponding cytosolic sucrose pools (Schneider et al., 2002; Walters et al., 2004). Under high light conditions, soluble sugar levels have been shown to decrease (Walters et al., 2004), while under a 12h photoperiod no significant changes in either sucrose, glucose or fructose were detectable (Schneider et al., 2002). This suggests that the sucrose levels are probably dependent on starch mobilization (see later for further discussion on starch degradation), which is again dependent on the rate and levels of the prevailing triose-P: Pi ratio in the respective sub-cellular compartments.

During sucrose synthesis, triose-P exported from the stroma may be converted to fructose-1,6-bisphosphate (F1,6BP) by the cytosolic isoform of aldolase. From this, the first monomer needed for sucrose synthesis is formed, namely, fructose-6-phosphate (F6P), facilitated by FBPase activity (Stitt and Heldt, 1985) (Fig 2.1). F6P is also converted to the other sugar used to produce sucrose, namely UDP-glc, by a

combination of hexose phosphate isomerase (HPI), PGM and UGPase activities (Fig 2.1). Sucrose can then be formed *via* two alternative routes. The first utilizes UDP-glc and F6P and is catalyzed by the enzymes sucrose phosphate synthase (SPS) and sucrose phosphate phosphatase (SPP) (Echeverría and Salerno, 1993; Baxter et al., 2003). On the other hand, sucrose synthases (SuSy) reversibly catalyzes sucrose formation from fructose and UDP-glc (as reviewed by Marino et al., 2008). While SPS mutants lead to significantly altered phenotypes and sucrose levels (Baxter et al., 2003), corresponding *Arabidopsis* mutants lacking the individual isoforms (or double combinations) of SuSy have no obvious growth or developmental phenotypes, with no significant alterations in starch, sugar or cellulose content under ambient conditions (Bieniawski et al. 2007), suggesting that SPS is the main sucrose synthesizing enzyme under these conditions. More apparent phenotypic alterations are, however, evident in *SuSy* mutants under oxygen deprivation, dehydration, cold treatment and sugar feeding (Bieniawska et al., 2007; Angeles-Núñez and Tiessen, 2010), suggesting that SuSy plays more intricate roles in carbon balances during, amongst others, abiotic stresses. More pronounced effects are, however, seen under ambient conditions with a reduction in starch content of maize upon silencing of *SuSy1* and *SuSy2* (Chourey et al., 1998), as well as an accumulation of reducing sugars and a reduction in starch content in potato tubers resulting from antisense inhibition of *SuSy* (Zrenner et al., 1995). In addition, the *Arabidopsis SuSy4* isoform is most abundantly expressed in the roots and appears to be primarily involved in sucrose hydrolysis (Bieniawska et al., 2007); leading to enhanced hexose phosphates pools as facilitated by hexokinase, fructokinase and UGPase activity (Zrenner et al., 1995).

Studies concerned with the regulation of sucrose synthesis have been primarily focused on the regulation of the penultimate step in sucrose synthesis, namely SPS. SPS genes fall into three distinct families and plants contain at least one gene from each family (Langenkämper et al., 2002). It has been shown that the phosphorylation of SPS by 14-3-3 proteins (Toroser et al., 1998) inhibits enzyme activity at low photosynthetic rates, while at high photosynthetic rates SPS responds to changing levels of the allosteric activator and inhibitor, G6P and Pi, respectively (Huber and Huber, 1992). There also appear to be differences between species in the light-dark regulation of SPS by increasing activity by covalent modification with ATP and the increase of the affinity of SPS for UDP-glc in the light (Lunn et al., 1997; Lunn et al., 2003). In the upstream step of these regulator molecules in sucrose synthesis, F1,6BP is converted to F6P in a reaction which is controlled by the cytosolic levels of F2,6BP (Fig 2.1). Therefore the activity of SPS and the rate of sucrose synthesis are controlled on a second level by the prevailing F2,6BP concentrations (Stitt and Heldt, 1985). The cytosolic concentration of F2,6BP is maintained by a bifunctional enzyme; fructose 6-phosphate, 2-kinase and fructose 2,6-bisphosphatase (F2KP) (Nielsen et al., 2004). An increase in the cytosolic concentration of triose-P as a result of an increased photosynthetic rate inhibits the formation of F2,6BP promoting the activity of cytosolic FBPase (cFBPase) and the synthesis of sucrose (Scott et al., 2000). Conversely, if the rate of sucrose synthesis exceeds the rate of photosynthesis, cytosolic Pi levels increase which promotes the synthesis of F2,6BP. This, in turn, decreases the activity of cFBPase and increase PFK activity which results in inhibition of sucrose synthesis (Scott et al., 2000).

When the rate of photosynthesis exceeds the rate of sucrose production, the triose-P synthesized in the stroma is rather directed towards starch formation. In a similar

biochemical reaction to sucrose synthesis, starch biosynthesis begins with the use of triose-P to synthesize G1P (Fig 2.1). AGPase is a key point of regulation in starch biosynthesis (Preiss et al., 1991; Martin and Smith, 1995; Fu et al., 1998; Geigenberger, 2003; Kötting et al., 2010) and catalyzes the formation of ADP-glucose; the primary glucosyl donor for the formation of the linear glucan molecules of which starch consists. These are then converted to starch by starch synthase (SS) isoforms (Patron and Keeling, 2005). AGPase is allosterically down- and up regulated by Pi and triose-P, respectively (Fu et al., 1998; as reviewed in Zeeman et al., 2007), and is further also known to be subjected to post translational redox modulation (Tiessen et al., 2003). Redox regulation is observed in both photosynthetic and non-photosynthetic tissues mediated by the plastidial ferredoxin/thioredoxin system, and this result in the activation during the day and inactivation at night of AGPase (Hendriks et al., 2003). AGPase also experiences short term redox regulation by a SNF1-related kinase decreasing its activity in response to decreased sucrose concentration (Tiessen et al., 2003). Feeding of trehalose to *Arabidopsis* leaves has been shown to stimulate starch synthesis accompanied by an activation of AGPase (Kolbe et al., 2005). Studies on transgenic *Arabidopsis* lines overexpressing trehalose phosphate synthase (TPS) and trehalose phosphate phosphatase (TPP) have shown that trehalose 6-phosphate (T6P) is essential for sugar utilization and growth (Kolbe et al., 2005), while genetic and biochemical evidence are mounting that T6P relays the cytosolic sucrose status to the plastid ensuring redox control of AGPase and starch synthesis independently of light (Kolbe et al., 2005). However, the exact molecular mechanism of how this is achieved remains to be elucidated.

Sugars have been shown, however, to act as signal molecules in the regulation and control of the expression of a diverse number of genes involved in many processes in plants (Xiao et al., 2000). The best studied thus far, namely hexokinase (HXK), is involved in sugar sensing and is sensitive to prevailing glucose levels. HXK is a dual functional enzyme with both catalytic and regulatory properties to fulfill these distinct roles (Xiao et al., 2000). Glucose and the glucose sensor HXK are responsible for the regulation of genes involved predominantly in photosynthesis, such as the small subunit of RuBisCo (*rbcS*), plastocyanin (*PC*) and chlorophyll a/b binding protein (*CAB1*), as well as the cell cycle and stress responses (Rolland and Sheen, 2005). Whilst T6P has been shown to be a potent inhibitor of yeast HXK (van Vaeck et al., 2001), complementary evidence in plants is still lacking. Alterations in trehalose metabolism lead; however, to significant changes in plant carbohydrate partitioning suggesting that some sensing and transduction could be operating *in planta* as well (as reviewed in Rolland et al., 2002). In potato tubers an increase in redox-activation of AGPase has been noted in lines with decreased plastidial adenylate kinase (ADK) activity (Oliver et al., 2008). A possible explanation for this is the presence of high levels of sucrose, activating AGPase via signals involving SNF-like protein kinases and T6P (Hendriks et al., 2003, Tiessen et al., 2003, Kolbe et al., 2005); however, these potato lines had no significant alterations in cellular concentration of sucrose (Oliver et al., 2008). Another possibility includes that energy sensing and signaling could be responsible for the redox-activation of AGPase. In support of this, adenine feeding to potato tuber discs has been shown to lead to increased cellular adenine levels accompanied by an activation of AGPase activity (Oliver et al., 2008). In contrast, the feeding of orotate (an intermediate of *de novo* uridine nucleotide biosynthesis) leads to increases in uridine nucleotide levels without affecting adenine nucleotide levels and results in increased sucrose degradation (Loef et al., 1999).

The resulting lower levels of sucrose could potentially decrease the redox activation of AGPase (Tiessen et al., 2003; Oliver et al., 2008).

While carbohydrate synthesis is an important component of metabolism, it is equally important that carbon catabolism and its modulation are matched. The first step in the hydrolysis of sucrose to glucose and fructose is mediated by invertases along with sucrose synthase (discussed above) (Tymowska-Lalanne and Kreis, 1998). Invertases are distinguished according to their location, solubility and pH optima and are thus located in the cell wall, cytoplasm, vacuole and plastid (Fig 2.1) (Tymowska-Lalanne and Kreis, 1998; Tamoi et al., 2010). Their expression has been shown to be significantly affected by sugars (Roitsch et al., 1995), biotic stress (Sturm and Chrispeels, 1990), gravity, temperature (Wu et al., 1993; Zhou et al., 1994), as well as development stage (Tymowska-Lalanne and Kreis, 1998). Vacuolar invertase has been shown to be essential for the mobilization of sucrose in sink organs and influences root growth and cell expansion in *Arabidopsis* (Sergeeva et al., 2006). Apart from an induction in cell wall invertase (CWI) expression in response to wounding and pathogen attack (Sturm and Chrispeels, 1990) it also plays a key role in development (Tymowska-Lalanne and Kreis, 1998). Recently, it has been shown that an isoform of CWI, *AtCWINV4*, is important in maintaining a sink for sugars in nectar production (Ruhlmann et al., 2010). Furthermore, a point mutation in plastidial neutral invertase leads to an inhibition of the development in the photosynthetic apparatus, as well as affects the carbon nitrogen balances in young *Arabidopsis* seedlings (Tamoi et al., 2010). A loss of one of the isoforms of cytosolic neutral invertase (NI) leads to a 30% reduction in *Arabidopsis* primary root extension as well as reduces leaf and silique expansion (Lou et al., 2007; Qi et al., 2007). In addition, a double mutant combination of NI further leads to severe growth retardation in

Arabidopsis (Barratt et al., 2009), suggesting that invertases is an important factor in maintaining sink to source balances. Starch degradation, on the other hand, is initiated in the dark by the phosphorylation of amylopectin at the C6 and C3 glucose residues by glucan water dikinase (GWD) and phosphoglucan water, dikinase (PWD), respectively (Ritte et al., 2002, 2006; Mikkelsen et al., 2004; Kötting et al., 2010) (Table 2.1). These disrupt the amylopectin molecule and allow access to the degradation enzymes β -amylase and isoamylase, which catalyze the formation of maltose and maltotriose, respectively (Lloyd et al., 2005). Maltotriose is cleaved into maltose and glucose by disproportionating enzyme 1 (DPE1). Maltose and glucose are exported to the cytosol by a maltose exporter and putative glucose export protein, respectively (Fig 2.1; Table 2.1). The main route in *Arabidopsis* leaves appears to be maltose export as mutations in the maltose transporter (*MEX1*) greatly inhibit starch degradation (Niittyla et al., 2004). Maltose in the cytosol is converted to glucose by disproportionating enzyme 2 (DPE2) (Chia et al., 2004; Lu and Sharkey, 2004; Lütken et al., 2010). It is speculated that the export of maltose from the chloroplast allows for its entry to the sucrose synthesis pathway downstream of F6P, ensuring that regulation by F2,6BP is further avoided (Nielsen et al., 2004).

Table 2.1 Summary of enzymes and transporters involved in carbohydrate catabolism and starch transport. Generalized names (and abbreviations) are given for enzymes involved in sucrose and starch degradation, as well as the (putative) transporters for the starch mobilization products. Corresponding enzyme commission (EC) numbers, and isoforms and AGI codes for the *Arabidopsis thaliana* orthologous are given. In addition, the general catalysis type and sub-cellular localization are described. Abbreviations: suc – sucrose; glu – glucose; fru – fructose; ER - endoplasmic reticulum.

Table 1: Showing different isoforms of enzymes involved with starch and sucrose degradation in Arabidopsis, the subcellular localization and mode of action

General name	EC Number	No of isoforms	AGI code	Reaction Type/ Mode of action	Subcellular localization
Sucrose degradation					
Sucrose synthase SuSY	EC. 2.4.1.13	6	At5g20830, At5g49190, At4g02280, At3g43190, At5g37180, At1g73370	Reversible hexosyl group transfer between sucrose and nucleotide sugar	Membrane bound, tonoplast, ER, plasma membrane, plastid
Neutral Invertase NI	EC. 3.2.1.26	4 Putative	At1g43600, At3g52600, At2g36190, At3g13784	Hydrolyze suc to glu and fru	Cytoplasm/mitochondrion/plastid
Cell wall invertase CWI	EC. 3.2.1.26	1	At3g13790	Hydrolyze suc to glu and fru	Cell wall
Acid invertase AI	EC. 3.2.1.26	1	At1g12240	Hydrolyze suc to glu and fru	Vacuole
Starch degradation					
Glucan,water dikinase GWD	EC 2.7.9.4	1	At5g26570	Starch phosphorylation	Chloroplast
Phosphoglucan,water dikinase PWD	EC 2.7.9.5	1	At5g26570	Starch phosphorylation	Chloroplast
β-amylase BAM1/3	EC 3.2.1.2	2	At3g23920/At4g17090	Malto-oligosacchrides to maltose	Chloroplast
Disproportionating enzyme 1 DPE 1	EC 2.4.1.25	1	At5g64860	Maltotriose metabolism	Chloroplast
Disproportionating enzyme 2 DPE 2	EC 2.4.1.25	1	At2g40840	Maltose metabolism	Cytosol
Transport					
Maltose Exporter MEX1	EC 3.6.3.19	1	At5g17520	Maltose export to cytosol	Chloroplast membrane
Glucose transporter GlcT	EC 2.7.1.69	1 Putative	-	Glucose export from plastid	Plastid

Research studies have further shown that starch degradation is linear at night and results in complete utilization of all starch by the onset of the following light period (Gibon et al., 2004; as reviewed in Smith and Stitt, 2007). As a consequence, plants exposed to altered day length change their carbohydrate partitioning accordingly and the rate of starch production is directly proportional to the amount of starch mobilized by the plant (Chatterton and Sivius, 1980; Gibon et al., 2004). For example, soybean plants grown under a 14h photoperiod allocate 60% of their total photoassimilate to starch synthesis, while plants exposed to half the time of sunlight allocate up to 90% of their total photoassimilate to starch biosynthesis (Chatterton and Silvius 1980). Accordingly, the rate of starch degradation at night is also adjusted to ensure that it is completely utilized by the onset of the following light period (Fondy and Geiger, 1985); a 4h darkness extension at the end of a night period results in complete cessation of root growth, which does not resume until several hours into the following light period, and is characterized by a large accumulation of carbohydrates as nothing is invested in growth during this time period (Gibon et al., 2004; as reviewed in Smith and Stitt, 2007). As is evident here, plant primary carbohydrate metabolism is subjected to a complex set of regulatory mechanisms involving both spatial and temporal aspects. A high degree of communication and control therefore needs to be exerted by the plant to ensure its success. This emphasizes the need for the development of new tools to aid those currently available and broaden our understanding of compartmentation in plant metabolism.

2.3 Transporters and compartmentation

While plant compartmentation ensures specificity in certain biosynthetic pathways, as well as allow for some pathways to be shared between compartments (Masakapalli et al., 2009), it becomes important to understand the exchange of metabolites and

hence communication between the different metabolic compartments. Of particular interest currently is the functional characterization of transport proteins because they are obvious points of regulation due to their role in facilitating the exchange of metabolites between these sub-cellular environments.

In this regard, proteomic studies from membrane-bound fractions in *Arabidopsis thaliana* has identified over 400 tonoplast enriched proteins to date (Carter et al., 2004); a quarter of which are still of unknown function. This suggests that the vacuole is a highly diverse organelle and illustrates the large scope for protein exploration and characterization of the tonoplast membrane. Similarly, the plastid envelope proteome has expanded significantly in recent years from 50 (Ferro et al., 2002) to over 480 membrane bound proteins (Ferro et al., 2010), with 85 proteins still with unknown functions. Recently, the plastidial proteome have differentiated between thylakoid, stromal and envelope fractions, which greatly facilitates biological interpretation of light-associated phenotypes or species differences (Peltier et al., 2006).

While functional characterization of the membrane bound transporters are an essential part of plant science currently, it requires laborious and tedious experimentation. In light of the presence of different isoforms, multi-enzyme complexes, as well as the occurrence of some transporters that have similar affinities for different substrates (Sauer et al., 2004), the task becomes even more daunting. The need for the development of high-throughput technologies that will aid in these analyses are thus essential.

2.4 Technologies available for studying plant compartmentation

2.4.1 Sub-cellular proteomics

Proteomics has been classically used as a tool to understand and predict sub-cellular metabolism. Organelle proteins, transcribed within the nucleus and translated in the cytosol, are transported to the appropriate compartments facilitated by signal or transit peptides that reside at or within the N- or C-terminal amino acid residues of the translated gene product. These peptides are recognized by specific protein complexes that facilitate import of the target protein to its destination (Nielsen et al., 1997). Mitochondrial and plastid signal peptides are recognized by the translocon on outer/inner membrane complex of mitochondria (TOM/TIM complex) and translocon on outer/inner envelope of chloroplast (TOC/TIC complex), respectively (Moghadam and Schleiff, 2005). Modern bioinformatic approaches have developed several algorithms in order to predict sub-cellular localization. Examples of databases that are available to aid in the sub-cellular prediction include TargetP (www.cbs.dtu.dk/services/TargetP/) and SignalP (www.cbs.dtu.dk/services/SignalP/). However, *in silico* prediction needs to be validated by biological confirmation, and fluorescent fusion proteins such as green fluorescent protein (GFP) are frequently used in this regard. These types of analyses have illustrated to date that, whilst the majority of proteins co-localize to their predicted targeting sites, unexpected localization may also occur, either as a result of misrecognition or neglect of the signal peptide by the plant (Haseloff et al., 1997), dual targeting mechanisms being employed or an exception to the target prediction programs. In addition, a major limitation of this kind of sub-cellular proteomics approach includes the disregard of post translational modification and its effect on metabolism.

Further methods which assist the study of proteomics include the use of cellular fractionation techniques. Proteins are extracted from the sub-cellular compartments

and separated according to mass and charge by two-dimensional gel electrophoresis. The proteins are then subjected to tryptic digests and at this point peptides can be analyzed by LC-MS for the identification of the proteins present. This technique has successfully been employed to assist the analysis of proteins contained in highly purified vacuolar membranes (Endler et al., 2006).

2.4.2 (Sub-cellular) metabolomics

Metabolomics can be defined as the measurement of a metabolite levels that reflect the biochemical state of a cell. Primary metabolite levels of interest have been frequently evaluated in the past by methods such as enzyme-linked assays, thin layer chromatography (TLC), high pressure liquid chromatography (HPLC) or nuclear magnetic resonance (NMR), and the analysis type is reliant on the metabolite (or class) of interest and restricted to a selected few. Hyphenated technologies (eg. gas chromatography mass spectrometry (GC-MS), liquid chromatography mass spectrometry (LC-MS) or LC-NMR, and variants of these) have greatly increased the spectral resolution and hence number of metabolites that can be profiled in a single plant extract or sample run (see for example Roessner et al., 2001; Sauer, 2007; Arrivault et al., 2009). Whilst metabolomics in itself relays no information on sub-cellular metabolite distribution, it becomes a powerful technique when employed in combination with other techniques that have conferred this type of resolution. For example metabolite profiling and flux measurements have been combined with fractionated proteins and, based on sub-cellular signal prediction, compartmentation in *C. reinhardtii* has been recently evaluated (Wienkoop et al., 2010).

Another useful technique to combine with metabolomics is that of cell fractionation. Plant organelles exhibit different characteristics (for example size, shape and

density), and based on differential centrifugation, enriched fractions of organelle types can be obtained. Both aqueous and non-aqueous fractionation (NAQF) can be used for this purpose. While aqueous fractionation is useful and relatively straightforward for isolation and characterization of genes and proteins in sub-cellular enriched environments, metabolite measurements rely on fast and effective quenching of metabolism and are severely compromised under these hydrated conditions (MacDougall et al., 1995). In contrast, NAQF is a fractionation technique that utilizes organic solvents, and hence ensures a moisture-free environment for cell fractionation. During NAQF, a homogenate of cells is loaded on a density gradient and organelle membranes are separated into fractions by ultra-centrifugation. Metabolites included in the compartment of interest adhere to the appropriate membrane, resulting in an enrichment of metabolites in a particular organelle of interest. In plant metabolism, this technique has been successfully employed to evaluate sub-cellular distribution of F_{2,6}BP in spinach (Stitt et al., 1983) adenylate and P_{Pi} distribution in soybean nodules (Kuzma et al., 1999) as well as, combined with GC-MS, allowed for the separation and sub-cellular enrichment of forty-six metabolites in potato tubers (Farre et al., 2008) and thirty-two metabolites in soybean leaves (Benkeblia et al., 2007).

2.4.3 Fluorescence resonance energy transfer (FRET) technology

While quantification of the sub-cellular metabolome has greatly advanced our current perception of plant metabolism and has the potential to lead to novel gene discoveries, the comprehensive characterization of metabolic networks and their functional operation would also rely on the rate a metabolite is synthesized, degraded or transported (the concepts of cycling, turnover and flux). Currently, a single optimized method provides an accurate account of sub-cellular flux in metabolism,

namely that of FRET. FRET refers to a quantum mechanical effect between a fluorescence donor and a suitable acceptor (Fehr et al., 2005). Specific metabolite binding proteins (MBPs) are coupled to chromophores such as the green fluorescence protein (GFP), yellow fluorescent protein (YFP) or cyan fluorescent protein (CFP) (van der Krogt et al., 2008), and plants can be transformed with the constructs leading to expression of these proteins in specific compartments. For metabolite analysis two unique FRET constructs are utilized by excitation of the protein complex by light of a short wavelength (436nm). This causes an energy emission from the fluorescence proteins which are recorded. Upon ligand (metabolite) binding the protein complex undergoes a conformational change, the proximity of the chromophores change and the fluorescence wavelength is altered accordingly. The ratio of emitted fluorescence from the two states (bound and unbound) is used to calculate the concentration of the metabolite and its flux. A number of plant FRET sensors have been developed to date and these include the glucose (Deuschle et al., 2006; Chaudhuri et al., 2008), sucrose (Chaudhuri et al., 2008) and phosphate (Gu et al., 2006) nanosensors. While the principle is universal for any metabolite in question, the number of metabolites co-profiled is limited to the amount of fluorescent sensors currently available.

In contrast to the limited number of metabolites (and subsequent flux) that can be co-profiled by FRET, an increase in the metabolite quantity involved in fluxes can be achieved by a combination of isotopic labelling experiments analyzed *via* hyphenated methodologies such as GC- and LC-MS (as reviewed in Allen et al., 2007). Further understanding of the extent of these on a sub-cellular level could greatly improve our current understanding of metabolic flux balancing analysis and isotope dilution factors encountered upon whole cell studies (Ratcliffe and Shachar-Hill, 2006).

2.4.4 Micro laser dissection

Lastly, a recent tool that has emerged as an alternative to study homogeneity in plant metabolism is that of laser capture micro dissection (LCMD) (Klink et al., 2005). LCMD makes use of a high intensity laser beam to isolate specific regions in a plant cell (as viewed under a microscope) for analysis. While it has been used to study DNA, RNA and protein levels in specific tissue types, it has also been suggested as an alternative to study metabolite levels on whole tissue or sub-cellular levels. However, while fast, effective cryo--sectioning of material could be achieved for a representation of the metabolome, such treatments have been known to result in ice formations in the vacuolar compartment and air spaces between cells in mature plant tissues. Therefore, the feasibility of this technique on metabolite levels might be restricted to dense cytoplasmic material or tissue that possess unique morphological characteristics, such as vascular elements or epidermal cell layers (Nakazono et al., 2003; Woll et al., 2005; Scanlon et al., 2009) . Previously LCMD was employed for cell wall polysaccharide analysis (Obel et al., 2009) and the scope remains for more cell-specific analysis; however, much work needs to be done before it is employed on a sub-cellular level. In addition, similar to the FRET technology mentioned above (section 2.4.3) methodologies like these are currently restricted to a few specialized laboratories due to the high cost associated with the equipment used to perform this analysis.

2.5 Layout of thesis

While it is evident from the preceding sections that methodologies are available to assist in the study of plant compartmentation, it is equally apparent that every technology suffers from a degree of constraint. Within the scope of research activities

conducted within our institute, accessible, cost-effective techniques to screen and profile proteins, metabolite levels and fluxes of interest in primary carbohydrate compartmentation has become essential, and motivates this study. Here I describe the development of a reverse-phase LC-MS method to allow for the simultaneous detection and quantification of phosphorylated and nucleotide sugars (Chapter 3). Chapter 4 will focus on the optimization and implementation of ^{13}C isotope labeling and non-aqueous fractionation of plant material to determine sub-cellular metabolite levels and isotopic label enrichment *via* GC- and LC-MS technology. Chapter 5 provides details on a yeast complementation used to screen for tonoplast bound import proteins involved in sucrose compartmentation. Chapter 6 is a summation of the experimental chapters, and will comment on the applicability and limitations of these technologies.

Chapter 3

Development of a reverse phase liquid chromatography-mass spectrometry method for detection and quantification of nucleotide and phosphorylated intermediates of primary metabolism

3.1 Introduction

High-throughput profiling technologies have come into focus as methods used to screen and characterize phenotypes of interest (Roessner et al., 2001; Arbona et al., 2010). Of these, the application of metabolomics (the metabolome being defined as the metabolite complement of a cell or tissue) has received particular interest due to the ease and manageability of conducting large scale experiments, as well as because the information produced can be directly related to the biochemical state of a cell or tissue type. Established methods such as enzyme-linked assays, high pressure liquid chromatography (HPLC) and nuclear magnetic resonance (NMR) are still used as a means to quantify these; however they exhibit some limitations. Spectrophotometric assays are dependent on the presence of proteins with specific activities which may not be readily available, while HPLC and NMR are relatively insensitive. Because of these drawbacks, novel technologies, such as gas chromatography mass-spectrometry (GC-MS), have been developed to analyze polar (Roessner et al., 2001; Benkeblia et al., 2007) and apolar (Dembitsky et al., 2001; Lytovchenko et al., 2009) metabolites. The nature of GC-MS analysis however, often hampers the reliable detection and quantification of charged compounds, like phosphorylated and nucleotide sugars. Profiling by this method relies on the compound of interest being vaporized in order for separation of compounds within complex extracts to occur in a capillary column. While this is applicable to a range of volatile compounds, chemical modification of non-volatile compounds (in a process

called derivitization) can also be employed to increase the volatility of the analyte of interest for gas chromatographic separation. More polar metabolites, however, such as ionic species containing phosphate groups, are not readily amenable to standard derivitization techniques and often result in artefact formation.

Phosphorylated metabolites often lie at crucial points in metabolic pathways, and their concentrations may have significant effects on the regulation of plant metabolism (Okar and Lange, 1999). They play fundamental roles in glycolysis, gluconeogenesis, the Calvin cycle, starch and cell wall biosynthesis. ADP-glucose, for example, is a precursor for starch biosynthesis and concentrations of ADP-glucose as well as the activity of ADP-glucose pyrophosphorylase (AGPase) (the enzyme responsible for its production) have been demonstrated to greatly affect levels of stored starch in *Arabidopsis thaliana* leaves and *Solanum tuberosum* tubers (Stark et al., 1992; Kolbe et al., 2005). On the other hand, some phosphorylated intermediates have been shown to be involved in signalling roles. Trehalose 6-phosphate acts as a redox activator of AGPase allowing for the light independent regulation of starch synthesis (Kolbe et al., 2005) while inositol 1,4,5-triphosphate is a signalling molecule which is very important for the gravitropic response in plants (Perera et al., 2001).

Liquid chromatography (LC) allows for the separation of a number of compounds according to their inherent chemical properties, interaction on a specified column and elution characteristics. Reverse phase LC involves the use of a non-polar column with an ion-pair reagent. This reagent displays both polar and non-polar properties allowing it to coat the column, while the compounds of interest adhere to it and are retained on the column as it pass through the matrix. Buffer lacking the ion-pair

reagent is used to elute the compounds from the column and, when it is linked to a MS the compounds can then be identified based on their mass-to-charge (m/z) ratios. One advantage of LC separation of analytes is that it does not require derivitization and, as separation is in the liquid phase, many compounds which are not readily detectable by GC-MS can be identified and quantified. Furthermore, LC, with the use of MS/MS, allows for the identification of isomeric compounds which might co-elute. The different fragmentation patterns and daughter ions may allow for further reliable identification. Such a technique was recently used for the identification and quantification of phosphorylated and nucleotide sugars in *A. thaliana* rosettes (Arrivault et al., 2009). The combination of separation and fragmentation technologies also facilitates in a) easier and more reliable metabolite identification and b) the possibility to determine isotopic label enrichments for down-stream flux analysis.

In this chapter, I present two optimized reverse phase LC-MS protocols for the simultaneous detection and measurement of phosphorylated and nucleotide compounds involved in primary carbon metabolism in *Arabidopsis* rosette leaves.

3.2 Results and Discussion

3.2.1 Evaluation of buffer and ion-pair composition on separation and detection of authentic phosphorylated and nucleotide standards

In order to evaluate chromatographic separation of phosphorylated and nucleotide sugars, twenty-nine authentic standards were injected onto a reverse phase LC column before being detected by a MS (Table 3.1). This was done in order to establish separation conditions, record retention times and fragmentation patterns to create a MS library of the compounds and to establish calibration curves for the

quantitative determination of metabolite concentrations. The standards for the analysis were selected firstly, for the roles which they play in primary plant metabolism and secondly for their availability. Many of the Calvin cycle intermediates are expensive, some of poor quality (Arrivault et al., 2009) or need to be synthesized, and were thus not considered for initial LC analyses.

The use of elution conditions with octylammonium acetate as the ion pair reagent and acetonitrile as elution buffer (OAAN method) led to the reliable detection and integration of seventeen distinguishable metabolites (Fig 3.1). These included ADP, ATP, ADP-glc, GDP, GDP-glc, GDP-fucose, GDP-mannose, gluconate 6-phosphate, GTP, Ins1,4,5TP, mannose 1-P, NADH, NADP, TDP-glc, TMP, T6P, TTP, UDP, UDP-xylose, UDP-galactose, UMP and UTP. Unfortunately several metabolites co-eluted under these conditions (Fig 3.1). These included the nucleotide sugars; however it was possible to distinguish between these due to differences in their m/z ratios. Also metabolites such as TDP-glucose are not expected to be present in plant extracts and, therefore, co-elution of these was not considered a problem. On the other hand, compounds with identical m/z ratios (like the mono- and disphosphate hexose sugars) could not be resolved using this method and the elution peak at RT 5.4 min and 9.3 min, and m/z of 259 and 339, respectively, represented the total hexose monophosphate and disphosphate pools (Fig 3.1). In order to separate these, two different strategies were evaluated.

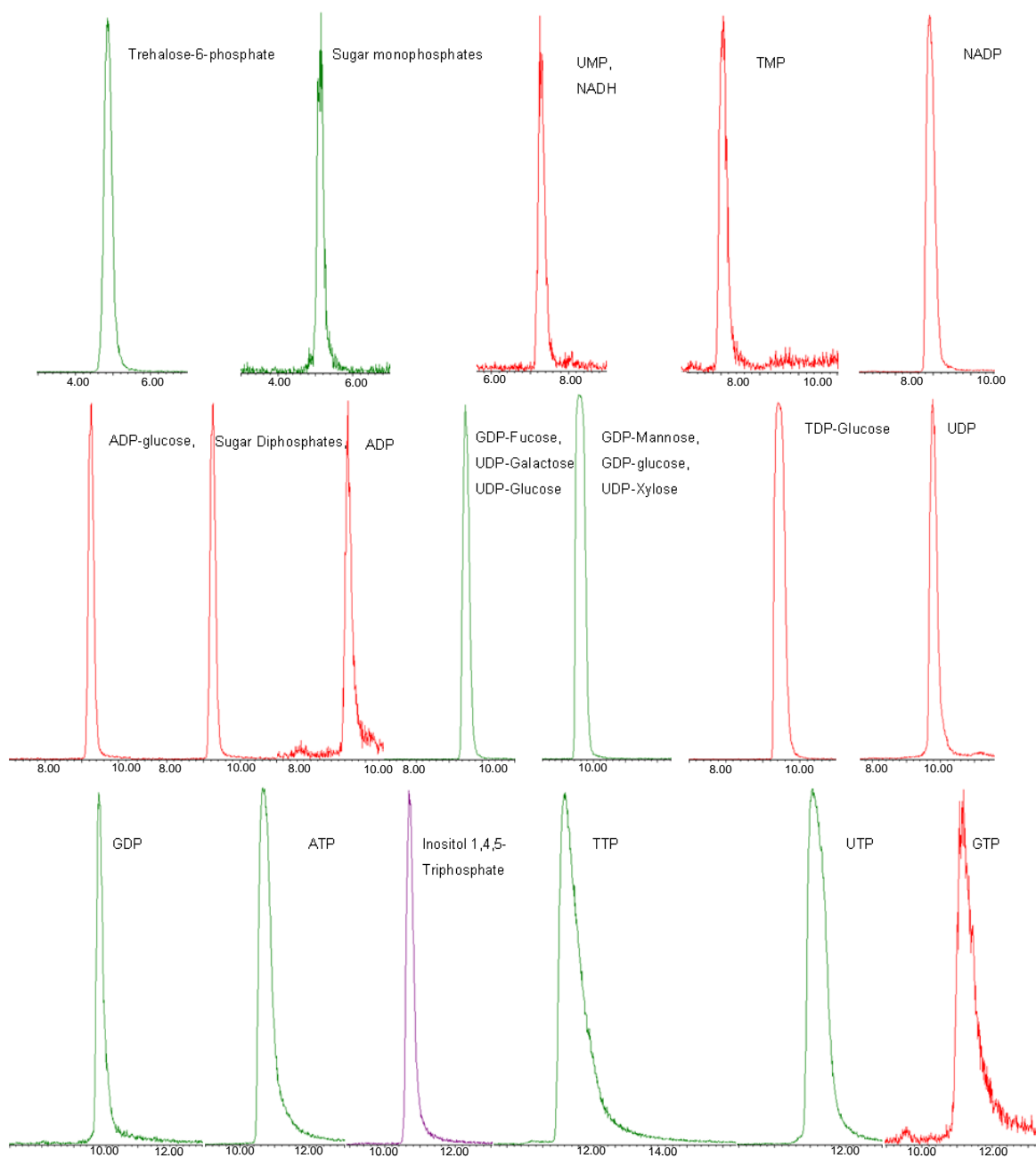


Fig 3.1. Elution pattern of metabolite standards on OAN gradient. Chromatograms displaying mass extractions of metabolite standards and their respective retention times.

Firstly, multiple reaction monitoring (MRM) was employed on the OAN gradient. This method has been previously used to identify co-eluting isomeric metabolites on a LC-MS system (Arrivault et al., 2009). Whilst LC separates compounds based on

their physiochemical properties and deliver it to the MS, a tandem or triple MS further fragment the parent ions from the first MS in order to obtain unique daughter fragments (Arrivault et al., 2009). An attempt was made to use MRM, however, in contrast to previous literature; a collision energy could not be found which yielded significantly different daughter ions or daughter ion ratios for the metabolites in question (data not shown).

For this reason a second set of elution conditions, namely tributylamine (TBAM) as an ion pair reagent and methanol as an elution buffer was used. TBAM elution resulted in adequate separation of the sugar monophosphates (G6P, F6P and G1P), and diphosphate (G1,6BP, F1,6BP and F2,6BP) authentic standards (Table 3.1) without the additional need for MRM scanning. However, this method failed to retain (or elute) the nucleotide and nucleotide-sugars (data not shown). Therefore, a combination of both methods, allowed for the separation and quantification of the phosphorylated and nucleotide compounds of interest.

In addition, no organic acids were detected using either elution methods (data not shown). Whilst chromatographic separation often results in non linear shifts in the retention times of metabolites, exogenous malate, aspartate, shikimate and citrate (7nM each) were added as time standards to correct for these shifts during pre-processing of the chromatography data.

3.2.2 Evaluation of linearity and reproducibility of Waters LC MS system

The linearity of the LC system was tested by running a dilution series of all standards in order to determine the detection limits and reliable quantification area for the plant extracts. A calibration curve was constructed for each of the metabolites and

indicated that all the standards performed linearly between the ranges of 250pM and 250µM with R^2 values > 0.90 (Table 3.1). As this is deemed a relevant physiological concentration range for most of the plant metabolites, recovery experiments were performed next. Quantification of the metabolite levels in the plant extracts was calculated and metabolite recoveries (by doubling the endogenous concentration) were estimated to vary between 65 and 115% (Table 3.1).

Table 3.1: Metabolite levels in *Arabidopsis* leaf tissue harvested at midday of a 12h photoperiod. Metabolites were detected with two LC-MS methods, the first an octylammonium acetate/acetonitrile (OAAN) gradient and the second a tributylamine/methanol (TBAM) gradient. (Metabolites detected in a method are denoted by a ✓ and those not detected are denoted by an x). Retention time is indicated, as well as the R² value which indicates the linearity of the system and the recovery percentage and endogenous leaf concentration for each metabolite is displayed. *nd* indicates a metabolite that was not detected in the plant extract.

Compound	OAAN	TBAM	Retention time (min)	R ²	Percentage recovery (%)	Leaf endogenous concentration (nmol.gFW ⁻¹)
ADP	✓	x	9.48	0.99	65	23.14 ± 2.63
ADP-Glucose	✓	x	9.34	0.93	99	3.39 ± 0.32
ATP	✓	x	10.65	0.98	70	74.93 ± 24.97
Fructose 1,6-bisphosphate	x	✓	49.82	0.98	95	17.28 ± 0.47
Fructose 2,6-bisphosphate	x	✓	50.76	0.90	90	2.38 ± 0.57
Fructose 6-phosphate	x	✓	8.13	0.94	78	61.84 ± 2.31
GDP	✓	x	9.78	0.98	<i>nd</i>	<i>nd</i>
GDP-fucose	✓	x	9.75	0.98	<i>nd</i>	<i>nd</i>
GDP-glucose	✓	x	9.61	0.91	<i>nd</i>	<i>nd</i>
GDP-mannose	✓	x	9.53	0.99	<i>nd</i>	<i>nd</i>
Gluconate 6-phosphate	✓	x	8.52	0.95	70	28.47 ± 0.76
Glucose 1,6-diphosphate	x	✓	53.76	0.94	89	4.05 ± 0.35
Glucose 1-phosphate	x	✓	7.2	0.99	93	5.45 ± 0.37
Glucose 6-phosphate	x	✓	7.07	0.95	105	136.44 ± 7.06
GTP	✓	x	11.18	0.80	<i>nd</i>	<i>nd</i>
Inositol 1,4,5-Triphosphate	✓	x	10.68	0.96	104	6.67 ± 0.66
Mannose 1-phosphate	✓	x	4.94	0.98	<i>nd</i>	<i>nd</i>
NADH	✓	x	7.38	0.98	101	32.41 ± 1.93
NADP	✓	x	8.9	0.92	97	2.52 ± 0.55
TDP-glucose	✓	x	9.61	0.76	<i>nd</i>	<i>nd</i>
TMP	✓	x	8.06	0.98	<i>nd</i>	<i>nd</i>
Trehalose 6-Phosphate	✓	x	4.83	0.94	94	4.49 ± 0.80
TTP	✓	x	11.61	0.98	<i>nd</i>	<i>nd</i>
UDP	✓	x	9.78	0.99	85	14.32 ± 0.86
UDP xylose	✓	x	9.67	0.92	98	11.97 ± 0.82
UDP-galactose	✓	x	9.6	0.93	<i>nd</i>	<i>nd</i>
UDP-glucose	✓	x	9.57	0.95	88	170.56 ± 7.13
UMP	✓	x	7.25	0.94	75	303.16 ± 4.40
UTP	✓	x	11.06	0.99	70	19.47 ± 1.45

3.2.3 Endogenous plant metabolite levels and recovery experiments

The levels of ADP, ATP, ADP-glc, UDP-glc, NADP, NAD, F6P, G1P, G6P and F1,6BP were in the same order of magnitude of those previously reported for *Arabidopsis* rosette leaves that were harvested in the light using a combination of enzymatic assays and ion pair chromatography (Arrivault et al., 2009). The concentration of UTP, UDP and UDP-xylose were at 19.26, 13.6 and 12.46 nmol.gFW⁻¹, respectively. UDP-xylose is a cell wall precursor and expected to be found at low concentrations. The phosphorylated signalling molecules T6P and Ins1,4,5TP were also detected at 4.25 and 7.14 nmol.g.FW⁻¹, respectively. The observed T6P levels is 40 times higher than expected, though, suggesting that another isomer (probably cytosolic sucrose 6-phosphate) is co-eluting with this metabolite. Also G16BP was detected at 4.05 nmol.g.FW⁻¹, which is slightly higher than expected and it is possible that it is co-eluting with another sugar di-phosphate thereby distorting the result. Unusually high levels of UMP are also observed (Table 3.1) possibly due to co-elution of an unknown metabolite of the same *m/z*. Metabolites not detected in the plant extracts (GDP, GDP-fucose, GDP-glucose, GDP-mannose, GTP, mannose-1-phosphate, TDP-glucose, TMP, TTP and UDP-galactose) were also exogenously (100µM in concentration) added to the extract in order to evaluate elution efficiency, and were recovered between 90 and 110% (data not shown).

Conclusion

In conclusion, although no single chromatographic protocol tested could satisfactorily separate all metabolites of interest in a single run, the integration of data resulting from a (single) methanol/chloroform extraction, run on an octylammonium acetate/acetonitrile and tributylamine/methanol gradient, respectively, resulted in the

detection and quantification of 29 phosphorylated and nucleotide sugar standards; 17 of which could be detected in the *Arabidopsis* leaf rosette tissue.

3.3 Materials and Methods

3.3.1 Chemicals

Tributylamine, metabolite standards (see Table 3.1) and organic acid time standards (citrate, malate, isocitrate, aconitate, shikimate) were purchased from Sigma-Aldrich (<http://www.sigmaaldrich.com>), while methanol, acetonitrile and biological agar were purchased from Merck (<http://www.merck.com>). Murashige and Skoog (MS) basal salt were obtained from Highveld Biological (South Africa) while the hydroponic nutrient mix was from Hygrotech (www.hygrotech.co.za). Octylammonium acetate was made by the careful addition of 0.1mol octylamine and 0.1mol acetic acid to 100ml diethyl ether on ice. This solution was gently stirred and cooled on dry ice to allow the salt to crystallize. The ether was removed, and the salt was washed twice with 50ml hexane.

3.3.2 Plant material and growth conditions

Arabidopsis thaliana (Heynh ecotype Col-0) seeds were surface sterilized by washing in 10% (v/v) aqueous sodium hypochlorite for 3min, followed by three washes in sterile dH₂O. The seeds were re-suspended in 500µl sterile dH₂O and plated onto half strength MS solidified with 0.7% (w/v) agar (pH 5.6), cold treated for 48h after which they were placed in a growth room under 16h/8h day/night cycle with a photosynthetic photon flux density of 50 µmol photons.m⁻².s⁻¹ at 23°C. Once the seedlings reached the four leaf stage they were transferred to 6cm pots containing coconut husk (www.starkeyayres.co.za) moistened with 1.5g.l⁻¹ hydroponic nutrient mix supplemented with 1.5g.l⁻¹ Ca(NO₃)₂. Plants were subsequently grown in a

12h/12h photoperiod at 23°C. After five weeks the plants were harvested, frozen in liquid nitrogen and kept at -80°C until analysis.

3.3.3 Metabolite extraction

Frozen plant material was homogenized using a pestle and mortar in liquid nitrogen and metabolites extracted by a chloroform/methanol method (Lunn et al., 2006) with modifications as specified by Arrivault et al. (2009). In brief, 250µl cold CHCl₃/CH₃OH (3:7, v/v) was added to 20mg plant material; the frozen mixture warmed to -20°C while shaking vigorously and then incubated for 2h at -20°C. Soluble metabolites were extracted from the CHCl₃ phase by the addition of 200µl dH₂O. The mixture was warmed to 4°C and centrifuged at 200xg for 4min. The upper aqueous phase was removed to a new 1.5ml eppendorf tube and stored at 4°C while the lower chloroform phase was re-extracted by the same process. The two extracts were combined and evaporated to dryness in a vacuum dryer (Genevac EZ-2, www.genevac.com) before being re-suspended in 150µl dH₂O. High molecular weight molecules were removed from the extract by passing through a 3kDa low binding regenerated cellulose membrane filter (Amicon, www.millipore.com).

3.3.4 LC MS analysis

3.3.4.1 Instrumentation details

Reverse phase chromatography was carried out on a Waters Aquity Ultra Performance LC coupled to a Micromass Q-TOF Ultima MS. It was operated in negative ion mode with a cone voltage of 35.0 V, a capillary voltage of 3.70 V, the source temperature was operated at 100°C and the desolvation temperature and gas were at 350°C. All other parameters were optimized for the best sensitivity on the machine.

Chromatographic column specification were as follow; a Waters Atlantis 10x150mm C18 3µm column (www.waters.com) coupled to an Agilent 10x30mm 3.5 µm bonus reverse phase guard column (www.agilent.com) was used in all the analyses. Chromatographic separation of nucleotides and nucleotide sugars were achieved by injecting 5µl extract or 1µl standard.

3.3.4.2 Octylammonium acetate/acetonitrile (OAAN) buffer composition and elution conditions

The octylammonium acetate/acetonitrile method consisted of buffer A made up of 10mM aqueous octylammonium acetate (pH3.0) and buffer B consisting of 95% acetonitrile (pH 3.0) (based on Vas et al., 2009). The linear gradient that was employed is as follows: 0 – 1min 100 – 95% A, 3min 90% A, 3.30 min 85% A, 4 min 85% A, 5 min 80% A, 5.30min 80% A, 6 min 70% A, 7 min 65% A, 8 min 60% A, 9 min 50% A, 14 min 50 % A, 20 min 21% A, 22 min 10 %A, 22.10 – 30 min 95% A. The flow rate was maintained at 0.06 ml/min throughout the run.

3.3.4.3 Tributylamine/methanol (TBAM) buffer composition and elution conditions

For the separation of sugar mono-and diphosphates a recent method was adapted (Arrivault et al., 2009). Buffer A consisted of 10mM aqueous tributylamine (pH 4.95, adjusted with acetic acid) and buffer B 100% methanol. The gradient was set as follows 0 – 5 min 95% A, 15 min 90% A, 22 min 85% A, 37 min 80% A, 40 min 65% A, 43 min 65% A, 47min 40% A, 50 min 40% A, 50.01min 10% A, 54 min 10% A, 54.01 95% A, 65 min 95% A. The flow rate was maintained at 0.06ml/min throughout the run.

3.3.5 Data acquisition and analysis

MassLynx V4.0 SP4 (www.micromass.co.uk) was used for instrument control and data acquisition, while for data pre-processing MetAlign v 200410. (www.metalign.wur.nl/UK/) was used for baseline correction, scaling and alignment (De Vos et al., 2007). The data matrix was generated by conversion of the MassLynx data files (.raw) to the NetCDF format by the DataBridge function of MassLynx 4.0. The parameters for the processing of data were as follows: Maximum amplitude: 10000; Peak slope factor: 1; Peak threshold factor: 1; Average peak width at half weight: 5; Scaling options: no; Maximum shift per scan: 35. Furthermore, peak filtering, peak binning, peak deconvolution and resulting metabolite annotation were manually performed from comparison with the authentic standards processed in parallel with the plant extracts.

Chapter 4

Sub-cellular distribution of non-steady state metabolite levels of an adenylate kinase mutant impaired in primary carbon metabolism in *Arabidopsis thaliana* rosette leaves

4.1 Introduction

Novel biological insights can be obtained from combined metabolomic and fluxomic approaches, yet the development and interpretation of high-throughput methods to study these on a sub-cellular level are in arrears. With the completion of the *Arabidopsis thaliana* genome sequencing project (*Arabidopsis* genome initiative, 2000) it has become apparent that functional gene annotation of distinct sub-cellular isoforms can lead to the identification of novel biochemical pathways (Araujo et al., 2010; Arsova et al., 2010), and the wealth of genomic, proteomic and metabolic platforms that have been established for this model species ease such research efforts. In addition, *Arabidopsis* is easily transformed *via Agrobacterium*-mediated infiltration and a large number of mutants and introgression lines are available from various resources (eg. SALK, GABI-Kat, NASC, RIKEN). This makes it an ideal species to study carbon interactions and regulation, and much has been learned from mutant characterization. For example, analysis of plants lacking phosphoglucomutase (*pgm*), ADP-glucose pyrophosphorylase (*agpase*) and the triose phosphate transporter (*tpt*) have told us much about their role in starch metabolism as well as its regulation (Caspar et al., 1985; Lin et al., 1988; Schneider et al., 2002; Gibon et al., 2004; Usadel et al., 2008).

In recent years, a number of studies have reported on sub-cellular metabolite levels in a range of crop species (Farré et al., 2008; Kuzma et al., 1999; Benkeblia et al.,

2007); however, only limited information regarding *Arabidopsis* sub-cellular metabolism (metabolite and flux information) has been published to date. The exception to this is the use of fluorescence resonance energy transfer (FRET) technology which is targeted to a specific metabolite. Examples of metabolite concentrations determined using FRET in sub-cellular compartments in *Arabidopsis* include ribose (Lager et al., 2003), glucose (Fehr et al., 2004), maltose (Fehr et al., 2002), sucrose (Lager et al., 2006) and phosphate (Lalonde et al., 2005).

Here I describe a method based on a non-aqueous cell fractionation principle and analysis of metabolite levels and label enrichments in *Arabidopsis* rosette leaf material in a mutant of an adenylate kinase isoform (*adk1*) (Carrari et al., 2005) and its Col-0 background. It was decided to perform this analysis on glucose fed leaf disc material for several reasons. Firstly, within our growth facilities, presently, uniform light and $\text{H}^{13}\text{CO}_3^-$ delivery cannot be controlled in order to ensure that each plant receives the same amount of isotopic label. As a validation method, any differences that would be observed between the genotypes should be attributed to their endogenous metabolism, and not these external parameters. Secondly, while *adk1* leads to significant changes in carbohydrate pools in the rosette leaves, more pronounced changes in root amino acid metabolism were evident upon continuous light conditions (Carrari et al., 2005). Glucose feeding has been known to result in the down-regulation of the expression of a number of photosynthetic genes (as reviewed in Rolland et al., 2006), and lead to a switch of autotrophic to heterotrophic metabolism. Therefore, more pronounced changes would be expected as time progress using this exogenous sugar supply. In addition, whilst energy-dependent hexokinase-associated sugar signaling mechanisms have profound impacts on plant growth (Xiao et al., 2000), glucose feeding in an energy impaired mutant would give

vital clues to the compensatory mechanism that *adk1* is exerting in order to maintain adenylate homeostasis. Lastly, as an additional control, prevailing cytosolic glucose levels have been measured with FRET technology in *Arabidopsis* epidermal cells of leaves perfused with glucose (Deuschle et al., 2006) and therefore this allows for a direct comparison to this more sophisticated technology.

Perturbations of adenylate homeostasis leads to unpredictable changes in sucrose and starch levels, the reason for which is not well understood (Regierer et al, 2002; Carrari et al., 2005; Olivier et al., 2008). Adenosine monophosphate kinase (ADK) catalyzes the reversible equilibration of ATP and AMP to ADP pools. Seven *Arabidopsis adk* isoforms have been identified and these are localized to either the plastid (*adk2* and *5*), mitochondria (*adk 6* and *7*) or cytosol (*adk 3* and *4*) (Lange et al., 2008). The remaining isoform, namely *adk1* has been previously reported to be localized to the plastid (Carrari et al., 2005), yet subsequent *in silico* signal peptide predictions and co-expression analysis, as well as additional GFP localization studies suggest that it might also be targeted to the mitochondria (Lange et al., 2008). The most plausible explanation for this is that *adk1* is targeted to both compartments (Lange et al., 2008). Due to the sub-cellular distribution of the isoforms and the various adenylate transporters identified on organellar membranes, it is also anticipated that a degree of redundancy in energy metabolism might exist (Carrari et al., 2005). In agreement, adenylate levels are almost equally distributed between the cytosol and plastid, with only 9% occurring in the mitochondria of potato tubers (Farré et al., 2001). Irrespective of whether *adk1* is plastidial, mitochondrial or co-localized, a mutation in the gene coding for it would be expected to lead to significant alterations in sub-cellular adenylate levels. On the other hand, if adenylate homeostasis is maintained either through carbon dispensary mechanism or

adenylate re-distribution, then these should become apparent by characterization of the sub-cellular metabolome and fluxome. However, the analysis tools to study such interactions remain expensive or under-developed.

The application of non aqueous fractionation (NAQF) combined with hyphenated technologies such as reverse phase liquid chromatography mass spectrometry (RPLC-MS) and gas chromatography mass spectrometry (GC-MS), as well as isotopic labeling was, therefore, assessed in *Arabidopsis thaliana* Col-0 and *adk1* mature rosette leaves in order to quantify metabolite levels and resulting isotopic label enrichments in three compartments, namely the cytosol, plastid and vacuole. It was apparent from this analysis that the three different sub-cellular compartments were easily distinguishable, and significant shifts in metabolite distribution existed between the mutant and wild type plants. These included the prevailing sucrose levels which was, curiously, significantly enhanced in the mutant plants and mainly distributed throughout the cytosolic fractions. Two additional fractions were enriched in cell wall precursors and organic acids (distinct from the vacuolar pool), respectively, suggesting that this technique also allowed for the distinction between the cell wall (pellet) and mitochondria, and will be validated in future. In combination with sub-cellular isotopic label enrichments (in the initial phases of processing), this would allow for vital information regarding metabolic organization upon energy deprivation and additional carbon supply.

4.2 Results

4.2.1 Evaluation of marker enzyme distribution and fractionation efficiency

In order to test the fractionation efficiency, marker enzymes predominant in a compartment were chosen and assayed to determine the fractions in which a specific

compartment was enriched (according to Stitt et al., 1983; Farré et al., 2001, 2008). AGPase and disproportionating-enzyme 1 (DPE1) were indicative of plastidial enrichment, while UDP-glucose pyrophosphorylase (UGPase) and pyrophosphate-dependent phosphofructokinase (PFK) were chosen as cytosolic marker enzymes, and α -mannosidase activity was used as a vacuolar marker. As a first experiment, time variation upon glucose feeding (as isotopic label supplied for fractional carbon enrichment studies) of these enzymes was assessed in total plant extracts (Fig 4.1).

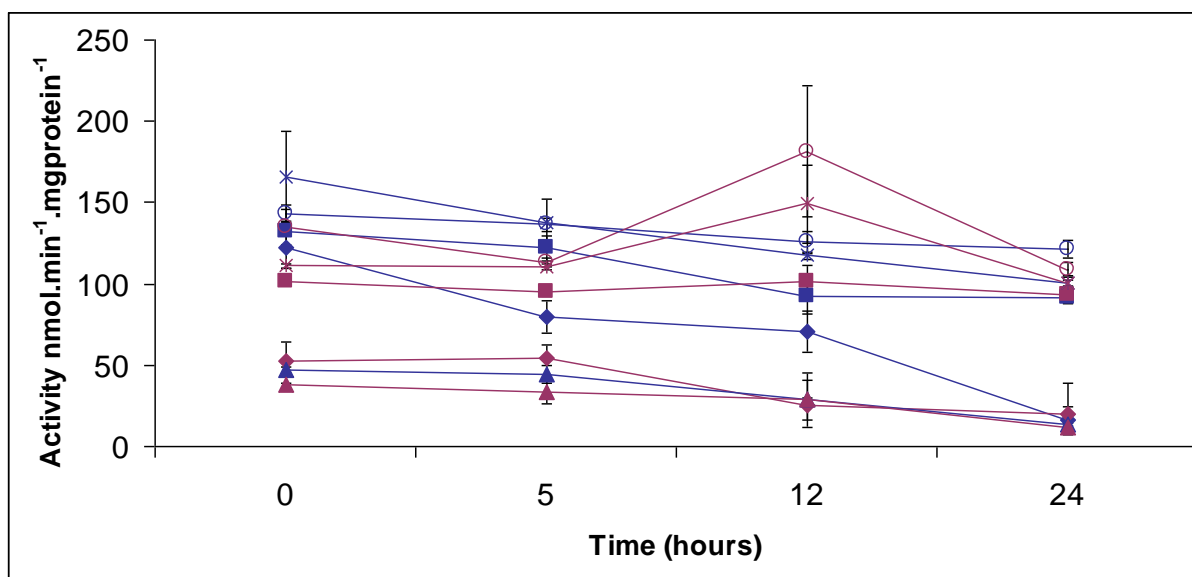


Fig 4.1 Assessment of marker enzyme activity variation in total protein extracts of Col-0 (blue) and *adk1* (purple) mutants in *Arabidopsis* mature rosette leaves at time points T0, T5, T12 and T24 after U-¹³C glucose feeding. Marker enzymes that were chosen as representative of the plastid, cytosol and vacuole are indicated as AGPase (◆) and DPE1 (■), UGPase (▲) and PFP (x), and α -mannosidase (○), respectively. Values are presented as means \pm SE of three individual plants.

Significant diurnal and genotypic variation could be observed in the wild-type and *adk1* mutant. Upon glucose feeding, AGPase and DPE1 activity progressively decreased over time in the wild-type background (Fig 4.1). Although UGPase and α -

mannosidase activity also decreased over time, this was less pronounced. Lastly, PFP activity did not vary over time in the Col-0 background (Fig 4.1). In the *adk1* mutant less diurnal variation in enzyme activity was observed upon glucose feeding, with the only significant decrease observed at T24 for the cytosolic markers (UGPase and PFP) and plastidial DPE1 at T12 (Fig 4.1). Genotypic comparison between wild-type and *adk1* reveal that at T24 all enzyme activities were of comparable value, and chosen as representative time point to assess fractionation efficiency due to the limited number of variables between the two genotypes in question. (For complete list of marker enzyme activities in the fractions of the genotypes at the various time points refer to Supplemental Table 4.1.) As an additional control the respective marker activities for the relevant compartments were also compared to each other (Fig 4.2). In this regard, because the cytosolic markers (PFP or UGPase) are equally distributed over the different fractions, it was decided to use them as a normalization control for plastid and vacuolar enrichment. Plastidial enrichment, as assessed by the relative ratios of AGPase: PFP or UGPase across the different fractions, were comparable between the wild-type and *adk1* mutant (Fig 4.3 a, b). Similar results were obtained for DPE1 (data not shown). However, α -mannosidase: PFP compared to α -mannosidase: UGPase activity were non-linearly correlated in the wild-type (Fig 4.3 c) due to unequal distribution of UGPase activity in the fractions. The reasons for this remain unclear; yet, PFP was chosen as cytosolic marker from this point onward.

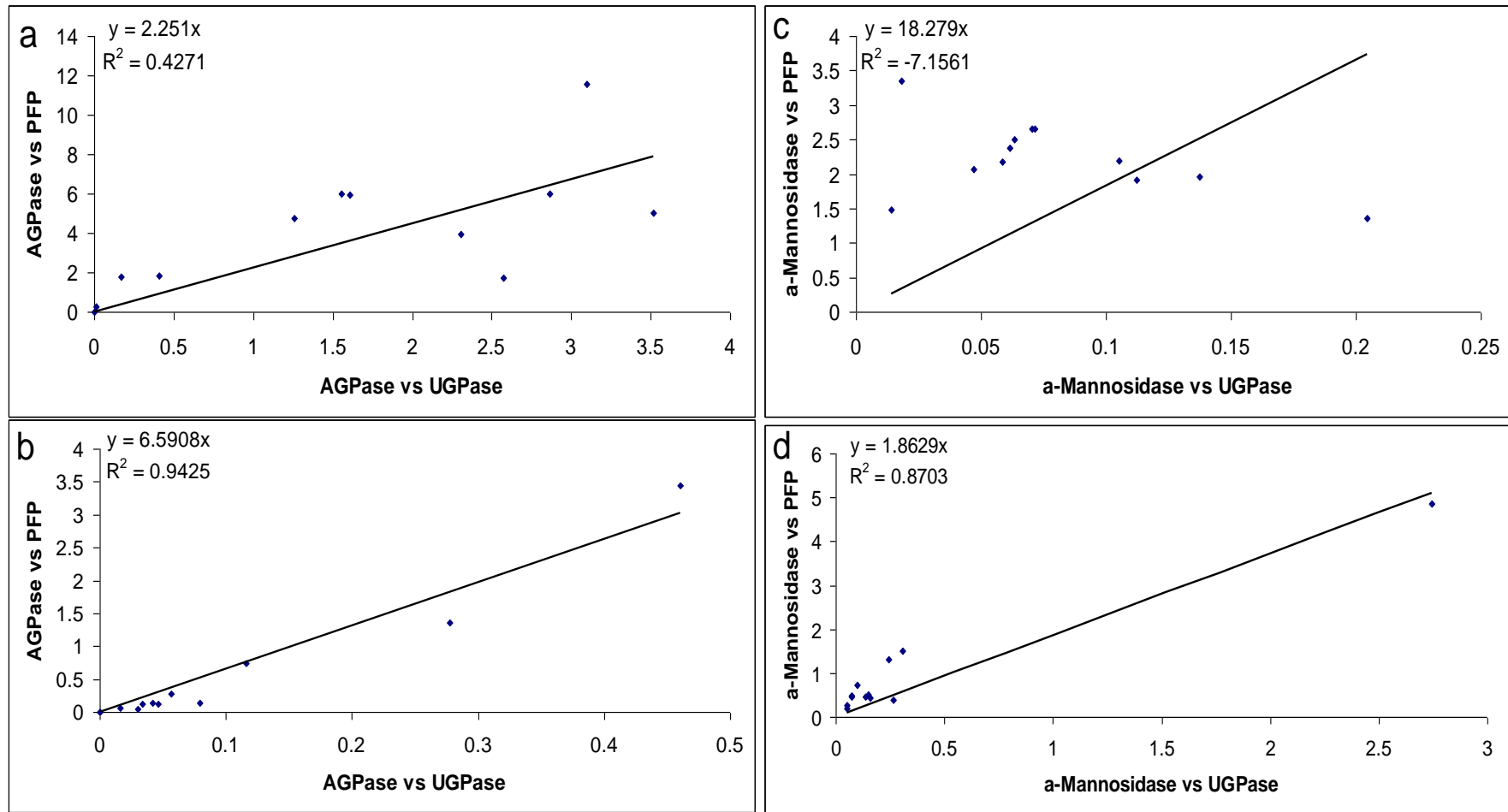


Fig 4.2 Linear correlation analysis of marker enzyme activities of plastidial and vacuolar enriched fractions normalized to the cytosolic control (AGPase:UGPase or PFP, and α -mannosidase:UGPase or PFP) of wild-type (a, c) and *adk1* mutant (b, d) upon and (U)- ^{13}C glucose feeding at T24.

With this in mind, marker enzyme distribution in the Col-0 and *adk1* mutant were assessed and indicated increased activity in fraction six (F6) and fraction two (F2) for the plastidial and vacuolar enrichments, respectively (Fig 4.3 a, b). The exception to this was the marker distribution of α -mannosidase in wild type which indicated less enrichment at this time point (Fig 4.3). However, in light of the pronounced activity of the vacuolar marker at T5 and T12 in the wild type (Supplemental Table 4.1), it was deemed as a reasonable indication of this sub-cellular enrichment. These fractionation distributions are consistent with those previously reported in the literature (Farré et al., 2001), and taken together with the time points T0, T5 and T12 fractions five to seven (F5-7), and fractions two to four (F2-4) was taken as reasonable representative fractions for the plastidial and vacuolar pools.

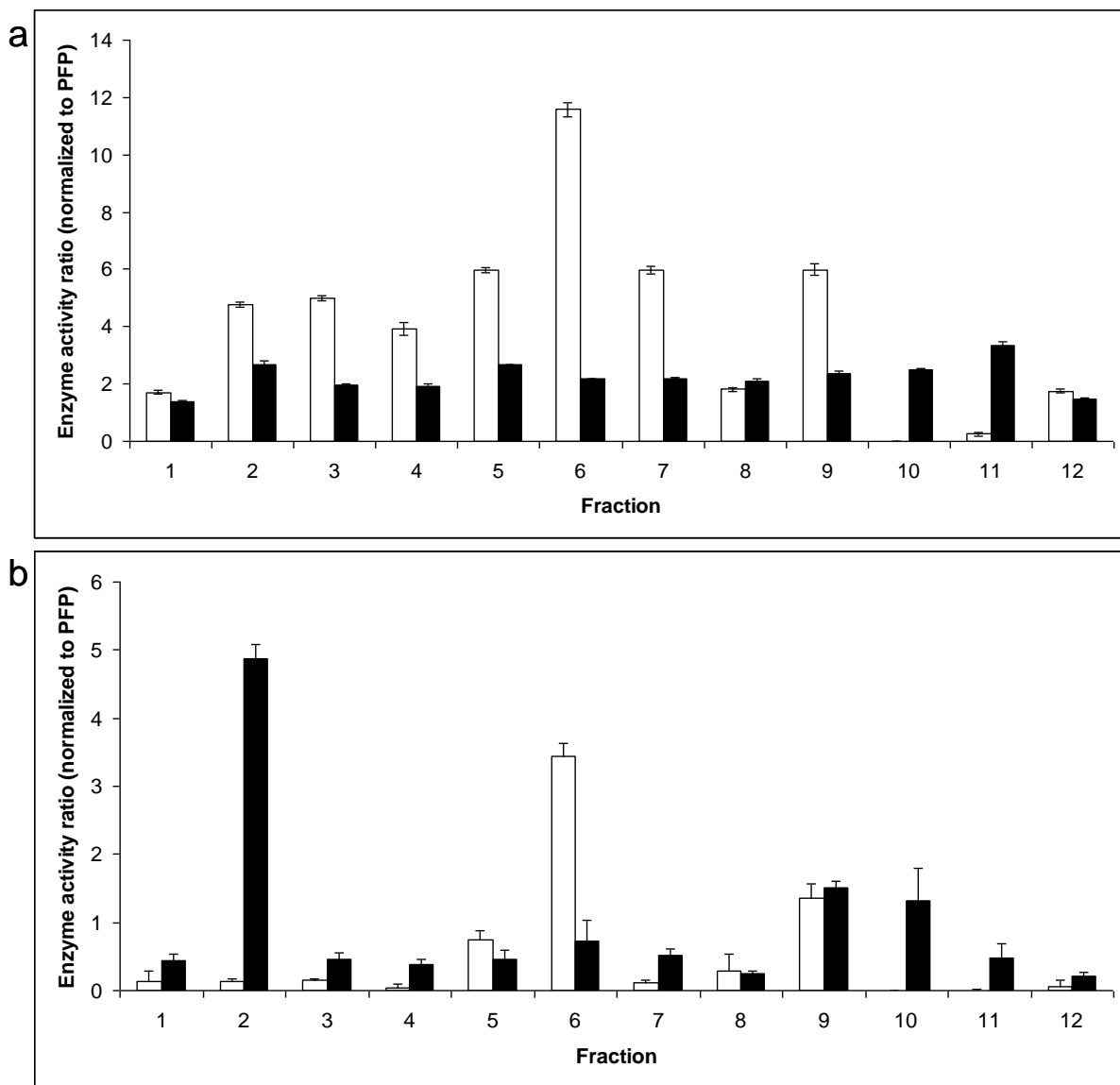
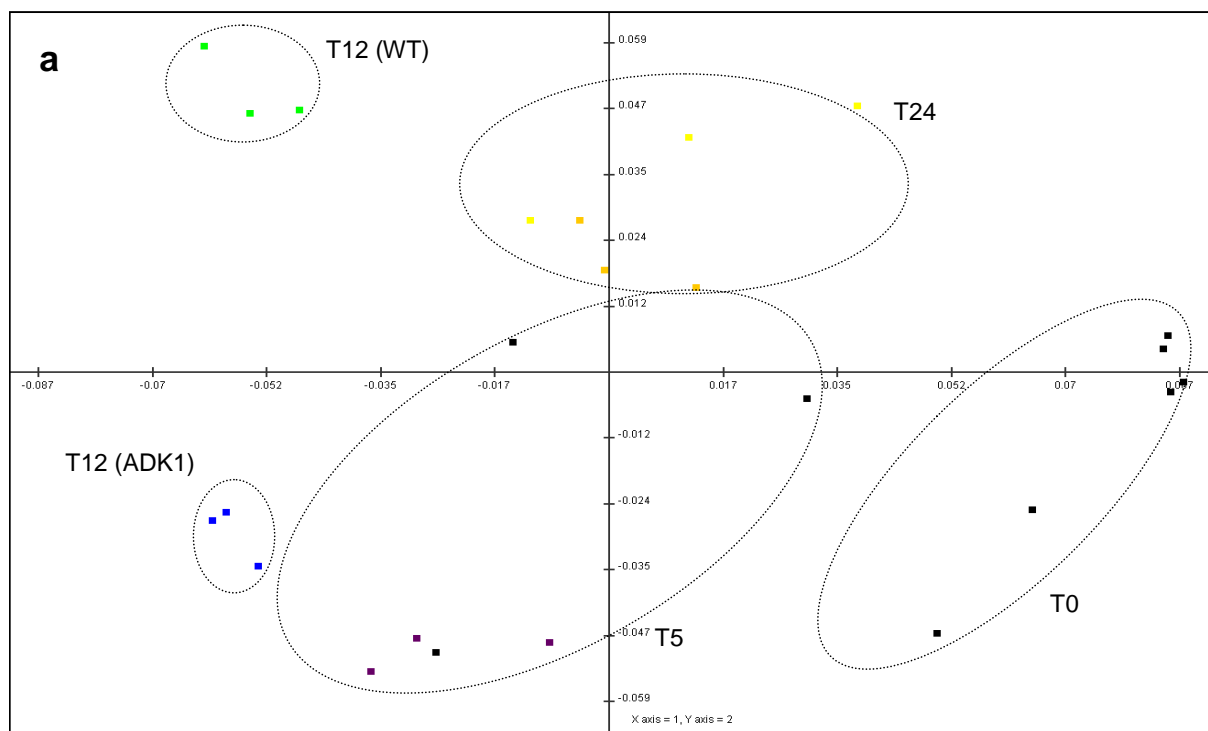


Fig 4.3 Plastidial AGPase (white) and vacuolar α -mannosidase (black) marker enzyme distribution assessed in non aqueous fractions of Col-0 (a) and *adk1* (b) rosette leaf material at T24. Values are presented as means \pm SE of three individual plants, and normalized to the cytosolic PFP marker.

4.2.2 Comparison of metabolite signatures between genotypes and time variation upon glucose feeding

Having assessed marker enzyme fraction enrichments in the plastid and vacuolar compartments, primary metabolites were profiled next *via* GC- and LC-MS technology. Between 31264 and 65135 non-supervised mass spectral tags (MSTs)

(Erban et al., 2007) were extracted from the chromatograms representing the total metabolite pools, and subjected to canonical correlation analysis. This was done to assess whether the feeding and time intervals were adequate to observe clear differences between the genotypes. It indicated that multivariate analyses could clearly distinguish between the different time points T0, T5, T12 and T24 upon glucose feeding (Fig 4.4 a, b). In addition, as time progressed the Col-0 and *adk1* genotypes could also be distinguished at T12 and T24 (Fig 4.4 a, b). In order to assess whether this was due to diurnal variation or glucose feeding, leaf material that was harvested at the four time points, but not subjected to glucose feeding, was also assessed (Fig 4.4 c). This indicated that, as expected, clear differences exist between the diurnal and glucose fed samples (Fig 4.4 c). However, it was still possible to distinguish between the different time points in the glucose fed samples, as well as genotype differences at T12 (Fig 4.4 c). This was not the case for the unlabeled samples (Fig 4.4 c).



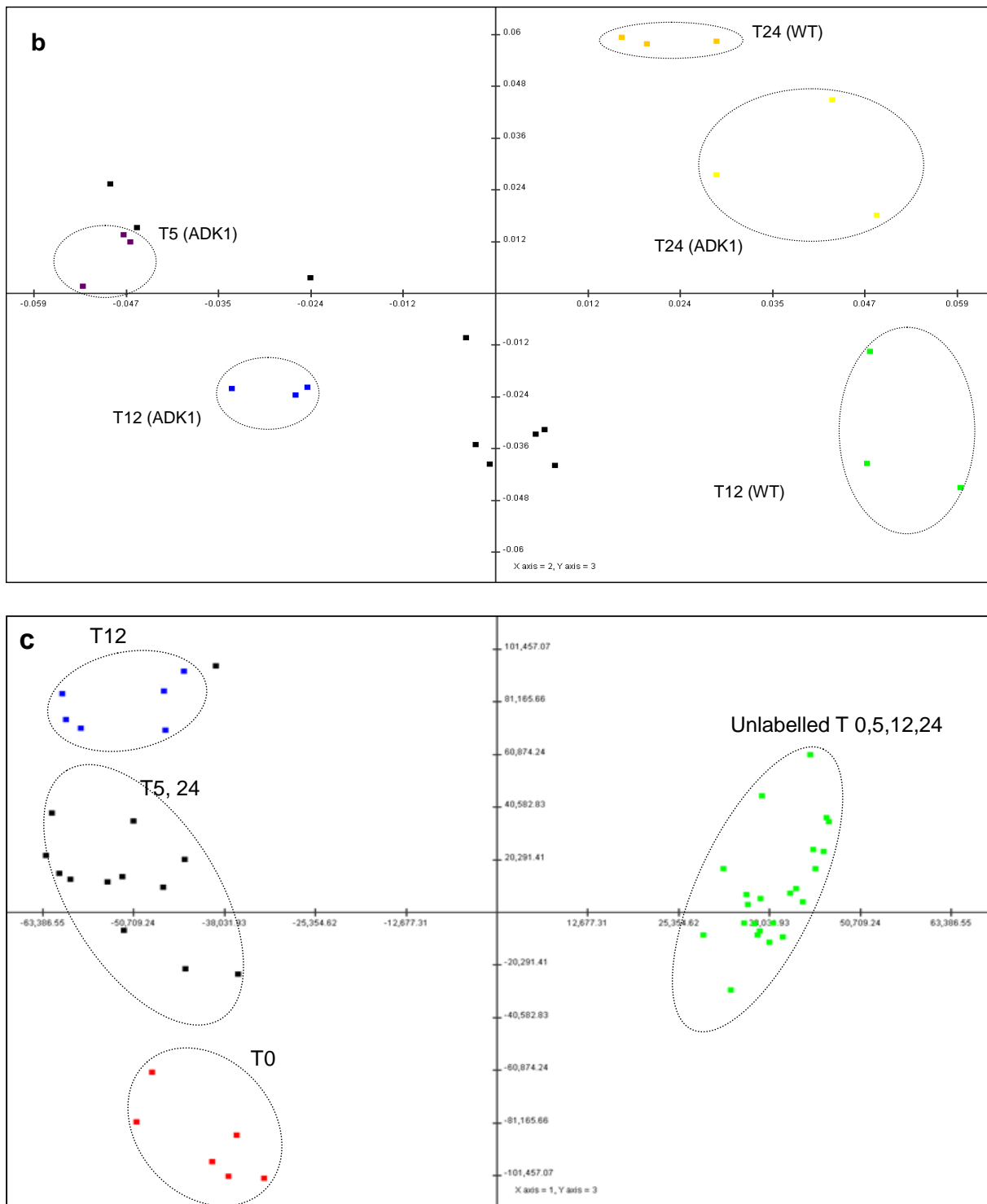


Fig 4.4 Canonical correlation analysis of mass spectral tags (MSTs) extracted from total plant extracts from Col-0 background and *adk1* mutant at four time points (i.e. T0, T5, T12 and T24) upon unlabeled and U-¹³C glucose feeding (a, b) and including diurnal variation at the same time points (c). CCA component scores are PC1 = 14.96% and PC2 = 7.56% (a), and PC2 and PC3 = 6.62% (b); combined with unlabeled metabolites, PC1 = 28.89% and PC 3 = 5.84% (c).

4.2.3 Analysis of primary metabolite levels in total fractionated leaf material

In order to assess more specific effects on primary metabolites, the levels of sugars, amino acids and organic acids as well as phosphorylated and nucleotide intermediates were quantified next (for general biosynthetic scheme of targeted metabolite analyses see Supplemental Fig 4.1). This indicated that the total levels of several key metabolites were significantly altered across all time points between the Col-0 and *adk1* genotypes over the 24h incubation period.

Many noticeable differences between the *adk1* mutant and the wild type at the specific time points were observed with the amino acid levels in the leaf rosettes (Fig 4.5). Methionine, glycine, glutamine, valine, leucine, phenylalanine, lysine and isoleucine were significantly increased at T0 in the mutant (Fig 4.5). After 5 hours of incubation on glucose, significant increases were further observed for tyrosine, and histidine. Curiously, although methionine, tryptophan, asparagine and proline levels also increased in both sets of plants, they did so far more rapidly in the wild type meaning that the mutant accumulated significantly less of these amino acids than the controls upon glucose feeding (Fig 4.5). Cystine, histidine, tyrosine and isoleucine levels were significantly increased after 12 hours of glucose feeding. Consistent with results obtained from plants exposed to continuous light (Carrari et al., 2005) leaf tyrosine, isoleucine, lysine and histidine (which are predominantly synthesized in the plastid) levels were all increased in the *adk1* mutant.

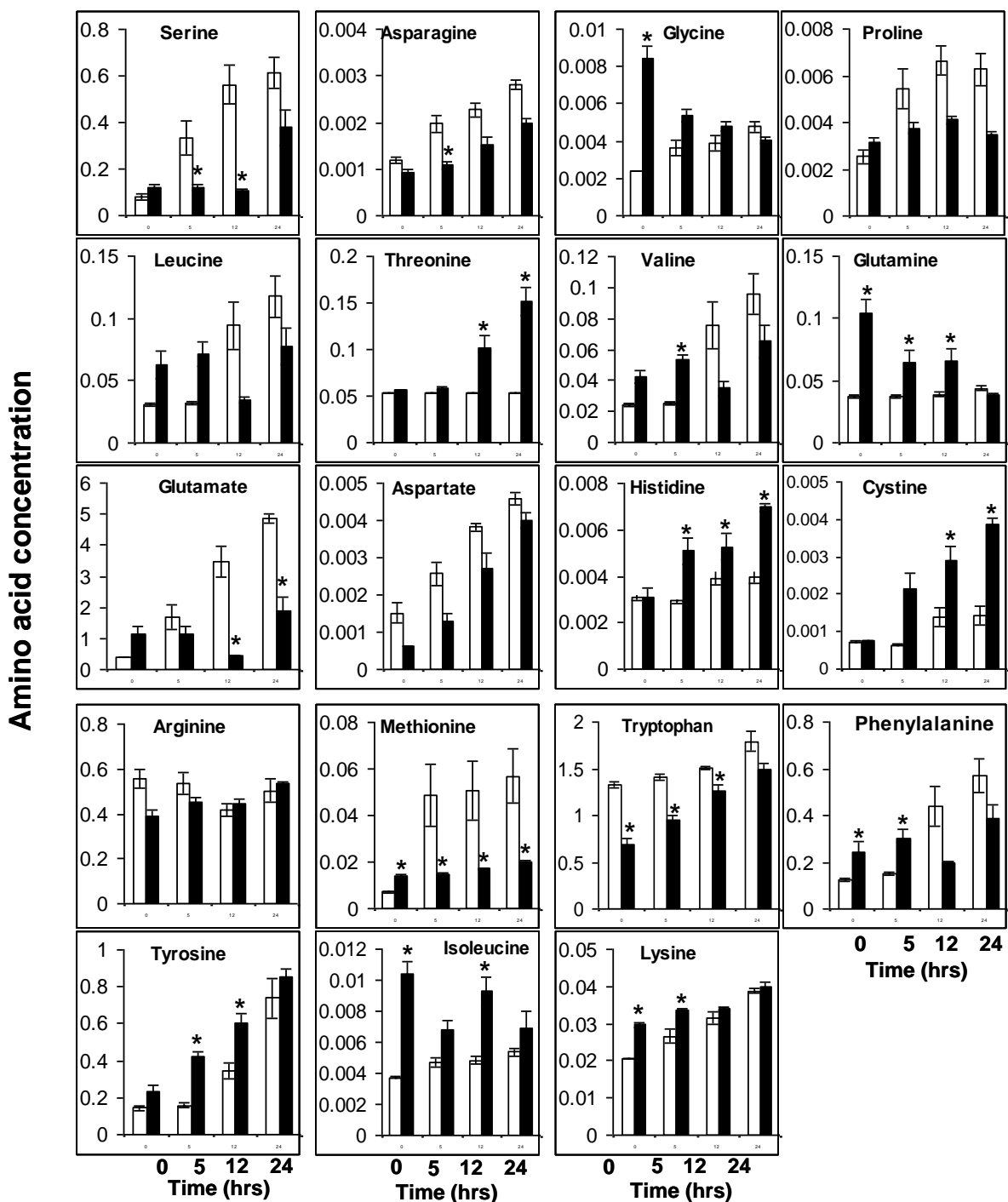


Fig 4.5 Amino acid concentrations (nmol.mm⁻²) in *Col-0* (white) and *adk1* (black) *Arabidopsis* leaf tissue. Leaf discs were incubated on unlabeled (U)-¹³C glucose grown in a 12h photoperiod and samples harvested at T0, T5, T12 and T24 (hours). The first three rows represents amino acids hypothesized to be synthesized in sub-cellular compartments other than the plastid and the last two rows amino acids thought to be synthesized in the plastid. Values are presented as means ± SE of three individual plants and values with an asterisk (*) were determined by

Students *t*-test to be significantly different ($P < 0.05$) from the respective wild-type time point.

In addition, the *adk1* mutant accumulated almost twice as much sucrose as the wild type plants at the onset of the experiment (Fig 4.6); however, the levels were equalized after 24 hours glucose addition. Similarly, starch levels were impaired in the mutant, especially at T12 when the wild type had significantly increased amounts of starch however, after 24 hours of incubation on glucose no difference in starch could be found (Fig 4.6). In addition, maltose concentrations were significantly decreased in the mutant at T12 and T24 (Fig 4.6). Furthermore, the levels of glucose increased throughout the experiment in both genotypes due to the substrate feeding although the levels were significantly lower in the mutant compared to the wild type at T5, T12 and T24 (Fig 4.6). The levels of fructose, in contrast, were comparable at all time points. Other minor sugars also responded to the glucose feeding in a similar response concerning time and genotype dependency of the substrate, including arabinose, mannose and myo-inositol (Fig 4.6).

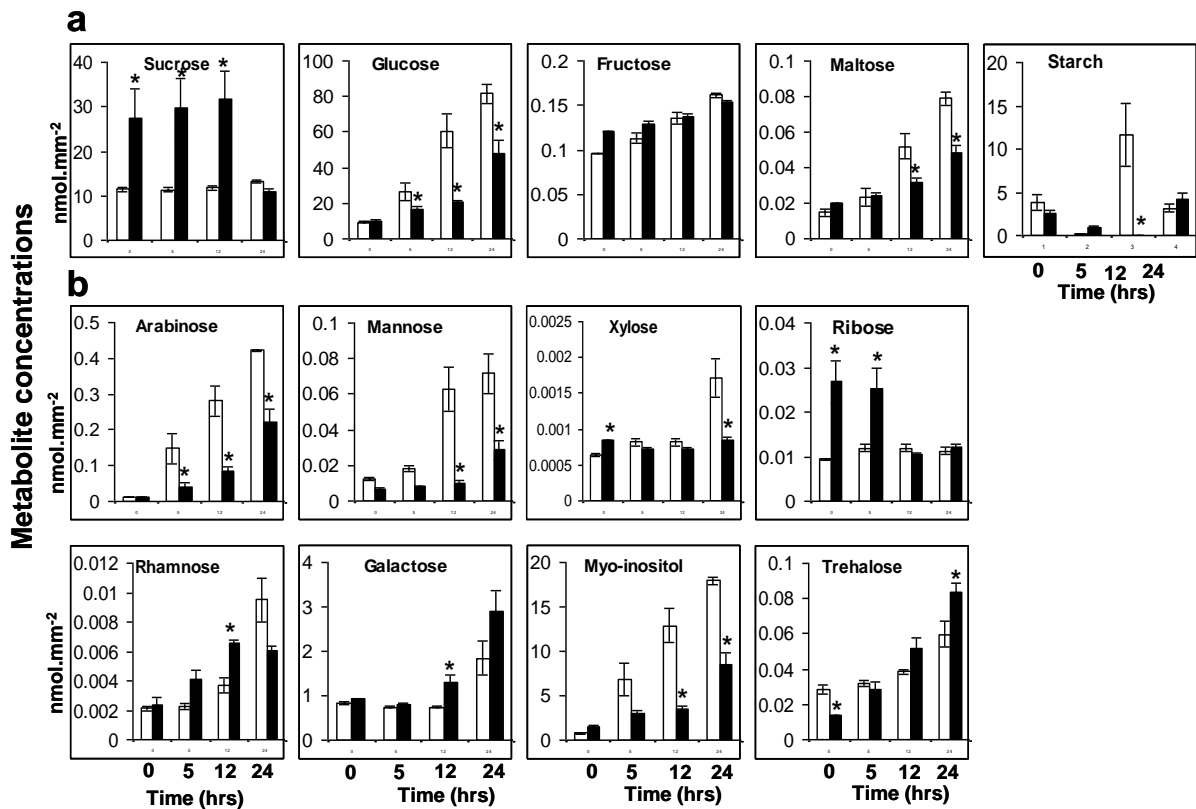


Fig 4.6 Sugar and starch concentrations (nmol.mm⁻²) in Col-0 (white) and *adk1* (black) *Arabidopsis* leaf tissue. Leaf discs were incubated on unlabeled (U)-¹³C glucose grown in a 12h photoperiod and samples harvested at T0, T5, T12 and T24 (hours). The top panel (a) represents major sugars involved in sucrose and starch metabolism and the bottom panel (b) represents minor sugars involved in other metabolic or signaling pathways. Values are presented as means \pm SE of three individual plants and values with an asterisk (*) were determined by Students *t*-test to be significantly different ($P < 0.05$) from the respective wild-type time point.

Analysis of organic acid levels (Fig 4.7) showed that after 12 hours the concentrations of maleate were significantly decreased in the mutant while those of succinate, shikimate, citrate, isocitrate, quinate and ascorbate were significantly increased relative to the respective wild type plant point as the incubation time progressed (Fig 4.7). As a metabolite that has been shown to be a sink of

photosynthate in the leaves (Pracharoenwattana et al., 2010) fumarate levels, as expected, decreased upon glucose feeding (Fig 4.7).

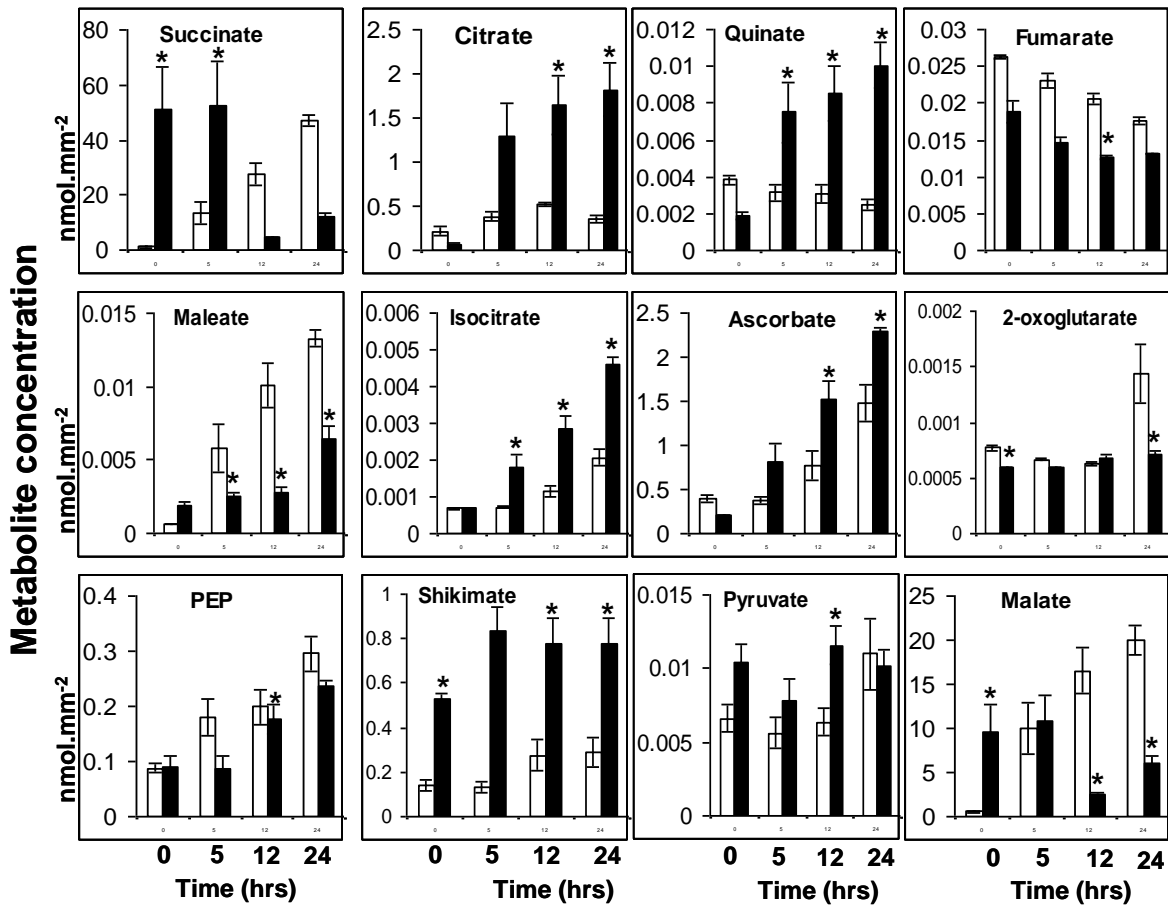


Fig 4.7 Organic acid concentrations (nmol.mm⁻²) in Col-0 (white) and *adk1* (black) *Arabidopsis* leaf tissue. Leaf discs were incubated on unlabeled (U)-¹³C glucose grown in a 12h photoperiod and samples harvested at T0, T5, T12 and T24 (hours). Values are presented as means ± SE of three individual plants and values with an asterisk (*) were determined by Students *t*-test to be significantly different (*P* < 0.05) from the respective wild-type time point.

In contrast to these metabolite alterations upon glucose feeding, very little changes were observed in the total unlabeled plant extracts at T5, T12 and T24 (Table 4.1).

Table 4.1 Primary metabolite levels (nmol.mm⁻²) of physiologically grown *Arabidopsis* Col-0 and *adk1* leaf rosette tissue, in a 12h photoperiod and measured at T0, T5, T12 and T24. Values are presented as means ± SE of three individual plants and values in bold were determined by Students *t*-test to be significantly different (*P*< 0.05) from the respective wild-type time point.

Metabolite	Time (hours)											
	0		5		12		24		0		24	
	Col-0	<i>adk1</i>	Col-0	<i>adk1</i>	Col-0	<i>adk1</i>	Col-0	<i>adk1</i>	Col-0	<i>adk1</i>	Col-0	<i>adk1</i>
asparagine (x10)	0.02 ± 0.01	0.02 ± 0.01	0.02 ± 0.01	0.02 ± 0.01	0.03 ± 0.01	0.02 ± 0.01	0.02 ± 0.00	0.03 ± 0.01	0.02 ± 0.01	0.03 ± 0.01	0.02 ± 0.01	0.03 ± 0.01
leucine	0.40 ± 0.03	0.44 ± 0.03	0.71 ± 0.38	0.45 ± 0.06	0.30 ± 0.01	0.49 ± 0.07	0.36 ± 0.06	0.37 ± 0.06	0.01 ± 0.00	0.04 ± 0.01	0.01 ± 0.00	0.04 ± 0.01
isoleucine (x10)	0.03 ± 0.01	0.05 ± 0.01	0.02 ± 0.01	0.02 ± 0.01	0.02 ± 0.00	0.04 ± 0.01	0.01 ± 0.00	0.04 ± 0.01	0.01 ± 0.00	0.04 ± 0.01	0.01 ± 0.00	0.04 ± 0.01
valine	0.04 ± 0.01	0.05 ± 0.00	0.04 ± 0.01	0.02 ± 0.00	0.05 ± 0.01	0.04 ± 0.00	0.06 ± 0.01	0.03 ± 0.01	0.06 ± 0.01	0.03 ± 0.01	0.06 ± 0.01	0.03 ± 0.01
methionine (x10)	0.21 ± 0.03	0.17 ± 0.03	0.17 ± 0.01	0.15 ± 0.02	0.07 ± 0.01	0.15 ± 0.02	0.13 ± 0.03	0.22 ± 0.01	0.10 ± 0.00	0.20 ± 0.08	0.09 ± 0.01	0.10 ± 0.01
proline (x100)	0.10 ± 0.01	0.11 ± 0.01	0.08 ± 0.03	0.08 ± 0.01	0.10 ± 0.00	0.08 ± 0.01	0.05 ± 0.00	0.08 ± 0.00	0.06 ± 0.01	0.10 ± 0.02	0.06 ± 0.01	0.10 ± 0.02
serine (x10)	0.07 ± 0.01	0.08 ± 0.01	0.09 ± 0.05	0.08 ± 0.01	0.09 ± 0.04	0.07 ± 0.01	0.07 ± 0.01	0.12 ± 0.03	0.06 ± 0.01	0.09 ± 0.01	0.06 ± 0.01	0.09 ± 0.01
threonine (x10)	0.24 ± 0.01	0.30 ± 0.05	0.27 ± 0.03	0.29 ± 0.01	0.19 ± 0.04	0.37 ± 0.08	0.33 ± 0.04	0.27 ± 0.05	0.07 ± 0.01	0.12 ± 0.03	0.06 ± 0.01	0.09 ± 0.01
alanine (x10)	0.05 ± 0.01	0.11 ± 0.02	0.06 ± 0.02	0.08 ± 0.01	0.07 ± 0.01	0.12 ± 0.03	0.06 ± 0.01	0.09 ± 0.01	0.07 ± 0.01	0.12 ± 0.03	0.06 ± 0.01	0.09 ± 0.01
glycine (x100)	0.50 ± 0.09	0.59 ± 0.22	0.06 ± 0.01	0.41 ± 0.05	0.45 ± 0.11	0.44 ± 0.06	0.09 ± 0.01	0.31 ± 0.12	0.50 ± 0.09	0.59 ± 0.22	0.06 ± 0.01	0.41 ± 0.05
trans-4-hydroxy-proline	0.10 ± 0.01	0.12 ± 0.01	0.12 ± 0.02	0.11 ± 0.01	0.07 ± 0.01	0.11 ± 0.02	0.10 ± 0.02	0.11 ± 0.02	0.10 ± 0.01	0.12 ± 0.01	0.10 ± 0.01	0.12 ± 0.01
cysteine	0.22 ± 0.03	0.42 ± 0.11	0.08 ± 0.02	0.16 ± 0.03	0.18 ± 0.03	0.22 ± 0.05	0.16 ± 0.05	0.19 ± 0.05	0.22 ± 0.03	0.42 ± 0.11	0.08 ± 0.02	0.16 ± 0.03
tryptophan (x10)	3.20 ± 0.72	2.93 ± 0.42	1.81 ± 0.70	3.87 ± 1.22	2.64 ± 0.56	4.27 ± 1.41	3.73 ± 0.99	2.85 ± 0.26	3.20 ± 0.72	2.93 ± 0.42	1.81 ± 0.70	3.87 ± 1.22
cystine (x10)	0.60 ± 0.12	0.10 ± 0.02	0.13 ± 0.01	0.14 ± 0.05	0.33 ± 0.10	0.28 ± 0.11	0.30 ± 0.15	0.48 ± 0.15	0.60 ± 0.12	0.10 ± 0.02	0.13 ± 0.01	0.14 ± 0.05
phenylalanine	0.14 ± 0.01	0.19 ± 0.01	0.26 ± 0.10	0.21 ± 0.01	0.21 ± 0.03	0.37 ± 0.09	0.16 ± 0.03	0.29 ± 0.04	0.14 ± 0.01	0.19 ± 0.01	0.26 ± 0.10	0.21 ± 0.01
glutamate	2.75 ± 0.43	3.20 ± 0.44	2.00 ± 0.13	1.72 ± 0.06	0.91 ± 0.08	1.82 ± 0.53	1.62 ± 0.23	2.21 ± 0.31	2.75 ± 0.43	3.20 ± 0.44	2.00 ± 0.13	1.72 ± 0.06
glutamine (x10)	0.19 ± 0.04	0.23 ± 0.04	0.23 ± 0.15	0.25 ± 0.03	0.12 ± 0.01	0.19 ± 0.05	0.18 ± 0.02	0.24 ± 0.04	0.19 ± 0.04	0.23 ± 0.04	0.23 ± 0.15	0.25 ± 0.03
arginine	0.38 ± 0.05	0.66 ± 0.10	0.43 ± 0.23	0.41 ± 0.03	0.22 ± 0.04	0.69 ± 0.19	0.47 ± 0.15	0.68 ± 0.26	0.38 ± 0.05	0.66 ± 0.10	0.43 ± 0.23	0.41 ± 0.03
lysine (x10)	0.65 ± 0.04	1.24 ± 0.10	0.63 ± 0.32	0.61 ± 0.02	0.72 ± 0.16	1.24 ± 0.27	0.71 ± 0.23	1.33 ± 0.30	0.65 ± 0.04	1.24 ± 0.10	0.63 ± 0.32	0.61 ± 0.02
histidine (x100)	0.31 ± 0.07	0.32 ± 0.09	0.60 ± 0.25	0.15 ± 0.04	0.13 ± 0.03	0.59 ± 0.19	0.50 ± 0.08	0.27 ± 0.11	0.31 ± 0.07	0.32 ± 0.09	0.60 ± 0.25	0.15 ± 0.04
tyrosine	0.14 ± 0.01	0.33 ± 0.10	0.23 ± 0.04	0.26 ± 0.03	0.20 ± 0.01	0.38 ± 0.09	0.20 ± 0.05	0.24 ± 0.03	0.14 ± 0.01	0.33 ± 0.10	0.23 ± 0.04	0.26 ± 0.03
aspartate (x100)	0.31 ± 0.05	0.41 ± 0.00	0.51 ± 0.40	0.37 ± 0.04	0.40 ± 0.12	0.42 ± 0.04	0.38 ± 0.10	0.55 ± 0.04	0.31 ± 0.05	0.41 ± 0.00	0.51 ± 0.40	0.37 ± 0.04
succinate	119.66 ± 5.51	117.04 ± 10.39	111.69 ± 30.39	123.84 ± 1.35	91.87 ± 9.31	57.78 ± 21.03	107.89 ± 18.07	126.86 ± 2.07	119.66 ± 5.51	117.04 ± 10.39	111.69 ± 30.39	123.84 ± 1.35
fumarate (x10)	0.18 ± 0.02	0.07 ± 0.02	0.14 ± 0.15	0.15 ± 0.07	0.21 ± 0.07	0.09 ± 0.02	0.12 ± 0.05	0.29 ± 0.04	0.18 ± 0.02	0.07 ± 0.02	0.14 ± 0.15	0.15 ± 0.07
malate	26.48 ± 2.53	32.16 ± 1.15	24.06 ± 1.40	21.09 ± 1.32	17.99 ± 0.35	34.87 ± 8.61	25.63 ± 4.83	39.21 ± 1.00	26.48 ± 2.53	32.16 ± 1.15	24.06 ± 1.40	21.09 ± 1.32
citrate	10.73 ± 1.03	10.85 ± 1.88	4.88 ± 1.09	2.89 ± 0.67	6.89 ± 2.90	8.06 ± 1.91	6.64 ± 1.92	11.64 ± 2.79	10.73 ± 1.03	10.85 ± 1.88	4.88 ± 1.09	2.89 ± 0.67
isocitrate (x100)	0.16 ± 0.01	0.19 ± 0.02	0.19 ± 0.01	0.16 ± 0.01	0.10 ± 0.01	0.35 ± 0.08	0.21 ± 0.04	0.17 ± 0.02	0.16 ± 0.01	0.19 ± 0.02	0.19 ± 0.01	0.16 ± 0.01
2-oxoglutarate (x100)	0.20 ± 0.07	0.15 ± 0.04	0.09 ± 0.03	0.16 ± 0.05	0.10 ± 0.02	0.09 ± 0.01	0.15 ± 0.05	0.10 ± 0.01	0.20 ± 0.07	0.15 ± 0.04	0.09 ± 0.03	0.16 ± 0.05
shikimate	0.59 ± 0.05	0.98 ± 0.24	0.38 ± 0.05	0.57 ± 0.07	0.44 ± 0.13	1.09 ± 0.31	0.48 ± 0.12	0.80 ± 0.22	0.59 ± 0.05	0.98 ± 0.24	0.38 ± 0.05	0.57 ± 0.07
pyroglutamate	0.11 ± 0.05	0.19 ± 0.06	0.06 ± 0.01	0.09 ± 0.01	0.14 ± 0.03	0.06 ± 0.01	0.07 ± 0.01	0.17 ± 0.08	0.11 ± 0.05	0.19 ± 0.06	0.06 ± 0.01	0.09 ± 0.01
quininate (x100)	0.55 ± 0.09	0.72 ± 0.09	0.58 ± 0.43	0.67 ± 0.14	0.59 ± 0.12	0.51 ± 0.02	0.62 ± 0.05	0.56 ± 0.02	0.55 ± 0.09	0.72 ± 0.09	0.58 ± 0.43	0.67 ± 0.14
ascorbate	0.28 ± 0.03	0.55 ± 0.14	0.27 ± 0.09	0.29 ± 0.02	0.22 ± 0.03	0.55 ± 0.11	0.30 ± 0.09	0.48 ± 0.18	0.28 ± 0.03	0.55 ± 0.14	0.27 ± 0.09	0.29 ± 0.02
galacturonic	0.09 ± 0.01	0.17 ± 0.04	0.09 ± 0.04	0.11 ± 0.01	0.08 ± 0.01	0.16 ± 0.03	0.09 ± 0.03	0.15 ± 0.05	0.09 ± 0.01	0.17 ± 0.04	0.09 ± 0.04	0.11 ± 0.01
glucuronic (x100)	0.78 ± 0.12	1.06 ± 0.26	0.59 ± 0.03	0.57 ± 0.13	0.65 ± 0.02	0.77 ± 0.04	0.49 ± 0.05	1.00 ± 0.19	0.78 ± 0.12	1.06 ± 0.26	0.59 ± 0.03	0.57 ± 0.13
pyruvate (x100)	1.00 ± 0.08	1.43 ± 0.12	0.90 ± 0.75	1.02 ± 0.22	1.08 ± 0.11	1.10 ± 0.09	0.82 ± 0.19	1.22 ± 0.30	1.00 ± 0.08	1.43 ± 0.12	0.90 ± 0.75	1.02 ± 0.22
PEP (x100)	1.53 ± 0.40	1.50 ± 0.19	1.30 ± 0.42	1.57 ± 0.24	1.12 ± 0.13	1.56 ± 0.62	1.31 ± 0.32	1.74 ± 0.21	1.53 ± 0.40	1.50 ± 0.19	1.30 ± 0.42	1.57 ± 0.24
glyceraldehyde (x100)	0.27 ± 0.07	0.15 ± 0.06	0.33 ± 0.36	0.38 ± 0.15	0.08 ± 0.01	0.58 ± 0.07	0.16 ± 0.06	0.44 ± 0.02	0.27 ± 0.07	0.15 ± 0.06	0.33 ± 0.36	0.38 ± 0.15
fructose (x10)	0.10 ± 0.01	0.16 ± 0.03	0.05 ± 0.02	0.15 ± 0.02	0.07 ± 0.01	0.10 ± 0.02	0.08 ± 0.01	0.12 ± 0.01	0.10 ± 0.01	0.16 ± 0.03	0.05 ± 0.02	0.15 ± 0.02
glucose	24.50 ± 5.62	23.59 ± 5.32	14.07 ± 5.56	13.04 ± 1.44	8.47 ± 1.03	15.17 ± 3.36	14.00 ± 1.44	19.12 ± 2.87	24.50 ± 5.62	23.59 ± 5.32	14.07 ± 5.56	13.04 ± 1.44
sucrose	10.85 ± 1.29	16.54 ± 3.89	16.61 ± 1.84	17.18 ± 3.83	8.67 ± 2.59	27.52 ± 8.71	21.58 ± 5.03	20.73 ± 1.99	10.85 ± 1.29	16.54 ± 3.89	16.61 ± 1.84	17.18 ± 3.83
trehalose	0.09 ± 0.01	0.17 ± 0.03	0.10 ± 0.04	0.12 ± 0.03	0.04 ± 0.01	0.11 ± 0.04	0.16 ± 0.05	0.14 ± 0.01	0.09 ± 0.01	0.17 ± 0.03	0.10 ± 0.04	0.12 ± 0.03
maltose (x10)	1.10 ± 0.16	1.26 ± 0.14	0.58 ± 0.00	0.39 ± 0.03	0.41 ± 0.03	1.09 ± 0.30	2.16 ± 0.12	1.43 ± 0.16	1.10 ± 0.16	1.26 ± 0.14	0.58 ± 0.00	0.39 ± 0.03
myo-inositol	13.20 ± 1.54	18.03 ± 2.89	11.86 ± 2.62	13.24 ± 0.94	8.37 ± 1.18	18.23 ± 5.61	13.29 ± 3.36	18.32 ± 2.98	13.20 ± 1.54	18.03 ± 2.89	11.86 ± 2.62	13.24 ± 0.94
mannose (x100)	6.00 ± 1.34	7.59 ± 1.05	11.16 ± 1.33	7.12 ± 0.49	4.63 ± 0.36	8.42 ± 2.46	7.72 ± 1.36	8.37 ± 0.12	6.00 ± 1.34	7.59 ± 1.05	11.16 ± 1.33	7.12 ± 0.49
mannitol	1.09 ± 0.34	2.13 ± 1.00	1.19 ± 0.75	5.86 ± 3.33	0.26 ± 0.03	0.66 ± 0.20	0.61 ± 0.08	2.21 ± 1.08	1.09 ± 0.34	2.13 ± 1.00	1.19 ± 0.75	5.86 ± 3.33
galactose	0.38 ± 0.08	0.37 ± 0.09	0.23 ± 0.10	0.20 ± 0.02	0.12 ± 0.01	0.24 ± 0.05	0.21 ± 0.02	0.31 ± 0.05	0.38 ± 0.08	0.37 ± 0.09	0.23 ± 0.10	0.20 ± 0.02
xylose (x10)	0.01 ± 0.00	0.03 ± 0.02	0.03 ± 0.01	0.02 ± 0.01	0.02 ± 0.01	0.03 ± 0.01	0.07 ± 0.02	0.07 ± 0.01	0.01 ± 0.00	0.03 ± 0.02	0.03 ± 0.01	0.02 ± 0.01
arabinose (x10)	0.26 ± 0.04	0.36 ± 0.06	0.49 ± 0.12	0.35 ± 0.02	0.21 ± 0.03	0.55 ± 0.14	0.44 ± 0.06	0.53 ± 0.07	0.26 ± 0.04	0.36 ± 0.06	0.49 ± 0.12	0.35 ± 0.02
ribose (x10)	0.32 ± 0.05	0.40 ± 0.05	0.48 ± 0.10	0.52 ± 0.04	0.31 ± 0.04	0.65 ± 0.16	0.54 ± 0.08	0.44 ± 0.01	0.32 ± 0.05	0.40 ± 0.05	0.48 ± 0.10	0.52 ± 0.04
rhamnose (x100)	0.11 ± 0.01	0.35 ± 0.15	0.33 ± 0.18	0.53 ± 0.11	0.43 ± 0.15	0.32 ± 0.06	0.43 ± 0.02	0.36 ± 0.14	0.11 ± 0.01	0.35 ± 0.15	0.33 ± 0.18	0.53 ± 0.11

In addition, while the majority of the metabolite levels displayed the same trend at T0 (comparing the labeled and unlabeled material), it is interesting to note that certain metabolite trends were highly variable, with trehalose, tryptophan, succinate and glycine levels variable between the independent experiments (Table 4.1, Fig 4. 5, Fig 4.6, Fig 4.7).

4.2.4 ¹³C label incorporation

Whilst prevailing metabolite levels give an indication of the post translational regulation that occurs in metabolism, two alternative parameters were further evaluated in this study that could contribute to a broader understanding of this. The first evaluated the isotopic label enrichment and the second the sub-cellular distribution of metabolites.

The analysis of label incorporation into selected primary metabolites (totals of fractionated material; Fig 4.8) revealed similar levels of ¹³C being incorporated into starch after 5 and 12 hours of incubation of wild type and mutant leaf discs, suggesting that starch biosynthesis was not compromised. Interestingly, the level of label incorporation in the starch breakdown product, maltose, is significantly enhanced in these conditions (Fig 4.8). Concerning sucrose metabolism, ¹³C labeling patterns were reciprocally reversed after 12 and 24 hours with the mutant containing significantly less label at 12 hours (Fig 4.8). Moreover, there was no significant difference in label incorporation in fructose during the course of the experiment (Fig 4.8) while the amount label incorporated into the sugar trehalose which was significantly reduced in the *adk1* mutant (Fig 4.8). Lastly, label incorporation of the branch chain amino acids isoleucine, leucine and valine (significantly increased at the initial time points of the experiment) indicated that, with the exception of

increased label incorporation of isoleucine, in the mutant no significant differences were evident (Fig 4.8).

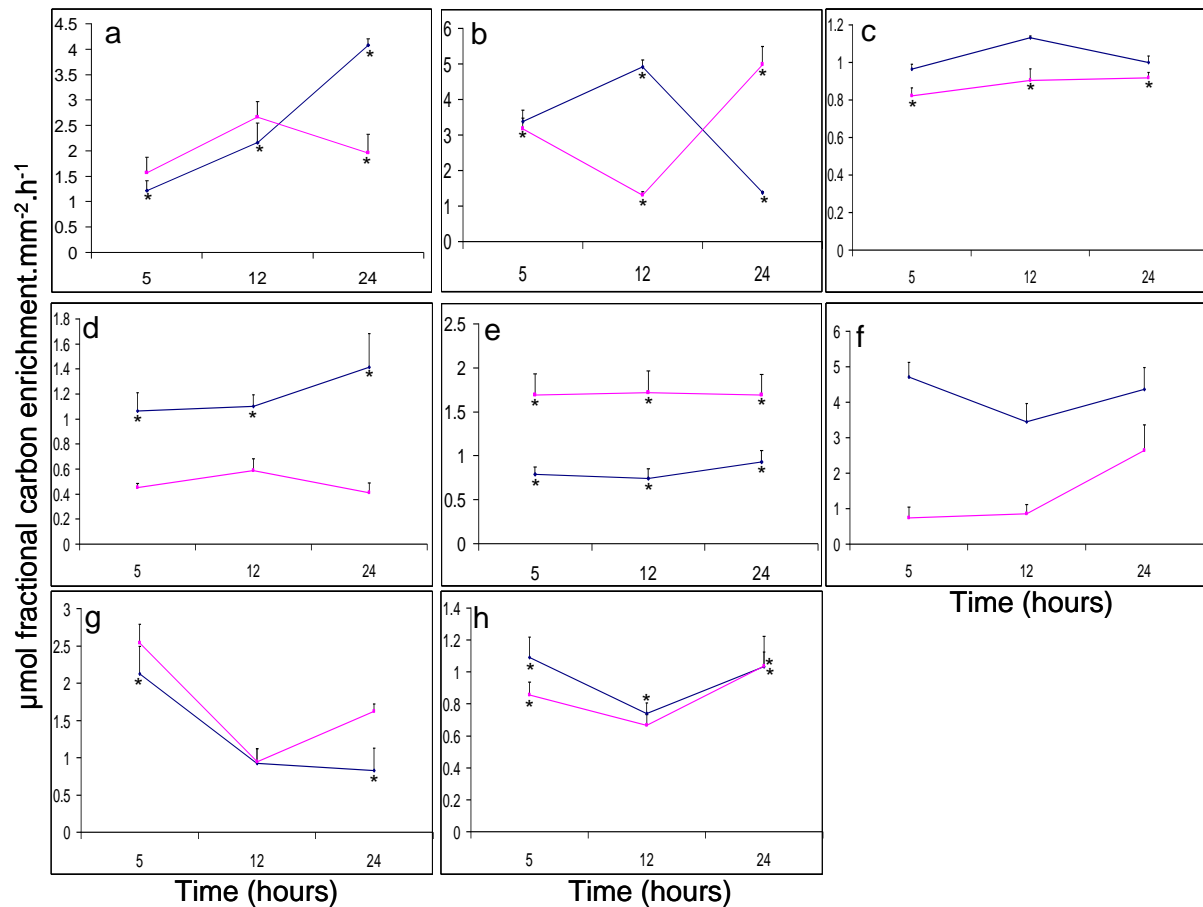


Fig 4.8 Fractional carbon enrichment (FCE) in Col-0 (blue) and *adk1* (purple) genotypes of a) starch, b) sucrose, c) fructose, d) trehalose, e) maltose, f) isoleucine, g) leucine and h) valine. Leaf discs were incubated on unlabeled (U)- ^{13}C glucose grown in a 12h photoperiod and samples harvested at 0, 5, 12 and 24h. FCE is corrected for natural abundant ^{13}C and the difference in label enrichment was calculated as in Roessner-Tunali et al. (2004). Values are presented as means \pm SE of three individual plants and values with an asterisk (*) were determined by Student *t*-test to be significantly different ($P < 0.05$) from the respective wild-type time point.

4.2.5 Sub-cellular metabolite levels and enrichments of primary metabolism in Col-0 and *adk1* rosette leaves

Next the sub-cellular distribution of these metabolites were evaluated and revealed a number of interesting results. Both the wild type and the *adk1* mutant showed valine enrichment in fraction 12 after 5 and 12 hours, while, at the same time points, the same fraction in the *adk1* mutant was further enriched with isoleucine and leucine levels. Glucose was observed to be evenly distributed through all fractions in the *adk1* mutant at all time points except for a slight enrichment in the vacuolar fraction at T12. In wild type plants on the other hand, glucose was observed in the vacuolar fractions (F2-4) at T5, T12 and T24 (Fig 4.9). Sucrose was also evenly distributed through all the fractions at all time points in the *adk1* mutant, while in the wild type enrichment was observed in the vacuolar fractions at T0 and T5 for the wild type. However, at T12 sucrose levels were more enriched in the plastidial fraction (F6-8) of the wild type while at T24 sucrose was distributed between the vacuole and plastid (Fig 4.10). Furthermore, trehalose levels were also enriched in the latter fractions (F9-12, which are possibly mitochondrially enriched due to high levels of mitochondrial metabolites eg. Malate and citrate) of the wild type plant for T0, T5 and T12 and evenly distribution at T24. The *adk1* mutant only showed enrichment of trehalose in the latter fractions at T5 and T12 while at T0 and T24 distribution was even throughout. Similarly, malate and citrate levels were enriched in the earlier fractions (F1-4) in the wild type while at T5 they were enriched in fraction 12 in the *adk1* mutant (Fig 4.11).

Moreover initial analysis of phosphorylated and nucleotide intermediates indicated that, ADP-glc was enriched in the plastidial fractions of wild type and mutant at the onset of the experiment, while GTP levels appear to be evenly distributed throughout fractions 1-10 (Supplemental Fig 4.2). A similar observation was made for NAD levels in the wild type and mutant. In addition, while UMP was detected in all the

fractions of the wild type plant, it was absent in the plastidial fraction of the mutant (Supplemental Fig 4.2). Other noticeable differences in the mutant were the enrichment of UDP and T6P in the plastidial fraction at T0 (Supplemental Fig 4.2). Higher abundant metabolites expected to be present at T0, as well as increases in metabolite concentrations as incubation time progress (at T5, T12 and T24) could not be detected to date, probably owing to their concentrations being too great (more starting material was used due to the fractionation technique employed) and leading to ion suppression in the MS. Analysis of these metabolites at lower concentrations is ongoing. In addition, the analysis of the fractional carbon enrichments (FCEs) (see section 4.2.4) in the fractionated material are underway, and should greatly enhance our understanding of the underlying fluxes involved in primary carbon metabolism.

a. Col-0

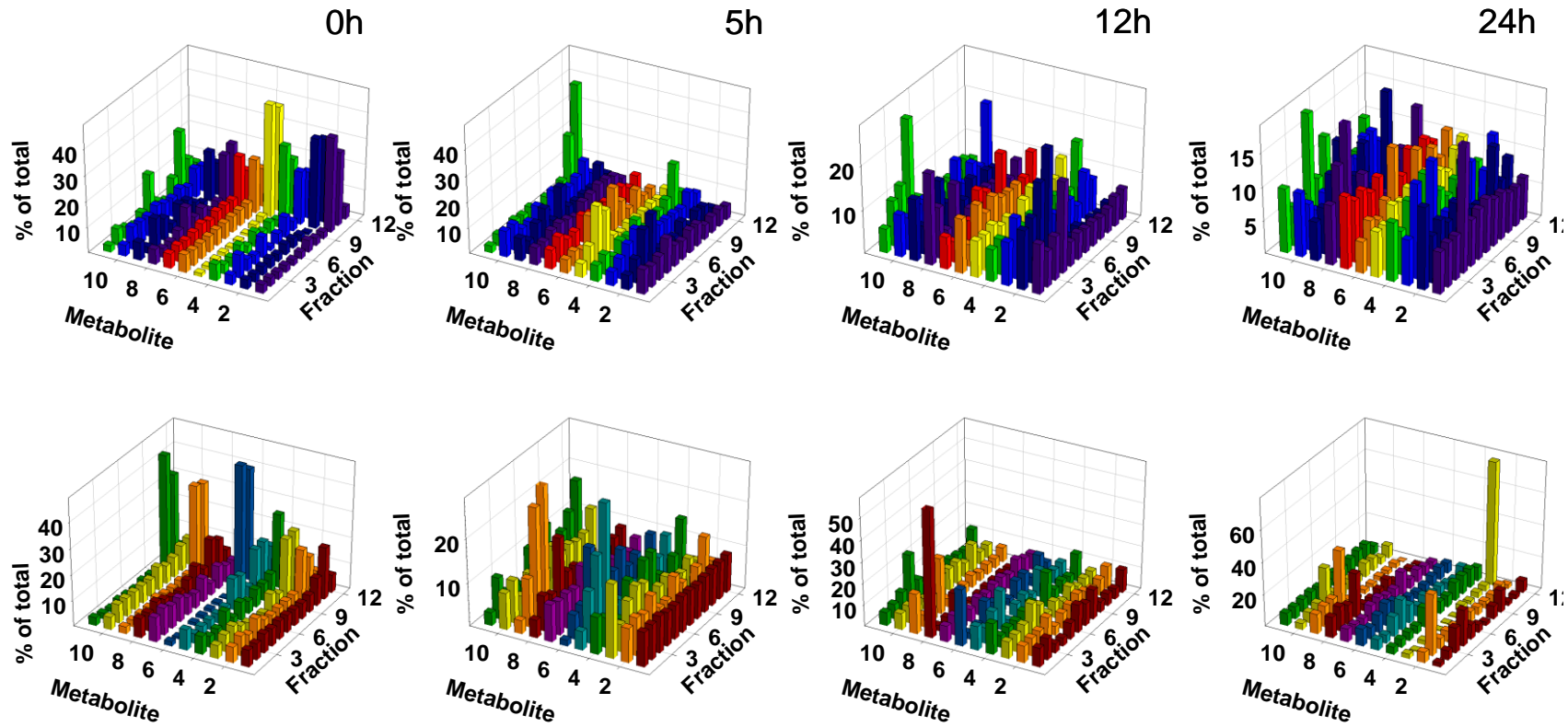


Fig 4.9 Amino acid concentrations (% of total) in Col-0 (a) and *adk1* (b) fractionated *Arabidopsis* leaf tissue. Leaf discs were incubated on unlabeled (U)-¹³C glucose grown in a 12h photoperiod and samples harvested at T0, T5, T12 and T24 (hours). (cont on next page, see key legend below).

b. *adk1*

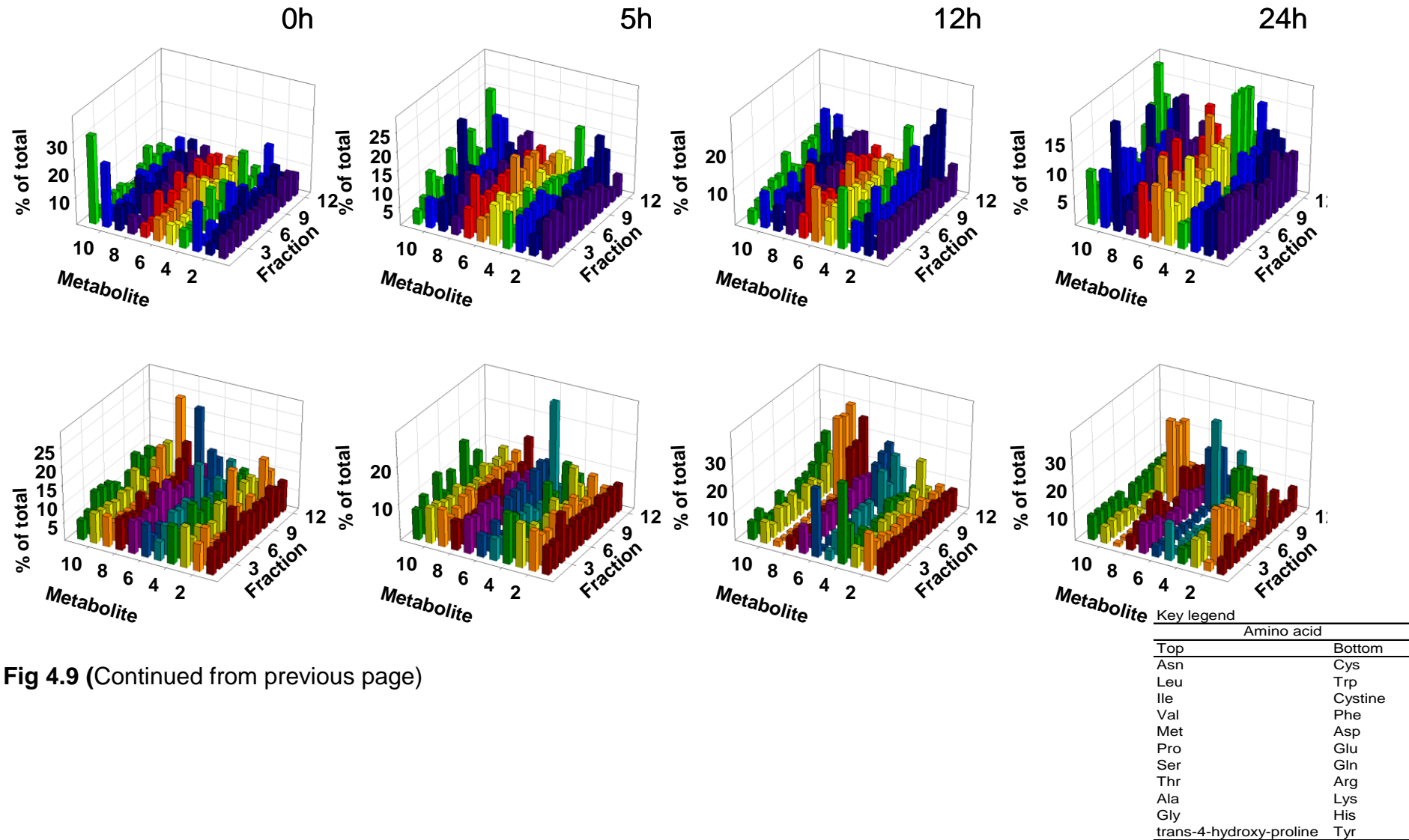
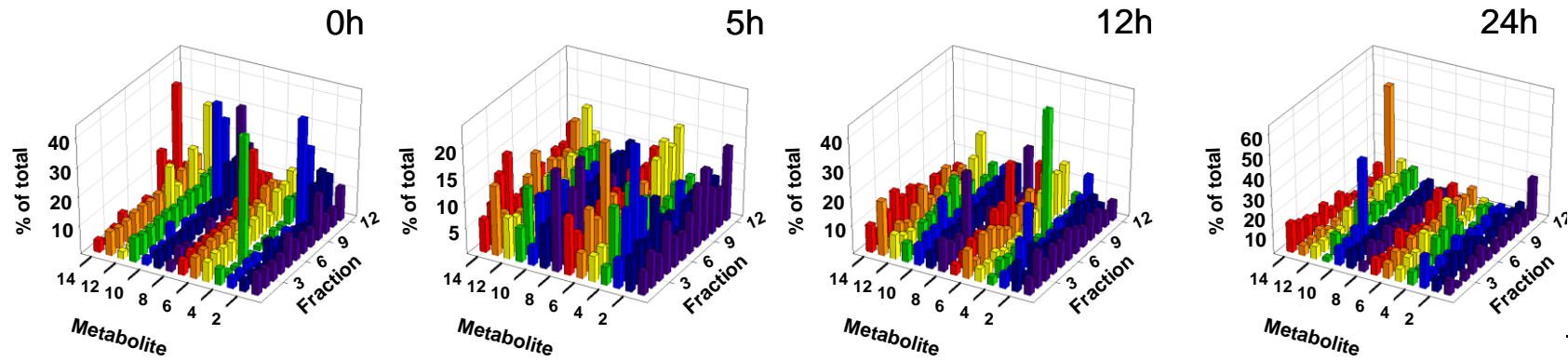
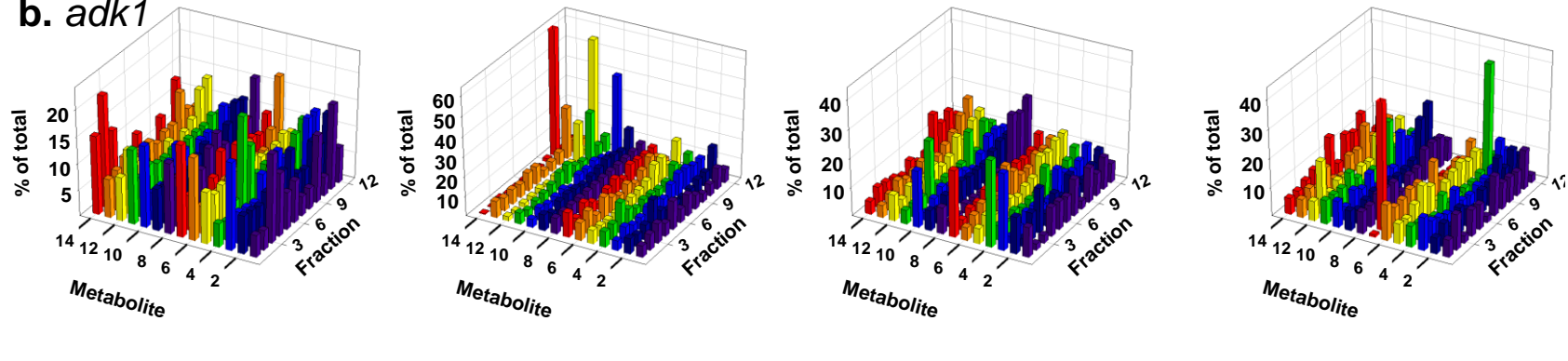


Fig 4.9 (Continued from previous page)

a. Col-0



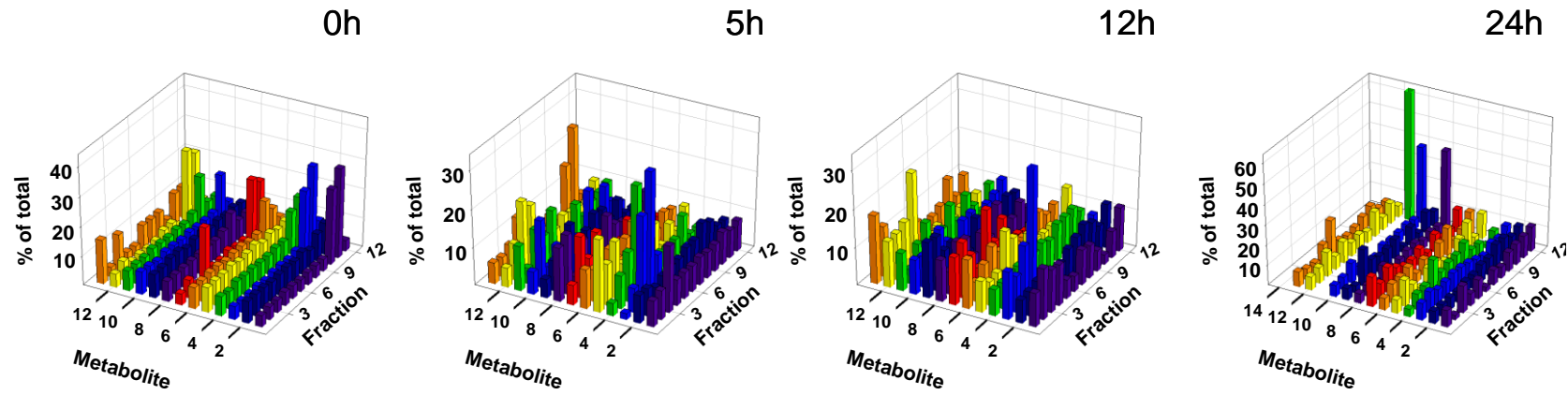
b. *adk1*



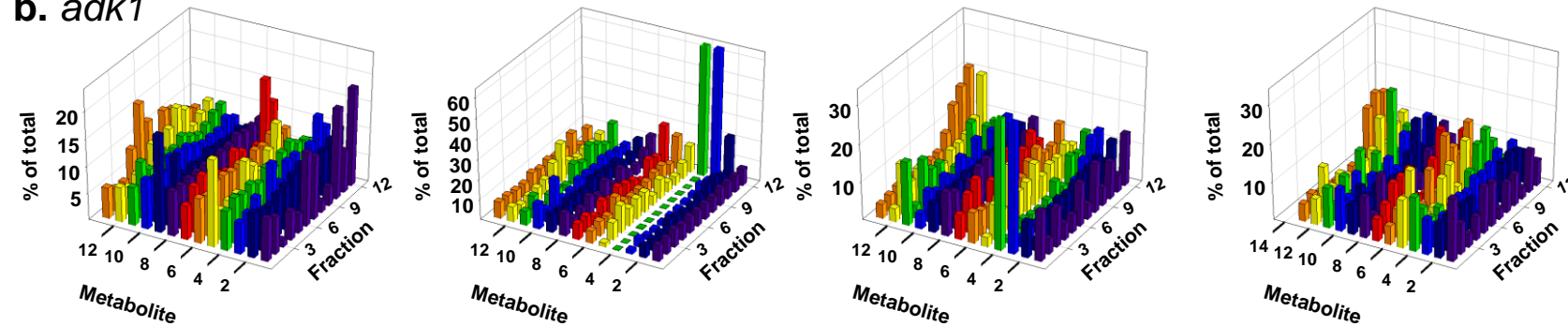
Key legend	
Metabolite	
1	glyceraldehyde
2	fructose
3	glucose
4	sucrose
5	trehalose
6	maltose
7	myo-inositol
8	mannose
9	mannitol
10	galactose
11	xylose
12	arabinose
13	ribose
14	rhamnose

Fig 4.10 Sugar and polyol concentrations (% of total) in Col-0 (a) and *adk1* (b) fractionated *Arabidopsis* leaf tissue. Leaf discs were incubated on unlabeled-¹³C glucose grown in a 12h photoperiod and samples harvested at T0, T5, T12 and T24 (hours). Values are presented as means of 3 individual plants. The metabolite numbers correspond to the metabolite annotation in the key legend (right).

a. Col-0



b. *adk1*



Key legend	
Metabolite	
1	succinate
2	fumarate
3	malate
4	citrate
5	isocitrate
6	2-oxogluterat
7	shikimate
8	pyroglutamate
9	maleate
10	quinate
11	ascorbate
12	pyruvate
13	PEP

Fig 4.11 Organic acid concentrations (% of total) in Col-0 (a) and *adk1* (b) fractionated *Arabidopsis* leaf tissue. Leaf discs were incubated on unlabeled-¹³C glucose grown in a 12h photoperiod and samples harvested at T0, T5, T12 and T24 (hours). Values are presented as means of 3 individual plants. The metabolite numbers correspond to the metabolite annotation in the key legend (right).

4.3 Discussion

Energy metabolism plays an important role in primary carbohydrate metabolism; however the extent of this, and the regulation it infers is poorly understood. One important feature of it is that adenylate homeostasis is a tightly regulated process and it is generally assumed that this is done at the expense of carbon utilization strategies. It would, therefore, be expected that the *adk1* mutant would be perturbed in adenylate homeostasis which would have secondary effects on carbon utilization. The modulators involved in this remain unknown.

Sucrose and starch metabolism

In this study, the *Arabidopsis adk1* mutant were characterized by significant changes in both sucrose and starch levels. Enhanced sucrose levels at T0, T5 and T12 were observed for the *adk1* mutant in the glucose fed material (Fig 4.6). In addition, sucrose levels were also significantly enhanced in unlabeled material at T0 and T12 (Table 4.1). Furthermore, in agreement with previous studies, starch levels were significantly decreased in the *adk1* mutant at the end of the light period (Fig 4.6). Curiously, this limitation is restored at T24 with supply of an additional carbon source (Fig 4.6). Isotopic label incorporation in the starch biosynthetic pathway in the wild type and mutant plant suggests that at T12 both genotypes were incorporating label at a similar rate (Fig 4.8). As time progress (T24), FCE in the wild type is significantly greater in the leaf disc than the mutant which, could either be due to the switch to heterotrophic metabolism in the wild type or, alternatively, the mutant that is utilizing carbon reserves in an energy conserving manner. Caution should however be exercised in the physiological interpretation of the results comparing *adk1* with Col-0 at time points T5, T12 and T24 due to pleiotropic effects related to the glucose treatment. Previously, it has been indicated that *Arabidopsis* leaf epidermal cells

exert little homeostatic control over glucose up-take (Deuschle et al., 2006), and, it was evident from my study that in the time points investigated, no saturation limit in was observed. From the sub-cellular metabolite analyses it is suggested that this glucose is primarily stored in the vacuolar compartment in the wild type plants (Fig 4.10).

In contrast to the wild type plant, the *adk1* mutant shows an equal distribution of sucrose in all the fractions whilst malate and citrate levels are concentrated in later eluting fractions which are presumed to be enriched in mitochondrial metabolites. This suggests that the *adk1* mutant is compensating for its defect in energy constituents by redirecting carbon towards metabolically active pools to generate as much energy and reducing equivalents as possible from existing carbon skeletons to be utilized for respiration. This is further validated in the mutant by the decrease in label incorporation into starch at T12 compared to T5 (Fig 4.8).

Plastidial aspartate amino acid family and its integration in the mitochondrial and cytosolic compartments

One plausible way of carbon liberation would be that of mitochondrial protein turnover during energy deprivation conditions. It was apparent from the metabolite profiling that a diversion in the amino acids synthesized from threonine appeared, with increases observed for the branched chain amino acids (BCAA) of valine, leucine and isoleucine, and a decrease in methionine levels (see Supplemental Fig 4.1 for biosynthetic scheme). The most likely explanation is that carbon flux is directed towards BCAA synthesis, at the cost of methionine anabolism. However, whilst BCAAs and methionine are predominantly synthesized in the plastids (as reviewed in Jander and Joshi, 2009), BCAAs also supply carbon sources for peptide

elongation, glucose and sucrose-linked branched chain esters, glutamate recycling, branched-chain fatty acid synthesis and respiration through synthesis of tricarboxylic acid cycle intermediates (Kandra et al., 1990; Walters et al., 2004; Kroumova et al., 1994; Däschner et al., 1999; Li et al., 2003; Beck et al., 2004; Taylor et al., 2004; Engqvist et al., 2009). In addition, in tomato, sub-cellular localizations of branched chain amino transferase (BCAT) isoforms, the first and last step of BCAA anabolism and catabolism, have been shown to be mitochondrial (*BCAT1* and *2*), plastidial (*BCAT3* and *4*) cytosolic (*BCAT 5*) and vacuolar (*BCAT 6*) localized (Maloney et al., 2010). In this data set, leucine and valine levels were enriched in the later eluting fractions (presently presumed mitochondrial enriched). In addition, both isoleucine and methionine levels are more equally distributed throughout the fractions, suggesting a cytosolic compartmentation. Isotopic label enrichments further suggest that BCAA biosynthesis is not significantly increased between the wild type and mutant (Fig 4.8). Therefore, the most likely explanation is that the occurrence of mitochondrial protein turnover possibly accounts for the elevated levels of these metabolites in the *adk1* mutant., and aid in the elevation of these energy deficient conditions.

Trehalose in mitochondrial fraction

Trehalose metabolism and signaling has gained tremendous popularity in recent years. In the majority of plants, trehalose occurs in trace amounts, yet several putative genes encoding enzymes for trehalose synthesis have been reported (Avonce et al., 2006; Lunn, 2007). In addition, many of these genes are subject to a high level of regulation at the transcriptional (Paul et al., 2008) and posttranslational (Harthill et al., 2006) level, suggesting an important function in metabolism. Moreover, mutants in the trehalose biosynthetic pathway lead to significant

morphological and biochemical changes. For example, *trehalose phosphate synthase 1 (TPS1)* has been shown to be essential for embryo development (Eastmond et al., 2002), normal vegetative growth and the transition to flowering (Van Dijken et al., 2004). The overexpression of TPS from different species, (eg. *otsA* coding for TPS in *E. coli*), results in changes of the use of sugar in seedlings (Schluepmann et al., 2003) and vegetative and photosynthetic phenotypes (Pellny et al., 2004; Almeida et al., 2007; Stiller et al., 2008). Contrasting effects are observed in these phenotypical parameters when plants express the *E. coli otsB* coding for trehalose-6-P phosphatase (TPP) (Schluepmann et al., 2003; Pellny et al., 2004). Trehalose is synthesized in the cytosol from UDPglc and G6P and trehalose 6-phosphate (T6P) formation is catalyzed by TPS and converted to trehalose by TPP. T6P responds to light and sugar signals in relation to the carbon status (Lunn et al., 2006), and therefore a role of T6P in signaling the sugar status of the cytosol to the chloroplast and inducing the activation of starch synthesis has been proposed. In this sub-cellular metabolome approach, trehalose concentrations were equally distributed at T0 and T24, suggesting a cytosolic participation in metabolism at these time points (Fig 4.9). Interestingly, apart from its role in cytosolic and plastidial metabolism, at T5 and T12 trehalose distribution was significantly enriched in fractions 9-12 in both ecotypes (Fig 4.10), suggesting that trehalose might have profound influences on mitochondrial metabolism. Sub-cellular localization and proteomic studies have identified thus far that the *Arabidopsis* trehalose phosphate synthase isoform, *TPS11* is mitochondrial localized (Heazlewood et al., 2004); yet possesses no functional catalytic activity (Vandensteene et al., 2010). Therefore, the physiological significance of mitochondrial trehalose remains unclear. However, preliminary evidence from a yeast *tps* mutant suggests that trehalose metabolism perturbs maximal respiratory activity and cytochrome c content through a hexokinase2/cAMP

dependent mechanism (Noubhani et al., 2009). Furthermore, *TPS 8-11* isoforms contain conserved BTB/POZ domain proteins that interact with cullin3 or bromodomain proteins, facilitating protein degradation or chromatin remodeling (Du and Poovaiah, 2004; Figueroa et al., 2005). One plausible explanation thus is that mitochondrial trehalose is modulating BCAA protein turnover in the mitochondria in the *adk1* mutant through metabolism of leucine and valine to drive alternative respiration processes. In support of this view, antisense constructs of plastidial ADK in potato tubers possess enhanced respiratory rates that were KCN-insensitive (Olivier et al., 2008). However, this hypothesis needs to be tested more vigorously with isolated mitochondria, and physiologically and molecularly assessed for changes, and if so, the potential targets involved in this response.

Plastidial sucrose content

Lastly, in this data set, plastidial enriched fractions containing sucrose have also been observed (Fig 4.10). The sub-cellular compartmentation of sucrose of NAQF plastid fractions have been previously reported in potato and maize (Shannon et al., 1998; Farre et al., 2001) and further substantiated on a molecular level. Fructan polymers utilizing sucrose as substrate have been successfully synthesized when targeted to tobacco and potato plastids (Gerrits et al., 2001). In addition, ectopic expression of a yeast invertase in the potato amyloplast leads to significant alteration in starch structure, and a 80% reduction in sucrose content (Gerrits et al., 2001). Furthermore, a point mutation in a plastidial invertase isoform has been shown to affect carbon and nitrogen balances in *Arabidopsis* seedlings (Tamoi et al., 2010). The physiological role of plastidial sucrose remains, however, unknown to date. Recent evidence suggests that it might form part of a complex signaling cascade involved in plastid-to-nucleus cross-talk (Cottage et al., 2010). Analysis of a plastidial

nucleoid-associated (PPR, pentatricopeptide repeat) protein mutant defective in retrograde signaling, namely *genomes uncoupled1 (gun1)*, shows alteration in sucrose and ABA responsiveness and has decreased anthocyanin content and *LHCB1* transcript accumulation (Cottage et al., 2010). *LHCB* acts as a transcriptional enhancer of retrograde signaling, and addition of external glucose to *Arabidopsis* seedlings reduces *LHCB* expression (Koussevitzky et al., 2007). Upon external sugar supply, it is known that nuclear and plastidial photosynthetic gene expression is significantly reduced (as reviewed in Rolland et al., 2006). In context with the aforementioned perturbation in steady state sucrose levels and subsequent shifts in sub-cellular compartmentation in the Col-0 ecotype compared to the *adk1* mutant, suggests that glucose feeding leads to enhanced plastidial sucrose levels which could be involved in the temporal switch of the wild-type plants to autotrophic metabolism. However, the *adk1* mutant appears to be unresponsive in this regard. Transcript profiling has revealed that *the adk1* mutation is negatively affected in photosynthetic gene expression (Lange et al., 2008); yet whether this is due to defective retrograde signaling or a more indirect effect remains to be demonstrated.

In conclusion, I have demonstrated here that NAQF of *Arabidopsis* rosette leaves leads to the identification of several significant metabolite changes in sub-cellular compartments with respect to both time intervals, as well as between the Col-0 background and *adk1* mutant that was characterized by enhanced sucrose and decreased starch levels. The combination of this and the use of analytical techniques along with isotopic ¹³C labeling has highlighted a number of areas where the further processing of the data obtained and carbohydrate flux analysis will allow for a better understanding for the metabolic changes observed.

4.4 Materials and Methods

4.4.1 Chemicals

All chemicals were obtained from Sigma-Aldrich (www.sigma-aldrich.co.za), with the exception of ascorbate, citrate, fructose, glucose, sucrose and phenylalanine from Merck (www.merck.com), and tartrate and nicotinate that were purchased from Saarchem (South Africa). F2,6BP was chemically synthesized as outlined by Niculescu et al. (1996). In brief, 10mg.ml⁻¹ F1, 6BP was cyclized by adding 50µl of 500mM 1-ethyl-3-(3-dimethylaminopropyl) carbodiimide (EDC) (in 200mM Hepes, pH 7.1) and incubating for 2h at 20°C. The cyclic intermediates was then hydrolyzed by addition of 50µl of 2.75M NaOH, and further incubated for 30min at 37°C. The formed F2,6BP was purified by fractional precipitation with the successive addition of ZnCl₂. F1,6BP was precipitated from the solution by the addition of ZnCl₂ to a final concentration of 2mM, incubation for 90min at room temperature, and the precipitate formed removed by filtration. A second addition of ZnCl₂ to a final concentration of 8mM, incubation for 90min at room temperature and filtration led to chemically pure F2,6BP to be obtained (Van Der Merwe, *unpublished data*).

4.4.2 Plant material and growth conditions

Arabidopsis thaliana (Heynh ecotype Col-0 and homozygous *adk1*) seeds were surface sterilized by washing in 10% (v/v) aqueous sodium hypochlorite for 3min, followed by three washes in sterile dH₂O. The seeds were resuspended in 500µl dH₂O and plated out onto half strength MS solidified with 0.7% (w/v) agar (pH 5.6). The seeds were cold treated for 48h after which they were placed in a growth room under 16h/8h day/night cycle with a photosynthetic photon flux density of 50µmol photons.m⁻².s⁻¹ at 23°C. Once the seedlings has reached the four leaf stage they were transferred to 6cm pots containing coconut husk (www.starkeyayres.co.za)

moistened with 1.5g.l^{-1} hydroponic nutrient mix supplemented with 1.5g.l^{-1} $\text{Ca}(\text{NO}_3)_2$. Plants were subsequently grown in a 12h photoperiod at 23°C . After five weeks, mature rosette leaves were isotopically labeled (see section 4.4.3), rapidly flash frozen in liquid nitrogen and kept at -80°C until sample analyses.

4.4.3 ^{13}C isotopic labeling

Isotopic feeding of Arabidopsis leaf discs was performed as described by Roessner-Tunali et al. (2004). Leaf discs (100mm^2 each) were punched out and washed three times in ice-cold 10mM MES-hydrate (pH 5.6) buffer. The leaf discs were incubated in 10mM MES-hydrate (pH5.6) supplemented with 20mM ^{13}C glucose in a total volume of 5ml in an 100ml Erlenmeyer flask with continuous shaking. The flasks were incubated for 0, 5, 12 and 24h, respectively under a 12/12 hour daylength. At the end of each time period the tissue was washed three times in 10mM MES-hydrate (pH 5.6), rapidly blotted dry and snap frozen in liquid nitrogen.

4.4.4 Non aqueous fractionation

The harvested tissue was homogenized in a tissue-lyzer (Qiagen, www.qiagen.com) by shaking at 30Hz for 30sec while maintaining a frozen temperature. Homogenized tissue was then freeze dried for 48h in a manifold freeze dryer (SP scientific, www.spscientific.com). The sample was resuspended in 20ml heptane/tetrachloroethylene (43:57 v/v) in a 50ml Corning ware tube and sonicated on an ethanol ice bath in three 30sec bursts with 20sec intervals in between at 40% power in a Labotech ultrasonic cleaner, (www.labotech.co.za). The solution was centrifuged at $4000\times g$ for 10min , the supernatant discarded and the pellet resuspended in 3ml heptane/tetrachloroethylene (43:57 v/v) solution. Aliquots of the extracts were taken at this stage for a representation of total protein and metabolite

pools. The remainder of the extract was loaded on a continuous 18ml heptane/tetrachloroethylene density gradient for ultra centrifugal cell fractionation. The gradient was loaded with an automatic Model 160 gradient former with a Tris pump cassette controlled by a Foxy Jr fraction collector (www.isco.com) at a constant flow rate of $1.8\text{ml}\cdot\text{min}^{-1}$, and consisted of a cushion of 100% tetrachloroethylene for 1min, followed by 80% heptane for 2min, 50% heptane for 4min and 5% heptane for 1 min.

The samples were centrifuged for 2.5h at $12000\times g$ in a Beckman ultracentrifuge (USA) at 4°C . Twelve blind fractions of 1.2ml were taken off each sample and divided for protein (200 μl) and metabolite LC-MS and GC-MS (500 μl each) determinations. The fractions were evaporated to dryness under vacuum in an airtight desiccator filled with silica gel and, upon dryness, stored in sealed plastic bags containing silica gel at -20°C .

4.4.5 Protein extraction and enzyme activity measurements

Protein was extracted from the evaporated samples with a protocol modified from (Geigenberger and Stitt, 1993). In brief, 200 μl of extraction buffer (50mM hepes, 5mM MgCl_2 , 1mM EDTA, 5mM DTT, 0.1% Triton and 10% glycerol) was added to the dried sample and sonicated at 40% power in a Labotech ultrasonic cleaner (www.labotech.co.za).

Total protein concentrations were determined by the Bradford protein determination method with bovine serum albumin (BSA) as a standard.

Marker enzyme determinations for each fraction were used to determine sub-cellular enrichment. For this purpose, five marker enzymes were chosen. For vacuolar enrichment α -mannosidase activity was determined according to Stitt et al. (1989). In brief, the hydrolysis of *p*-nitrophenyl- α -*p*-mannosidase to *p*-nitrophenol is determined spectrophotometrically at 405nm. Plastidial and cytosolic fractions were determined by maximal catalytic activity of disproportionating enzyme 1 (DPE1) and AGPase, and UGPase and PFP, respectively. AGPase, UGPase and PFP activity were measured by the sensitive glycerol-3-phosphate cycling assays previously described (Gibon et al., 2004). The activity of DPE1 was assayed by measuring the production of glucose from maltotriose (Takaha et al., 1995).

4.4.6 Primary metabolite profiling

Metabolites were extracted by resuspension in 7.5nM ribitol aqueous solution. The samples were vortexed and sonicated in a sonication bath until complete resuspension of the pellet, before being evaporated to dryness in a vacuum dryer (Genevac EZ-2, www.genevac.com).

The samples were subsequently derivatized in 60 μ l of 15mg.ml⁻¹ methoxyamine-HCl in pyridine. The samples were vortexed and incubated at 50°C for 1h, and 60 μ l of *N*-methyl trimethylsilylfluoroacetamide (MSTFA) and 1% (v/v) trichlormethylchlorosilane (TMCS) was added and the sample further incubated at 50°C for 1h. The samples were then transferred to glass inserts and analyzed by GC-QUAD MS technology.

The GC MS system was composed of an Agilent technologies 6890N network GC system coupled to an Agilent 5975 MS (www.agilent.com), Chromatographic separation was performed on a 10m guard column, 30m Restek column

(www.restek.com) with a 2.5 μ m film thickness. Running conditions were followed as described in Roessner et al. (2001). Helium was used as a carrier gas at a flow rate of 1ml.min⁻¹. The injection temperature was set at 230°C, the interface at 250°C and the ion source at 200°C. The oven temperature was set at 70°C for 5min followed by 5°C.min⁻¹ increase to 310°C with 1 min of heating at 310°C. The system was equilibrated for 6min at 70°C before the injection of the next sample.

Instrument control and data acquisition was performed by the MSD Chemstation software (v 02.00.237, www.agilent.com). Data pre-processing for baseline correction, scaling and alignment was conducted with MetAlign software, with parameters as specified in “Platform for Riken Metabolomics” (<http://prime.psc.riken.jp/lcms/>) (MetAlign v 200410. www.metalign.wur.nl/UK/). For targeted metabolite analyses, authentic standards and calibration curves were constructed, and metabolite identities and annotations were cross-checked with the Golm metabolome database (csbdb.mpimp-golm.mpg.de/csbdb/gmd/gmd).

4.4.7 Phosphorylated and nucleotide profiling

LC-MS metabolite extraction and analysis was conducted as in Chapter 3 (refer to sections 3.2.4 and 3.2.5). In brief, total extracts and fractions were analyzed by reverse phase chromatography carried out on a Waters Aquity Ultra Performance LC coupled to a Micromass Q-TOF Ultima MS. Nucleotide sugars were separated on an octylammonium acetate/acetonitrile gradient and phosphorylated sugars on a tributylamine/methanol gradient. MassLynx V4.0 SP4 (www.micromass.co.uk) was used for instrument control and data acquisition, while for data pre-processing MetAlign v 200410. (www.metalign.wur.nl/UK/) was used for baseline correction, scaling and alignment (De Vos et al., 2007). The data matrix was generated by

conversion of the MassLynx data files (.raw) to the NetCDF format by the DataBridge function of MassLynx 4.0. The parameters for the processing of data were as follows: Maximum amplitude: 10000; Peak slope factor: 1; Peak threshold factor: 1; Average peak width at half weight: 5; Scaling options: no; Maximum shift per scan: 35. Furthermore, peak filtering, peak binning, peak deconvolution and resulting metabolite annotation were manually performed from comparison with the authentic standards processed in parallel with the plant extracts.

4.4.8 ^{13}C enrichment calculations

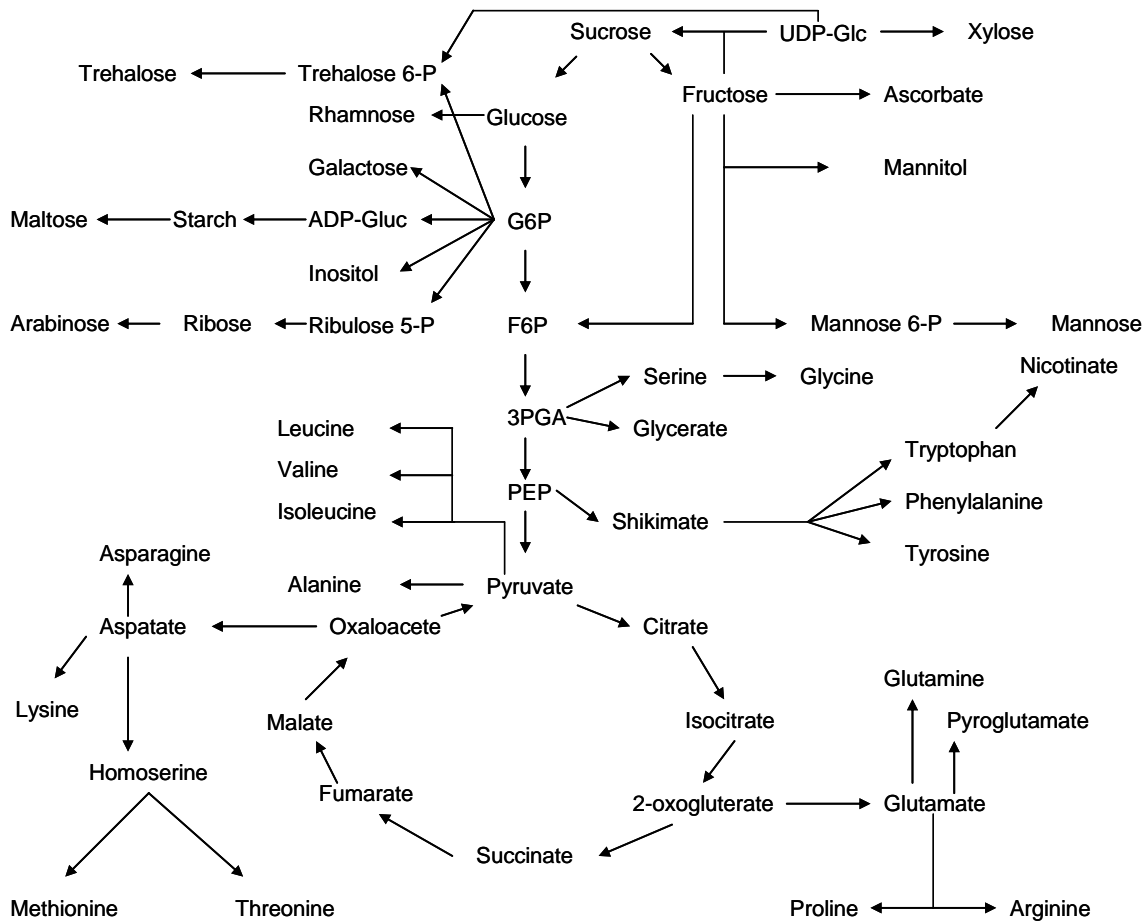
For polar metabolites, ^{13}C labeling patterns were analysed as described previously (Giegé et al., 2003; Roessner-Tunali et al., 2004). Fractional enrichment of metabolites was calculated by directly comparing replicate samples incubated in unlabeled ^{13}C glucose with those incubated in glucose of natural abundance as previously described by Roessner-Tunali et al. (2004).

4.4.9 Starch measurements and ^{13}C glucose incorporation

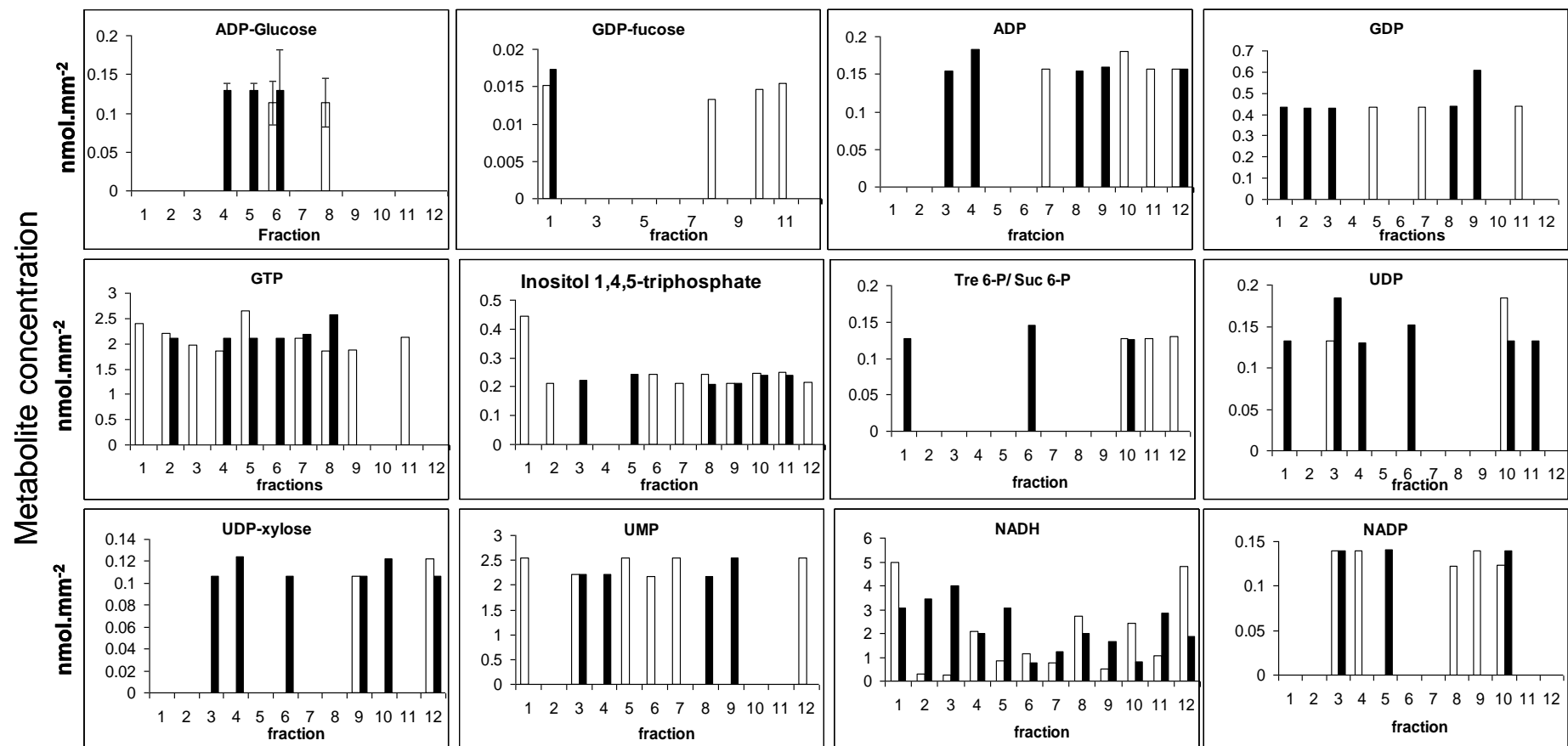
Leaf discs were labeled with unlabeled- ^{13}C glucose as described in 4.4.3. Leaf discs were then snap frozen in liquid nitrogen and homogenized in a tissue-lyzer (Qiagen, www.qiagen.com) by shaking at 30Hz for 30sec. Starch was then extracted from the homogenate as described in (Kempa et al., 2007) with 300 μl of pre-cooled methanol. Ribitol (7nM) was added as an internal standard, 300 μl of chloroform was then added and the mix was centrifuged. The pellet was washed twice with ethanol and incubated with 460 μl 0.2M KOH at 85°C for 1h, and the pH was adjusted with 140 μl 1M acetic acid. The supernatant was incubated with 1U of amyloglucosidase (www.sigmaaldrich.com) for 3hrs and free glucose was quantified by GC-MS.

4.4.10 Statistical analyses

Unless otherwise specified, statistical analyses were performed using the *t*-test embedded in the Microsoft Excel software (Microsoft, Seattle). Only the return of a *P* value < 0.05 was designated significant. Canonical correlation analyses were performed in the TMEV program (Saeed et al., 2003).



Supplemental Fig 4. General biosynthetic scheme of metabolites selected for the targeted metabolome analyses.



Supplemental Fig 4.2 Fractionation of nucleotide and phosphorylated sugars at T0, Col-0 (white) and *adk1* (black) *Arabidopsis* leaf tissue. Leaf discs were incubated on U-¹³C glucose with a 12h photoperiod. Values are presented as means ± SE of three individual plants.

Table 4.4 supplemental table, complete list of marker enzyme activities over 4 time points (0, 5, 12 and 24 hours). Values are presented as means \pm SE of three individual plants and values with an asterisk (*) were determined by Students *t*-test to be significantly different ($P < 0.05$) from the respective wild-type time point.

Marker Enzyme		Fraction																											
		1	2	3	4	5	6	7	8	9	10	11	12	1	2	3	4	5	6	7	8	9	10	11	12				
AGPase	T0	Col-0	0.09 \pm 0.03	0.06 \pm 0.01	0.08 \pm 0.02	0.08 \pm 0.01	0.07 \pm 0.00	0.06 \pm 0.02	0.05 \pm 0.00	0.05 \pm 0.01	0.07 \pm 0.01	0.07 \pm 0.01	0.06 \pm 0.01	0.05 \pm 0.01	0.05 \pm 0.01	0.05 \pm 0.01	0.05 \pm 0.01	0.05 \pm 0.01	0.05 \pm 0.01	0.05 \pm 0.01	0.05 \pm 0.01	0.05 \pm 0.01	0.05 \pm 0.01	0.05 \pm 0.01	0.05 \pm 0.01	0.05 \pm 0.01			
		<i>adk1</i>	0.05 \pm 0.00	0.05 \pm 0.01	0.06 \pm 0.00	0.06 \pm 0.01	0.05 \pm 0.00	0.06 \pm 0.01	0.05 \pm 0.00	0.06 \pm 0.01	0.05 \pm 0.01	0.06 \pm 0.01	0.06 \pm 0.01	0.05 \pm 0.01	0.05 \pm 0.01	0.05 \pm 0.01	0.05 \pm 0.01	0.05 \pm 0.01	0.05 \pm 0.01	0.05 \pm 0.01	0.05 \pm 0.01	0.05 \pm 0.01	0.05 \pm 0.01	0.05 \pm 0.01	0.05 \pm 0.01	0.05 \pm 0.01	0.05 \pm 0.01		
		T5	Col-0	0.23 \pm 0.23	0.36 \pm 0.36	0.91 \pm 0.91	0.04 \pm 0.24	1.47 \pm 0.86	4.61 \pm 3.09	5.74 \pm 1.77	3.27 \pm 3.27	0.00 \pm 0.00	-0.02 \pm 0.02	0.00 \pm 0.00	0.73 \pm 0.73	0.23 \pm 0.23	0.36 \pm 0.36	0.91 \pm 0.91	0.04 \pm 0.24	1.47 \pm 0.86	4.61 \pm 3.09	5.74 \pm 1.77	3.27 \pm 3.27	0.00 \pm 0.00	1.96 \pm 1.99	2.14 \pm 2.14	0.00 \pm 0.00		
		<i>adk1</i>	0.23 \pm 0.23	0.36 \pm 0.36	0.91 \pm 0.91	0.04 \pm 0.24	1.47 \pm 0.86	4.61 \pm 3.09	5.74 \pm 1.77	3.27 \pm 3.27	0.00 \pm 0.00	1.96 \pm 1.99	2.14 \pm 2.14	0.00 \pm 0.00	0.07 \pm 0.04	0.24 \pm 0.06	0.11 \pm 0.03	0.09 \pm 0.06	0.06 \pm 0.03	0.28 \pm 0.08	0.17 \pm 0.09	0.08 \pm 0.07	0.18 \pm 0.06	0.26 \pm 0.16	0.39 \pm 0.11	0.10 \pm 0.07	0.03 \pm 0.02		
		T12	Col-0	0.07 \pm 0.04	0.24 \pm 0.06	0.11 \pm 0.03	0.09 \pm 0.06	0.06 \pm 0.03	0.06 \pm 0.03	0.28 \pm 0.08	0.17 \pm 0.09	0.08 \pm 0.07	0.18 \pm 0.06	0.26 \pm 0.16	0.39 \pm 0.11	0.10 \pm 0.07	0.03 \pm 0.02	0.28 \pm 0.02	0.21 \pm 0.12	0.20 \pm 0.08	0.14 \pm 0.09	0.27 \pm 0.09	0.19 \pm 0.10	0.02 \pm 0.01	0.13 \pm 0.09	0.26 \pm 0.16	0.51 \pm 0.06	0.11 \pm 0.08	
		<i>adk1</i>	0.03 \pm 0.02	0.28 \pm 0.02	0.21 \pm 0.12	0.20 \pm 0.08	0.14 \pm 0.09	0.27 \pm 0.09	0.19 \pm 0.10	0.02 \pm 0.01	0.13 \pm 0.09	0.26 \pm 0.16	0.51 \pm 0.06	0.11 \pm 0.08	0.37 \pm 0.07	0.40 \pm 0.14	0.31 \pm 0.13	0.22 \pm 0.03	0.18 \pm 0.03	0.13 \pm 0.11	0.13 \pm 0.07	0.07 \pm 0.04	0.16 \pm 0.08	0.00 \pm 0.00	0.02 \pm 0.01	0.14 \pm 0.07	0.14 \pm 0.07		
		T24	Col-0	0.37 \pm 0.07	0.40 \pm 0.14	0.31 \pm 0.13	0.22 \pm 0.03	0.18 \pm 0.03	0.13 \pm 0.11	0.13 \pm 0.07	0.07 \pm 0.04	0.16 \pm 0.08	0.00 \pm 0.00	0.02 \pm 0.01	0.14 \pm 0.07	0.32 \pm 0.05	0.23 \pm 0.05	0.17 \pm 0.05	0.23 \pm 0.04	0.16 \pm 0.09	0.12 \pm 0.07	0.12 \pm 0.09	0.22 \pm 0.13	0.00 \pm 0.00	0.01 \pm 0.01	0.12 \pm 0.06	1.29 \pm 0.68	1.34 \pm 0.10	
		<i>adk1</i>	0.32 \pm 0.05	0.23 \pm 0.05	0.18 \pm 0.04	0.17 \pm 0.05	0.23 \pm 0.04	0.16 \pm 0.09	0.12 \pm 0.07	0.12 \pm 0.09	0.22 \pm 0.13	0.00 \pm 0.00	0.01 \pm 0.01	0.12 \pm 0.06	1.29 \pm 0.68	1.34 \pm 0.10	1.47 \pm 0.15	1.20 \pm 0.09	1.36 \pm 0.06	1.45 \pm 0.06	1.12 \pm 0.14	1.33 \pm 0.06	1.32 \pm 0.10	1.36 \pm 0.11	1.48 \pm 0.21	1.37 \pm 0.36	0.91 \pm 0.47	1.23 \pm 0.13	
		T0	Col-0	1.29 \pm 0.68	1.34 \pm 0.10	1.47 \pm 0.15	1.20 \pm 0.09	1.36 \pm 0.06	1.45 \pm 0.06	1.12 \pm 0.14	1.33 \pm 0.06	1.32 \pm 0.10	1.36 \pm 0.11	1.48 \pm 0.21	1.37 \pm 0.36	2.59 \pm 0.29	2.18 \pm 0.40	1.82 \pm 0.32	1.54 \pm 0.25	1.53 \pm 0.25	1.37 \pm 0.20	1.29 \pm 0.19	1.48 \pm 0.12	1.55 \pm 0.30	1.45 \pm 0.06	1.29 \pm 0.15	2.38 \pm 0.39	2.23 \pm 0.13	1.87 \pm 0.44
		<i>adk1</i>	0.91 \pm 0.47	1.23 \pm 0.13	1.36 \pm 0.23	1.13 \pm 0.03	1.31 \pm 0.09	1.33 \pm 0.07	1.15 \pm 0.11	1.26 \pm 0.09	1.24 \pm 0.06	1.18 \pm 0.08	1.27 \pm 0.02	1.19 \pm 0.25	2.59 \pm 0.29	2.18 \pm 0.40	1.82 \pm 0.32	1.54 \pm 0.25	1.53 \pm 0.25	1.37 \pm 0.20	1.29 \pm 0.19	1.48 \pm 0.12	1.55 \pm 0.30	1.45 \pm 0.06	1.29 \pm 0.15	2.38 \pm 0.39	2.23 \pm 0.13	1.87 \pm 0.44	
		T5	Col-0	2.59 \pm 0.29	2.18 \pm 0.40	1.82 \pm 0.32	1.54 \pm 0.25	1.53 \pm 0.25	1.37 \pm 0.20	1.29 \pm 0.19	1.48 \pm 0.12	1.55 \pm 0.30	1.45 \pm 0.06	1.29 \pm 0.15	2.38 \pm 0.39	2.23 \pm 0.13	1.87 \pm 0.44	1.64 \pm 0.27	1.54 \pm 0.25	1.53 \pm 0.25	1.30 \pm 0.15	1.34 \pm 0.22	1.30 \pm 0.13	1.62 \pm 0.31	1.54 \pm 0.15	1.42 \pm 0.28	2.08 \pm 0.47	1.50 \pm 0.08	1.78 \pm 0.04
		<i>adk1</i>	2.23 \pm 0.13	1.87 \pm 0.44	1.64 \pm 0.27	1.54 \pm 0.25	1.53 \pm 0.25	1.30 \pm 0.15	1.34 \pm 0.22	1.30 \pm 0.13	1.62 \pm 0.31	1.54 \pm 0.15	1.42 \pm 0.28	2.08 \pm 0.47	1.50 \pm 0.08	1.78 \pm 0.04	1.48 \pm 0.05	1.23 \pm 0.01	1.26 \pm 0.06	1.21 \pm 0.09	1.51 \pm 0.17	1.30 \pm 0.04	1.24 \pm 0.07	1.29 \pm 0.09	1.61 \pm 0.16	3.52 \pm 0.77	1.63 \pm 0.05	1.79 \pm 0.04	
	T12	Col-0	1.50 \pm 0.08	1.78 \pm 0.04	1.48 \pm 0.05	1.23 \pm 0.01	1.26 \pm 0.06	1.21 \pm 0.09	1.51 \pm 0.17	1.30 \pm 0.04	1.24 \pm 0.07	1.29 \pm 0.09	1.61 \pm 0.16	3.52 \pm 0.77	1.63 \pm 0.05	1.79 \pm 0.04	1.67 \pm 0.15	1.34 \pm 0.11	1.29 \pm 0.10	1.28 \pm 0.08	1.37 \pm 0.06	1.33 \pm 0.06	1.30 \pm 0.07	1.41 \pm 0.09	1.86 \pm 0.24	3.96 \pm 0.50	3.13 \pm 0.79	2.35 \pm 0.53	
	<i>adk1</i>	1.63 \pm 0.05	1.79 \pm 0.04	1.67 \pm 0.15	1.34 \pm 0.11	1.29 \pm 0.10	1.28 \pm 0.08	1.37 \pm 0.08	1.34 \pm 0.26	1.44 \pm 0.39	1.18 \pm 0.19	1.13 \pm 0.22	1.19 \pm 0.15	2.22 \pm 0.17	2.75 \pm 0.41	1.88 \pm 0.23	1.65 \pm 0.29	1.38 \pm 0.11	1.19 \pm 0.08	1.14 \pm 0.12	1.05 \pm 0.13	1.37 \pm 0.30	1.58 \pm 0.51	1.32 \pm 0.41	1.15 \pm 0.11	1.82 \pm 0.36	3.13 \pm 0.79	2.35 \pm 0.53	
	T24	Col-0	3.13 \pm 0.79	2.35 \pm 0.53	2.13 \pm 0.49	1.42 \pm 0.14	1.35 \pm 0.22	1.33 \pm 0.26	1.44 \pm 0.39	1.31 \pm 0.26	1.18 \pm 0.19	1.13 \pm 0.22	1.19 \pm 0.15	2.22 \pm 0.17	2.75 \pm 0.41	1.88 \pm 0.23	1.65 \pm 0.29	1.38 \pm 0.11	1.19 \pm 0.08	1.14 \pm 0.12	1.05 \pm 0.13	1.37 \pm 0.30	1.58 \pm 0.51	1.32 \pm 0.41	1.15 \pm 0.11	1.82 \pm 0.36	0.59 \pm 0.20	0.38 \pm 0.14	
	<i>adk1</i>	2.75 \pm 0.41	1.88 \pm 0.23	1.65 \pm 0.29	1.38 \pm 0.11	1.19 \pm 0.08	1.14 \pm 0.12	1.05 \pm 0.13	1.37 \pm 0.30	1.58 \pm 0.51	1.32 \pm 0.41	1.15 \pm 0.11	1.82 \pm 0.36	0.59 \pm 0.20	0.38 \pm 0.14	0.47 \pm 0.04	0.40 \pm 0.08	0.42 \pm 0.04	0.20 \pm 0.10	0.32 \pm 0.03	0.44 \pm 0.06	0.35 \pm 0.09	0.39 \pm 0.03	0.39 \pm 0.05	0.46 \pm 0.15	0.39 \pm 0.03	0.27 \pm 0.08		
UGPase	T0	Col-0	0.59 \pm 0.20	0.38 \pm 0.14	0.47 \pm 0.04	0.40 \pm 0.08	0.42 \pm 0.04	0.20 \pm 0.10	0.32 \pm 0.03	0.44 \pm 0.06	0.35 \pm 0.09	0.39 \pm 0.03	0.39 \pm 0.05	0.46 \pm 0.15	0.39 \pm 0.03	0.27 \pm 0.08	0.36 \pm 0.08	0.34 \pm 0.03	0.41 \pm 0.04	0.29 \pm 0.01	0.23 \pm 0.07	0.42 \pm 0.04	0.39 \pm 0.12	0.49 \pm 0.12	0.36 \pm 0.04	0.37 \pm 0.15	0.39 \pm 0.03	0.27 \pm 0.08	
		<i>adk1</i>	0.39 \pm 0.03	0.27 \pm 0.08	0.36 \pm 0.08	0.34 \pm 0.03	0.41 \pm 0.04	0.29 \pm 0.01	0.23 \pm 0.07	0.42 \pm 0.04	0.39 \pm 0.12	0.49 \pm 0.12	0.36 \pm 0.04	0.37 \pm 0.15	0.38 \pm 0.11	0.40 \pm 0.08	0.38 \pm 0.03	0.35 \pm 0.02	0.35 \pm 0.06	0.23 \pm 0.02	0.28 \pm 0.06	0.26 \pm 0.13	0.21 \pm 0.04	0.13 \pm 0.02	0.27 \pm 0.11	0.75 \pm 0.08	0.27 \pm 0.08	0.36 \pm 0.08	
		T5	Col-0	0.38 \pm 0.11	0.40 \pm 0.08	0.38 \pm 0.03	0.35 \pm 0.02	0.35 \pm 0.06	0.23 \pm 0.02	0.28 \pm 0.06	0.26 \pm 0.13	0.21 \pm 0.04	0.13 \pm 0.02	0.27 \pm 0.11	0.75 \pm 0.08	0.27 \pm 0.08	0.36 \pm 0.08	0.34 \pm 0.03	0.41 \pm 0.04	0.29 \pm 0.01	0.23 \pm 0.07	0.42 \pm 0.04	0.39 \pm 0.12	0.49 \pm 0.12	0.36 \pm 0.04	0.37 \pm 0.15	0.39 \pm 0.03	0.27 \pm 0.08	0.36 \pm 0.08
		<i>adk1</i>	0.27 \pm 0.02	0.36 \pm 0.10	0.33 \pm 0.02	0.34 \pm 0.02	0.30 \pm 0.02	0.23 \pm 0.02	0.27 \pm 0.06	0.18 \pm 0.10	0.17 \pm 0.09	0.15 \pm 0.06	0.42 \pm 0.02	0.47 \pm 0.10	0.17 \pm 0.12	0.12 \pm 0.06	0.50 \pm 0.13	0.26 \pm 0.06	0.19 \pm 0.10	0.14 \pm 0.07	0.31 \pm 0.07	0.18 \pm 0.10	0.15 \pm 0.09	0.15 \pm 0.06	0.42 \pm 0.02	0.47 \pm 0.10	0.17 \pm 0.12	0.12 \pm 0.06	0.50 \pm 0.13
		T12	Col-0	0.12 \pm 0.06	0.50 \pm 0.13	0.26 \pm 0.06	0.19 \pm 0.10	0.14 \pm 0.07	0.31 \pm 0.07	0.18 \pm																			

Chapter 5

The development of a yeast functional complementation system to identify tonoplast-localized sucrose transport proteins from *Arabidopsis thaliana*

5.1 Introduction

Sucrose, a common disaccharide in plants, plays integral roles as an energy source and storage reserve and its hydrolysis drives basic processes such as glycolysis and the electron transport chain. It seems a sensible adaptation of plant cells to store this inert molecule in order to effectively and efficiently maintain carbon skeletons in times of need. The major storage organelle in plant cells is represented by the vacuole and may account for ~80-90% of the total cell volume (Maeshima, 2001). To enter the vacuole sucrose must cross the tonoplast membrane and, in C4 plants, transport is active and dependant on a pH gradient developed by proton translocating ATPases and pyrophosphatases (Leigh, 1984; Preisser and Komor, 1991).

In *Arabidopsis thaliana* nine sucrose transporter-like sequences have been identified to date (designated *AtSUT1* to 9; Table 5.1) and some have been functionally characterized (Sauer, 2007). The nine transporters are divided into groups according to tissue specificity, sub-cellular localization and biological function with transporters *AtSUT1*, 2 and 5 to 9 localized to the plasma membrane and responsible for phloem loading and sucrose import into sink tissue (Schulze et al., 2003; Sauer, 2007). *AtSUT3*, which is also plasma membrane bound, is different in that it contains 15-20% more amino acids and has been demonstrated to have a higher affinity for sucrose uptake than any of the other transporters (Meyer et al., 2004), while *AtSUT6* and 7 are presumed to be pseudogenes. *AtSUT4* is the only *Arabidopsis* sucrose transporter which has been shown to localize to the tonoplast membrane (Endler et

al., 2006) and analysis of the homologous gene products from both barley (*HvSUT2*) and lotus (*LjSUT4*) demonstrates that they also localize to the vacuolar membrane (Endler et al., 2006; Reinders et al., 2008). It has been suggested, however, that AtSUT4 and HvSUT2 are involved with sucrose export to the cytosol (Kühn and Grof, 2010) based on the kinetic parameters of the transport proteins (Weschke et al., 2000; Weise et al., 2000). In addition, these transporters have an affinity for a range of glucosides, suggesting that their main role may not be in sucrose transport. The high K_m of LjSUT4 for sucrose (16mM) (Reinders et al., 2008) further suggests that the proposed high affinity sucrose tonoplast import proteins have not yet been identified.

It is apparent that, based on analysis of the barley and *Arabidopsis* tonoplast proteomes, many vacuolar bound proteins remain to be characterized (Endler et al., 2006). The elusive tonoplast bound sucrose import protein remains of particular interest. One strategy to identify such transporters is by the use of a functional complementation expression screen to test for activity in a yeast mutant. The first sucrose transporter identified this way transformed a spinach cDNA library into a yeast mutant (Δ SUC2) which lacks an extracellular invertase, and had been engineered to express a plant sucrose synthase in the cytosol (Riesmeier et al., 1992). When grown on sucrose containing media as a sole carbon source, only the complemented cells which are able to take it up survive.

Table 5.1 The family of sucrose transporters identified in *Arabidopsis thaliana*. The nine isoforms are described according to tissue specificity, sub-cellular localization and biological function. Abbreviations: N/A - not applicable

Transporter	Cellular Localization	Subcellular localization	Function	Reference
AtSUT1	Pollen tubes, faniculi and placenta	Plasma membrane	Modulation of water potential	Stadler et al., 1999
AtSUT2	Companion cells	Plasma membrane	Phloem loading	Barker et al., 2000
AtSUT3	Sieve elements	Plasma membrane	Phloem loading	Meyer et al., 2004
AtSUT4	Source and sink tissue	Tonoplast membrane	Sucrose transport	Endler et al., 2006
AtSUT5	Endosperm	Plasma membrane	Biotin transport in addition to sucrose	Baud et al., 2005
AtSUT6	Pseudogene	-	N/A	Sauer et al., 2004
AtSUT7	Pseudogene	-	N/A	Sauer et al., 2004
AtSUT8	Floral tissue	Plasma membrane	Solute transport across membranes	Sauer et al., 2004
AtSUT9	Floral tissue	Plasma membrane	Sucrose import into cytosol	Sauer et al., 2004

In this chapter I describe the development of a similar system designed to identify tonoplast sucrose transporters. The same yeast mutant (Δ SUC2) was engineered to express both a plasma membrane bound sucrose importer (*SoSUT1*) and vacuolar acid invertase (*INV-19*) genes. In this case *SoSUT1* would transport sucrose into the cytosol, but the cells should only survive if the sucrose is transported into the vacuole where it can be acted upon by the invertase. I screened this system using an *Arabidopsis* cDNA library and identified 39 complementation clones. The sequence identities of these were determined, and will be discussed in context with current literature of membrane bound proteins.

5.2 Results

5.2.1 Yeast engineering for complementation screening

A *S. cerevisiae* mutant (Δ SUC2) (Brachmann et al., 1998) is unable to metabolize sucrose as a result of the absence of invertase activity and is an auxotrophic mutant for the amino acids histidine, leucine, lysine and uracil. The Δ SUC2 mutant was sequentially transformed with plasmids containing plant sequences coding for a plasma membrane bound sucrose transport protein *SoSUT1* and a vacuolar invertase *INV-19*. The transformed mutant was designated Δ SUC2::pPVD1-*SoSUT1*::YCPlac111-*INV-19*.

The engineered yeast was transformed with an *A. thaliana* cDNA library contained in the shuttle vector pFL61 (Minet et al., 1992), and approximately 100 000 colonies were subsequently screened by growing on minimal media containing sucrose. This number of colonies was chosen as it should allow for an adequate coverage of the *A. thaliana* genome. (An approximate 25 000 genes exist in the genome, therefore a 4

fold representation of expressed genes within the library should theoretically have been screened).

5.2.2 Analysis of plant sequences

Thirty nine colonies were identified as being able to grow on the media (Table 5.2), the library plasmids within them extracted and the inserts sequenced. These data were compared to the NCBI database (www.ncbi.nlm.nih.gov) using the Basic Local Alignment Search Tools (blastn and blastx) algorithms. Of the sequences showing high homology to known plant genes, clones 5, 15, 30, 35, and 36 were interesting (Table 5.2). Clone 5 encodes a zinc finger protein and clone 30 a putative protein kinase, while sequences 35 and 36 encode for putative ATP-binding proteins (Table 5.2). Transformant 15 was identified as an exocyst subunit (subunit EXO70) (Table 5.2). Furthermore, an enolase gene is encoded by one of the sequences (clone 25).

Table 5.2 Sequence identities of positive colonies from a yeast complementation screen for tonoplast localized sucrose transporters. DNA sequences were compared to the NCBI database to identify possible function and assign an accession and AGI number to the relevant sequences. [(✓) - insert isolated from library plasmid, and (x) – no insert isolated.]

Transformant	Insert	Gene	Accession number	E-value	AGI Number
1	✓	Plasma membrane intrinsic protein	NP_001078067	9x10 ⁻¹²²	AT2G45960
2	✓	Predicted protein (<i>Populus trichocarpa</i>)	EEE75392	2x10 ⁻³⁰	-
3	✓	Chlorophyl a/b binding protein	AAM12979	1x10 ⁻¹¹⁴	AT5G01530
4	✓	No sequence homology to <i>A. thaliana</i>	-	-	-
5	✓	Zinc finger protein	NP_182290	7x10 ⁻¹⁰⁸	AT2G47680
6	✓	Hypothetical protein	AAP22496	7x10 ⁻²⁶	AT2G45760
7	✓	Predicted protein (<i>Populus trichocarpa</i>)	EEE75392	2x10 ⁻³⁰	-
8	✓	Predicted protein (<i>Populus trichocarpa</i>)	EEE75393	2x10 ⁻³⁰	-
9	✓	Predicted protein (<i>Populus trichocarpa</i>)	EEE75394	1x10 ⁻³⁰	-
10	✓	β-glucosidase	AAB38783	2x10 ⁻⁹¹	-
11	x				
12	✓	No sequence homology to <i>A. thaliana</i>	-	-	-
13	✓	UDP-glucuronate decarboxylase	NP_001078768	2x10 ⁻¹⁵⁸	AT5G59290
14	✓	RNA binding protein	NP_566850	9x10 ⁻¹³⁵	AT3G29390
15	✓	Exocyst sub-unit	NP_200909	7x10 ⁻⁷	AT5G61010
16	x				
17	✓	Predicted protein (<i>Populus trichocarpa</i>)	EEE75392	3x10 ⁻⁶⁸	-
18	✓	Oxygen binding/ thalianol hydroxylase	NP_851153	7x10 ⁻¹⁴³	AT5G48000
19	✓	Oxygen binding/ thalianol hydroxylase	NP_851154	3x10 ⁻¹⁶¹	AT5G48230
20	✓	Putative alanine aminotransferase	AAK25905	4x10 ⁻⁹¹	AT1G23310
21	✓	No sequence homology to <i>A. thaliana</i>	-	-	-
22	✓	Hypothetical protein	NP_568055	2x10 ⁻³¹	AT4G39235
23	✓	Hypothetical protein	AAM62578	1x10 ⁻³²	-
24	✓	Glutathione reductase	NP_189059	1x10 ⁻⁵	AT3G24170
25	✓	Enolase	AAM12985	4x10 ⁻¹¹⁹	AT2G36530
26	✓	Predicted protein (<i>Populus trichocarpa</i>)	EEE75392	2x10 ⁻³⁰	-
27	x				
28	✓	40S ribosomal protein	NP_567104	5x10 ⁻⁷⁹	AT3G60770
29	x				
30	✓	ATP-binding protein	NP_172853	9x10 ⁻⁴³	AT1G14000
31	x				
32	x				
33	x				
34	x				
35	✓	ATP-binding protein	NP_568203	1x10 ⁻²⁹	AT5G08670
36	✓	ATP-binding protein	NP_568203	1x10 ⁻⁸⁶	AT5G08670
37	x				
38	✓	Hypothetical protein	NP_196959	4x10 ⁻²³	AT5G14550
39	x				

Interestingly, 4 sequences showed homology to unknown or predicted *Arabidopsis* sequences which are as yet uncharacterized. An analysis of hydrophobic regions

was conducted using the prediction program Hydrophobicity plot (<http://www.vivo.colostate.edu/molkit/hydrophathy/>) and the Kyte-Doolittle algorithm to determine potential membrane spanning regions on the uncharacterized proteins. It was found that the hypothetical protein encoded by sequence 38 displayed a region of hydrophobicity, however it was only one region and this indicates the protein is most likely membrane attached. The three other uncharacterized proteins, clones 6, 22 and 23 did not display any hydrophobic regions. Furthermore, co-expression analysis performed on the program Expression angler (Toufighi et al., 2005) suggest that the hypothetical protein, encoded for by the sequence isolated from clone 38 revealed its co-expression with that of a putative hexose phosphate transporter, however further *in silico* investigation into the sub-cellular localization of the protein (<http://bar.utoronto.ca/efp/cgi-bin/efpWeb.cgi>) suggested the clone was either an extracellular protein or localized to the mitochondrion (data not shown).

5.3 Discussion

Sucrose storage hinges on transport and is a critical point of research in terms of plant metabolism. To comprehend the intricacies of sucrose storage, an understanding of its distribution between photosynthetic and non-photosynthetic tissues is essential. In plants, leaves and stems represent the primary site of photosynthesis and are the tissues of carbon fixation and sucrose production. In contrast, seeds, roots and tubers are dependent on photosynthetically fixed carbon and, therefore, a net flow of carbohydrate is observed from the site of synthesis to organs of storage or photosynthetically inactive tissues (Riesmeier et al., 1992). Sucrose must cross the plasma membrane from the apoplasm to enter sieve tube elements or companion cells (where concentrations are 8-10 fold higher than in the cytosol) for transport *via* phloem tissue (Meyer et al., 2004) to areas of storage. This

transport is mediated by sucrose transport proteins which are there to ensure phloem loading and to maintain phloem flux (Kühn and Grof, 2010). Once it has been transported to the storage organs the carbohydrate must then either be metabolized or stored in the vacuole.

The plant vacuole is an important organelle and is responsible not only for the storage of sucrose but also for other carbohydrates, secondary metabolites and even compounds which are toxic to the plant (Endler et al., 2006). As with the phloem, sucrose in storage tissues is imported into the vacuole against a concentration gradient and this must be achieved by a sucrose import protein. In species that store large quantities of sucrose, such as sugarcane, researchers have recently focused on increasing cellular and vacuolar sucrose concentrations in order to increase yield (Groenewald and Botha, 2008). It has been demonstrated that the targeting of sucrose isomerase (SI) to the vacuole allowed for a doubling of the total amount of stored carbohydrate there (Wu and Birch, 2007) indicating that the storage capacity has not been reached. The identification of a sucrose import protein would help in the study of these transport process and may help in increasing sucrose storage in commercial crops.

The yeast complementation system developed in this chapter was designed to allow the screening of an *Arabidopsis thaliana* cDNA library (Minet et al., 1992) in order to isolate genes coding for tonoplast sucrose transporters. For this purpose, a *Saccharomyces cerevisiae* mutant (BY4742), which is unable to metabolize sucrose to its monomers (Brachmann et al., 1998), was used. The mutant lacks extracellular invertase activity and is unable to grow on media where sucrose is the sole carbon source. The yeast was sequentially transformed with two vectors allowing expression

of both a plasma membrane bound sucrose transport gene, (*SoSUT1*) (Riesmeier et al 1993) and a potato vacuolar targeted invertase (*INV19*) (Zrenner et al 1995). The proteins encoded by these genes should facilitate firstly sucrose import and, if it is then further transported into the vacuole, its degradation (Fig 5.2).

An *A. thaliana* cDNA library was transformed into the yeast and sequences allowing growth on Yeast Nitrogen Base (YNB) supplemented with sucrose as a carbon source were investigated. A vacuolar sucrose transport protein would likely have a number of properties, the lack of which would allow for the rejection of some of the identified sequences as candidate genes. Firstly the protein would have to be present in the tonoplast, so sequences encoding proteins that have been demonstrated to be present in other compartments can be ignored. This would include sequences such as that encoding the chlorophyll *a/b* binding protein, which is localized in the chloroplast as well as the ribosomal protein, the oxygen binding/ thalianol hydroxylase and the alanine aminotransferase sequences. Secondly, it should contain hydrophobic regions that would allow it to span the tonoplast membrane. Many of the previously characterized proteins identified in this screen, such as enolase (sequence 25) and the glutathione reductase, are hydrophilic and can thus be classified as false positives.

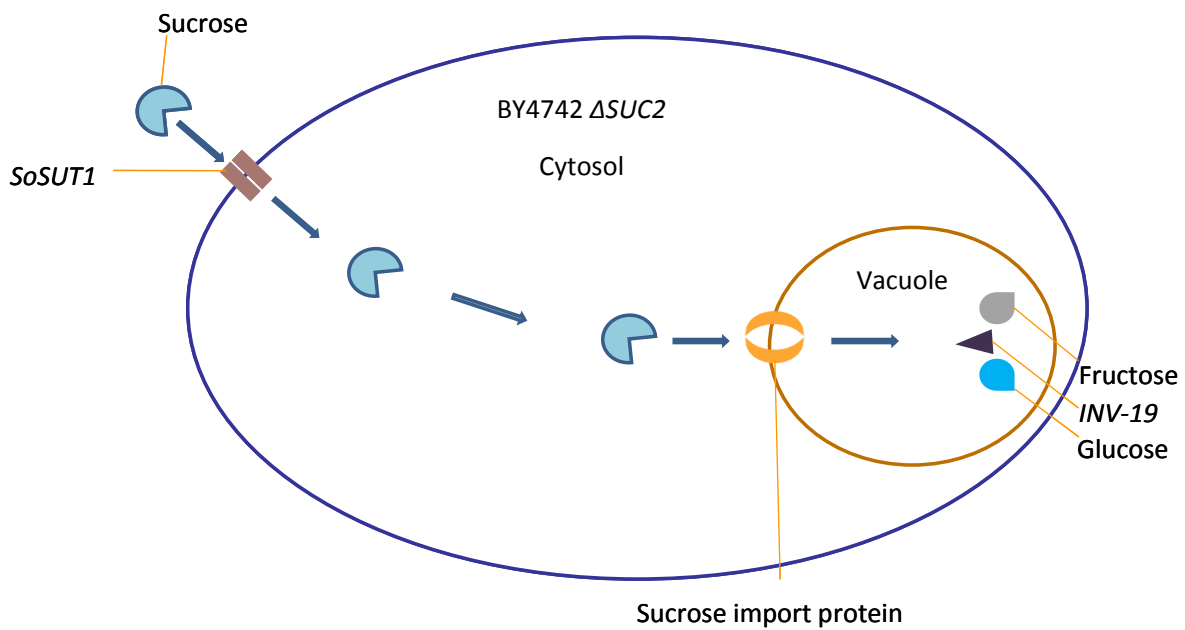


Fig 5.1 Schematic representation of the yeast complementation system designed to screen for putative vacuolar sucrose importers. A yeast invertase mutant showing the transport of sucrose into the yeast cell by a plasma membrane sucrose transporter (SoSUT1), the subsequent transport into the vacuole by a putative tonoplast bound sucrose import protein and hydrolysis of sucrose by a vacuolar invertase (INV-19), allowing for the survival of the yeast.

Of the known proteins, only one (sequence 15) fulfils both these criteria. This encodes a small sub-unit of the exocyst gene family which is involved in exocytosis. Some members of the family are responsible for vesicular transport from the Golgi apparatus to the plasma membrane (TerBush et al., 1996; Synek et al., 2006); however, this particular subunit has been shown to localize to the tonoplast membrane (Synek et al., 2006). This sequence, therefore, can be classed as a candidate gene for further study. Currently insertion mutants in the At5g61010 gene are being isolated and they will be analyzed using non-aqueous fractionation techniques in order to examine vacuolar sucrose concentrations. In addition a FRET protein that can sense sucrose will be targeted to the vacuole in yeast which is also

expressing the exocyst protein. This will allow the examination of sucrose concentrations within the vacuole.

In addition, several sequences encoding hypothetical proteins with no known function were identified (Table 5.1). As their sub-cellular location is unknown, hydrophobic regions of the proteins were evaluated. Only one of them (sequence 38) contained a, small, hydrophobic domain making it unlikely that any of the sequences are transporters. The expression of the unknown genes was also examined to see if they co-expressed with proteins likely to be involved in vacuolar sucrose storage, such as *vPPase* and *vATPase* genes, however, none of them did. Taken together these data provide no evidence that any of the unknown proteins are a vacuolar sucrose transport protein.

Although there is no obvious mechanism why several of the soluble proteins would lead to the growth phenotype, there are theoretical reasons as to how some of them might complement the mutation. For example, the zinc-finger protein identified (sequence 5) is a transcription factor. Six invertase genes are present within the yeast genome, although they are normally not expressed when grown under the described conditions and it is possible that a plant transcription factor could lead to their up-regulation which would allow the yeast to be able to degrade sucrose and survive.

Obviously, the functioning of this complementation system is based on a number of assumptions. The first of these is that the plant tonoplast sucrose importer will target to the same membrane in yeast. Factors affecting protein targeting to the vacuolar membrane are not as well understood as with other organelles, such as the

chloroplast or mitochondria. A number of studies have demonstrated that *Arabidopsis* vPPase proteins also target to the tonoplast in yeast (Kim et al., 1994; Pérez-Castiñeira et al., 2002), however, AtSUT4 (which is located in the vacuolar membrane in *Arabidopsis*) (Endler et al., 2006) was functionally characterized by expression in the yeast plasma membrane (Weise et al., 2000). The second assumption is that the sucrose importer is encoded by a single gene. If this is not the case then the complementation system will not work. The final assumption is that the gene is present in the library that is being used in the screen. This library (Minet et al., 1992) was constructed from RNA isolated from whole, young *Arabidopsis* seedlings which may, or may not, express the protein of interest. It is interesting to note that no cytosolic invertase or sucrose synthase proteins were isolated in the screen, which may indicate that the plants were not expressing genes involved in sucrose metabolism at the time the RNA used to produce the library was isolated. One way to exploit the complementation system further, therefore, would be to isolate a cDNA library from, for example *Arabidopsis* leaf discs fed with extracellular sucrose which would be expected to up-regulate genes involved in sucrose storage and degradation; or from plants that store large amounts of sucrose, such as sugarcane.

In summary, I identified several genes that allowed a yeast mutant to grow on sucrose. The system was designed to allow identification of vacuolar sucrose importers, however, only one of the sequences appear to encode a protein that is localized to the tonoplast. This protein will be studied further, but additionally a new library would be manufactured which may stand a better chance of succeeding in the isolation of a sucrose import protein.

5.3 Experimental procedures

5.3.1 Chemicals, enzymes and plasmids

All chemicals used in this study were purchased from Sigma-Aldrich (<http://www.sigmaaldrich.com>) unless otherwise stated. Restriction enzymes and kits were purchased from Fermentas (www.fermentas.com).

5.3.2 Vector construction

The vector pPVD1 containing a membrane bound sucrose transport protein sequence *SoSUT1* (kind gift of Colin Olhoff, Institute of Plant Biotechnology, Stellenbosch University) in parallel with the vacuolar invertase sequence *INV-19* (kind gift of Prof. Uwe Sonnewald, University of Erlangen, Germany; (Zrenner et al., 1996) were ligated into the plasmid YCPlac111 (Gietz and Akio, 1988). The constitutive promoters phosphoglycerate kinase (PGK) and the lactose operon (*lacZ*) controlled the levels of expression in the plasmids, respectively.

The pFL61 library plasmid containing the sequence of interest was isolated from the yeast, the insert excised by digestion with *NofI*. This was separated from the plasmid by agarose gel electrophoresis and the fragment isolated from the gel, following which it was ligated into the same sites in the cloning vector pBK-CMV (www.stratagene.com).

5.3.3 Yeast transformation

The Δ SUC2 mutant was sequentially transformed with the pPVD1-*StSUT1* and YCPlac111-*INV19* construct using the lithium acetate transformation protocol (Becker and Lundblad, 2001). These were inoculated in 5ml of yeast nitrogen base (YNB) minimal liquid media and grown overnight to an optical density of between 3.0 and

4.0 (OD₆₀₀). One ml of the starter culture was then inoculated in 200ml of YNB minimal liquid media and grown for 3 – 4h until an OD₆₀₀ of 0.4 – 0.6 was reached. The cells were centrifuged at 4000xg at room temperature for 5min, and the cell pellet was re-suspended in 10ml of sterile dH₂O and sedimented again by centrifugation as described above. The supernatant was decanted and the cells re-suspended in 700µl of lithium acetate buffer (100mM LiAC in TE buffer) and 10µl of 20mg.ml⁻¹ herring sperm DNA were mixed with 2µl of 5µg.µl⁻¹ of plasmid DNA inoculated with 100µl of the yeast suspension. Following this, 600µl of PEG solution (40% (w/v) PEG 4000, 100mM LiAC in TE buffer), were added to each tube. The mixture were incubated for 30min at 30°C and transferred for a further incubation at 42°C for 15min. The cells were centrifuged at 10000xg for 5sec and the pellet re-suspended in 140µl 1x TE buffer. Sixty µl of the transformation mix was plated onto selective media consisting of YNB agar containing the appropriate amino acids with glucose as a carbon source. The plates were incubated for 3 days at 30°C until colony growth was observed.

5.3.4 Transformation with an *A. thaliana* cDNA library

Following the successful transformation and growth of the mutant Δ SUC2::pPVD1-SoSUT1::YCPlac111-INV-19 on selection media the modified yeast mutant was transformed (as described above) with an *A. thaliana* cDNA (Minet et al., 1992) library.

5.3.5 DNA isolation from complemented yeast colonies

Yeast minimal media supplemented with sucrose was inoculated with the relevant transformant from the library screen and incubated overnight at 30°C on a shaker. One ml of the culture was taken and centrifuged at 16000xg for 4min. The pellet was

re-suspended in 600µl of 67mM K₂HPO₄, 1% (w/v) driselase and incubated for 1h at 37°C. Plasmid isolation with a geneJET plasmid miniprep kit was performed according to the manufacturer's recommendations (www.fermentas.com).

5.3.6 Insert sequencing

Isolated sequence contained in the plasmid pBK-CMV was sequenced on an ABI3730xl DNA analyzer by a commercial service (Central Analytical Facility, Stellenbosch University).

5.3.7 *In silico* analysis

Sequence identity was compared to known plant sequences by the BLAST algorithmns (www.ncbi.nlm.nih.gov). Hydrophobicity plot (<http://www.vivo.colostate.edu/molkit/hydropathy/>) was used to determine hydrophobic regions on hypothetical proteins. Co-expression analysis was conducted with expression angler (http://bar.utoronto.ca/ntools/cgi-bin/ntools/expression_angler.cgi) and an expression profile was created with the use of eFP browser (<http://bar.utoronto.ca/efp/cgi-bin/efpWeb.cgi>).

Chapter 6

General conclusion

This study was primarily concerned with the development of analytical and biochemical tools to aid in the understanding of sub-cellular metabolism.

In regards to this, in Chapter 3 I describe the development of a reverse phase liquid chromatography coupled to a mass spectrometer to identify and quantify phosphorylated and nucleotide compounds. Currently, 29 authentic standards could be identified within an acceptable confidence range, of which 17 has been identified in *Arabidopsis* extracts. Progress is underway to include more standards in this analysis to increase the current library size. The inclusion of Calvin cycle intermediates especially will take priority (Arrivault et al., 2009), although these metabolites are expensive or need to be chemically synthesized. One way I suggest to improve the current method is to also include ^{13}C labeled and deuterated internal standards for each analyte of interest, although this will increase the cost of the analysis significantly since these are either expensive or not commercially available. Another useful adaption of the method would be to use the multiple reaction monitoring (MRM) scanning for MS/MS data generation. Although this would not resolve certain isomeric compounds co-eluting within our chromatographic set-up (discussed in Chapter 3), the application of this in positive metabolite identification in complex biological matrixes would certainly ease downstream automated software development. Such MS2T libraries have been successfully generated for LC-MS profiled plant secondary metabolites (Matsuda et al., 2009), and remains an attainable prospect for ionic specie library compilations. The adaptation of current semi-automated software for metabolite identification is currently underway, using

both scaling, alignment and baseline correction procedures from the user-driven interface of MetAlign, combined with Perl scripts to aid in peak filtering, picking, binning and data deconvolution.

The application of this technique, in parallel with those of gas chromatography mass spectrometry (GC-MS) was next applied to cell fractions to distinguish metabolite distributions within *Arabidopsis* rosette leaves (Chapter 4). This indicated that as little as 30mg of plant material was enough to detect and quantify primary metabolites such as sugars (and polyols), organic – and amino acids. However, with the enhanced sensitivity of the LC-MS system, only low abundant phosphate-containing metabolites were detected (either at T0 or T5). The most plausible reason is that the extracts are too concentrated; leading to ion suppression within the MS. Current analysis is underway with 100-fold diluted samples to analyze these metabolite concentrations *in vivo*. Furthermore, this technique was also combined with isotope labeling to provide information regarding the viability of distinguishing sub-cellular fluxes *via* this approach. While analyses is still ongoing, it is evident that the label enrichment in the total fractionated aliquots gave informative details on branch chain amino acid biosynthesis, sucrose hydrolysis and starch metabolism between the wild type and an *adk1* mutant (Chapter 4), and the scope remains for this to be validated on sub-cellular levels. As was evident from the analysis, fractions enriched in either cell wall precursors or organic acid metabolism (with enriched isotopic label enrichment) were also identified, and marker enzyme activities (cellulose synthase, succinyl CoA ligase and cytochrome c oxidase) are currently being conducted in order to elucidate the identities of the fractions. Furthermore, whilst this experiment was not set-up to acquire physiological information regarding the *adk1* mutant, and its biological effect, it is evident that the genetic perturbation extent over several sub-

cellular compartments. Therefore, the assessment of the sub-cellular maximal catalytic activity of ADK could provide interesting information regarding adenylate homeostasis.

In my last experimental chapter (Chapter 5) I constructed a yeast complementation screen in order to identify candidates for tonoplast-localized sucrose importers. A positive aspect from my preliminary results indicate that several known vacuolar membrane spanning or –associated coding sequences were targeted, indicating that compartmentation is taken into account. However, the lack of obvious false positives expected during this screen (cytosolic invertase or sucrose synthases) suggests that a cDNA library from a plant (such as sugarcane or sugarbeet) or specific treatment which is known to accumulate high levels of sucrose could be more beneficial. If the correct transporter is identified, the application of the techniques developed in Chapters 3 and 4 will assist in the characterization of the biological role of this gene in sucrose transport and storage.

Angeles-Núñez, J. and Tiessen, A. (2010). *Arabidopsis* sucrose synthase 2 and 3 modulate metabolic homeostasis and direct carbon towards starch synthesis in developing seeds. *Planta*.

Arabidopsis genome initiative (2000). Analysis of the genome sequence of the flowering plant *Arabidopsis thaliana*. *Nature*, **408**, 796-815.

Araujo, W. L. et al. (2010). Identification of the 2-Hydroxyglutarate and Isovaleryl-CoA Dehydrogenases as Alternative Electron Donors Linking Lysine Catabolism to the Electron Transport Chain of *Arabidopsis* Mitochondria. *Plant Cell*, tpc.110.075630.

Arbona, V. et al. (2010). Common and divergent physiological, hormonal and metabolic responses of *Arabidopsis thaliana* and *Thellungiella halophila* to water and salt stress. *Journal of Plant Physiology*, **In Press, Corrected Proof**.

Arrivault, S. et al. (2009). Use of reverse-phase liquid chromatography, linked to tandem mass spectrometry, to profile the Calvin cycle and other metabolic intermediates in *Arabidopsis* rosettes at different carbon dioxide concentrations. *The Plant Journal*, **59**, 826-839.

Arsova, B. et al. (2010). Plastidial Thioredoxin z Interacts with Two Fructokinase-Like Proteins in a Thiol-Dependent Manner: Evidence for an Essential Role in Chloroplast Development in *Arabidopsis* and *Nicotiana benthamiana*. *Plant Cell*, tpc.109.071001.

- Baena-Gonzalez, E. et al.** (2007). A central integrator of transcription networks in plant stress and energy signalling. *Nature*, **448**, 938-942.
- Barnes, S. A. et al.** (1994). Alteration of the amount of the chloroplast phosphate translocator in transgenic tobacco affects the distribution of assimilate between starch and sugar. *Plant Physiol.*, **106**, 1123-1129.
- Barratt, D. H. P. et al.** (2009). Normal growth of *Arabidopsis* requires cytosolic invertase but not sucrose synthase. *Proceedings of the National Academy of Sciences*, **106**, 13124 -13129.
- Baxter, C. J. et al.** (2003). Elevated sucrose-phosphate synthase activity in transgenic tobacco sustains photosynthesis in older leaves and alters development. *J. Exp. Bot.*, **54**, 1813-1820.
- Beck, H. C. et al.** (2004). Catabolism of leucine to branched-chain fatty acids in *Staphylococcus xylosus*. *J. Appl. Microbiol.*, **96**, 1185-1193.
- Becker, D. M. and Lundblad, V.** (2001). Introduction of DNA into yeast cells. *Curr Protoc Mol Biol*, **Chapter 13**, Unit13.7.
- Benkeblia, N. et al.** (2007). Metabolite profiling and assessment of metabolome compartmentation of soybean leaves using non-aqueous fractionation and GC-MS analysis. *Metabolomics*, **3**, 297-305.
- Bieniawska, Z. et al.** (2007). Analysis of the sucrose synthase gene family in

Arabidopsis. *The Plant Journal*, **49**, 810-828.

Blanchard, J. L. and Lynch, M. (2000). Organellar genes: why do they end up in the nucleus? *Trends in Genetics*, **16**, 315-320.

Brachmann, C. B. et al. (1998). Designer deletion strains derived from *Saccharomyces cerevisiae* S288C: A useful set of strains and plasmids for PCR-mediated gene disruption and other applications. *Yeast*, **14**, 115-132.

Carrari, F. et al. (2005). Deficiency of a Plastidial Adenylate Kinase in *Arabidopsis* Results in Elevated Photosynthetic Amino Acid Biosynthesis and Enhanced Growth. *Plant Physiol.*, **137**, 70-82.

Carter, C. et al. (2004). The vegetative vacuole proteome of *Arabidopsis thaliana* reveals predicted and unexpected proteins. *Plant Cell*, tpc.104.027078.

Caspar, T. et al. (1985). Alterations in growth, photosynthesis, and respiration in a starchless mutant of *Arabidopsis thaliana* (L.) deficient in chloroplast phosphoglucomutase activity. *Plant Physiol*, **79**, 11-17.

Chatterton, N. J. and Sivius, J. E. (1980). Photosynthate partitioning into leaf starch as affected by daily photosynthetic period duration in six species. *Physiologia Plantarum*, **49**, 141-144.

Chaudhuri, B. et al. (2008). Protonophore- and pH-insensitive glucose and sucrose accumulation detected by FRET nanosensors in *Arabidopsis* root tips. *Plant J*,

56, 948-962.

Chia, T. et al. (2004). A cytosolic glucosyltransferase is required for conversion of starch to sucrose in *Arabidopsis* leaves at night. *Plant J*, **37**, 853-863.

Chourey S. et al. (1998). Genetic evidence that the two isozymes of sucrose synthase present in developing maize endosperm are critical, one for cell wall integrity and the other for starch biosynthesis. *Molecular and General Genetics MGG*, **259**, 88-96.

Cottage, A. et al. (2010). The *Arabidopsis* plastid-signalling mutant gun1 (genomes uncoupled1) shows altered sensitivity to sucrose and abscisic acid and alterations in early seedling development. *J. Exp. Bot.*, **61**, 3773-3786.

Cruz, J. A. et al. (2008). Metabolite profiling of Calvin cycle intermediates by HPLC-MS using mixed-mode stationary phases. *Plant J*, **55**, 1047-1060.

Däschner, K. et al. (1999). In plants a putative isovaleryl-CoA-dehydrogenase is located in mitochondria. *Plant Mol. Biol*, **39**, 1275-1282.

Dembitsky, V. M. et al. (2001). branched alkanes and other apolar compounds produced by the *Cyanobacterium Microcoleus vaginatus* from the negev desert. *Russian Journal of Bioorganic Chemistry*, **27**, 110-119.

Deuschle, K. et al. (2006). Rapid metabolism of glucose detected with FRET glucose nanosensors in epidermal cells and intact roots of *Arabidopsis* RNA-

silencing mutants. *Plant Cell*, **18**, 2314-2325.

De Vos, R. C. et al. (2007). Untargeted large-scale plant metabolomics using liquid chromatography coupled to mass spectrometry. *Nat. Protocols*, **2**, 778-791.

Du, L. and Poovaiah, B. (2004). A novel family of Ca²⁺-calmodulin-binding proteins involved in transcriptional regulation: interaction with fsh/ring3 class transcription activators. *Plant Mol Biol*, **54**, 549-569.

Echeverría, E. and Salerno, G. (1993). Intracellular localization of sucrose-Phosphate Phosphate in photosynthetic cells of lettuce (*Lactuca sativa*). *Physiologia Plantarum*, **88**, 434-438.

Endler, A. et al. (2006). Identification of a vacuolar sucrose transporter in barley and *Arabidopsis* Mesophyll cells by a tonoplast proteomic approach. *Plant Physiol.*, **141**, 196-207.

Engqvist, M. et al. (2009). Two D-2-hydroxy-acid dehydrogenases in *Arabidopsis thaliana* with catalytic capacities to participate in the last reactions of the methylglyoxal and beta-oxidation pathways. *J. Biol. Chem*, **284**, 25026-25037.

Erban, A. et al. (2007). Nonsupervised construction and application of mass spectral and retention time index libraries from time-of-flight gas chromatography-mass spectrometry metabolite profiles. *Methods Mol. Biol*, **358**, 19-38.

Farre, E. M. et al. (2008). Analysis of subcellular metabolite levels of potato tubers

(*Solanum tuberosum*) displaying alterations in cellular or extracellular sucrose metabolism. *Metabolomics*, **4**, 161-170.

Farre, E. M. et al. (2001). Analysis of the compartmentation of glycolytic intermediates, nucleotides, sugars, organic acids, amino acids, and sugar alcohols in potato tubers using a nonaqueous fractionation method. *Plant Physiol.*, **127**, 685-700.

Fehr M et al. (2005). Development and use of fluorescent nanosensors for metabolite imaging in living cells.

Fehr, M. et al. (2002). Visualization of maltose uptake in living yeast cells by fluorescent nanosensors. *Proceedings of the National Academy of Sciences of the United States of America*, **99**, 9846 -9851.

Fehr, M. et al. (2004). Live imaging of glucose homeostasis in nuclei of COS-7 cells. *J Fluoresc*, **14**, 603-609.

Fernie, A. et al. (2002). Antisense repression of cytosolic phosphoglucomutase in potato (*Solanum tuberosum*) results in severe growth retardation, reduction in tuber number and altered carbon metabolism. *Planta*, **214**, 510-520.

Ferro, M. et al. (2002). Integral membrane proteins of the chloroplast envelope: Identification and subcellular localization of new transporters. *Proceedings of the National Academy of Sciences of the United States of America*, **99**, 11487 -11492.

- Figueroa, P. et al.** (2005). *Arabidopsis* has two redundant cullin3 proteins that are essential for embryo development and that interact with RBX1 and BTB proteins to form multisubunit E3 ubiquitin ligase complexes in Vivo. *Plant Cell*, **17**, 1180-1195.
- Fondy, B. R. and Geiger, D. R.** (1985). Diurnal changes in allocation of newly fixed carbon in exporting sugar beet leaves. *Plant Physiol.*, **78**, 753-757.
- Fragoso, S. et al.** (2009). SnRK1 isoforms AKIN10 and AKIN11 are differentially regulated in *Arabidopsis* plants under phosphate starvation. *Plant Physiol.*, **149**, 1906-1916.
- Fu, Y. et al.** (1998). mechanism of reductive activation of Potato tuber ADP-glucose pyrophosphorylase. *Journal of Biological Chemistry*, **273**, 25045 -25052.
- Geigenberger, P.** (2003). Regulation of sucrose to starch conversion in growing potato tubers. *J. Exp. Bot.*, **54**, 457-465.
- Geigenberger, P. and Stitt, M.** (1993). Sucrose synthase catalyses a readily reversible reaction in vivo in developing potato tubers and other plant tissues. *Planta*, **189**, 329-339.
- Gerrits, N. et al.** (2001). Sucrose Metabolism in Plastids. *Plant Physiol.*, **125**, 926-934.

Gibon, Y. et al. (2004a). A robot-based platform to measure multiple enzyme activities in *Arabidopsis* using a set of cycling assays: comparison of changes of enzyme activities and transcript levels during diurnal cycles and in prolonged darkness. *Plant Cell*, **16**, 3304-3325.

Gibon, Y. et al. (2004b). Adjustment of diurnal starch turnover to short days: depletion of sugar during the night leads to a temporary inhibition of carbohydrate utilization, accumulation of sugars and post-translational activation of ADP-glucose pyrophosphorylase in the following light period. *Plant J*, **39**, 847-862.

Gietz, R. and Akio, S. (1988). New yeast-*Escherichia coli* shuttle vectors constructed with in vitro mutagenized yeast genes lacking six-base pair restriction sites. *Gene*, **74**, 527-534.

Glinski, M. and Weckwerth, W. (2005). Differential multisite phosphorylation of the trehalose-6-phosphate synthase gene family in *Arabidopsis thaliana*. *Molecular & Cellular Proteomics*, **4**, 1614-1625.

Groenewald, J. and Botha, F. (2008). Down-regulation of pyrophosphate: fructose 6-phosphate 1-phosphotransferase (PFP) activity in sugarcane enhances sucrose accumulation in immature internodes. *Transgenic Research*, **17**, 85-92.

Gu, H. et al. (2006). A novel analytical method for in vivo phosphate tracking. *FEBS Letters*, **580**, 5885-5893.

Harthill, J. E. et al. (2006). Phosphorylation and 14-3-3 binding of *Arabidopsis* trehalose-phosphate synthase 5 in response to 2-deoxyglucose. *The Plant Journal*, **47**, 211-223.

Haseloff, J. et al. (1997). Removal of a cryptic intron and subcellular localization of green fluorescent protein are required to mark transgenic *Arabidopsis* plants brightly. *Proceedings of the National Academy of Sciences of the United States of America*, **94**, 2122 -2127.

Häusler, R. E., Baur, B., et al. (2000). Plastidic metabolite transporters and their physiological functions in the inducible crassulacean acid metabolism plant *Mesembryanthemum crystallinum*. *The Plant Journal*, **24**, 285-296.

Häusler, R. E., Schlieben, N. H., et al. (2000). Control of carbon partitioning and photosynthesis by the triose phosphate/phosphate translocator in transgenic tobacco plants (*Nicotiana tabacum* L.). I. Comparative physiological analysis of tobacco plants with antisense repression and overexpression of the triose phosphate/phosphate translocator. *Planta*, **210**, 371-382.

Häusler, R. E. et al. (1998). Compensation of decreased triose phosphate/phosphate translocator activity by accelerated starch turnover and glucose transport in transgenic tobacco. *Planta*, **204**, 366-376.

Heazlewood, J. L. et al. (2004). Experimental analysis of the *Arabidopsis* mitochondrial proteome highlights signaling and regulatory components,

provides assessment of targeting prediction programs, and indicates plant-specific mitochondrial proteins. *Plant Cell*, **16**, 241-256.

Heineke, D. et al. (1994). Effect of antisense repression of the chloroplast triose-phosphate translocator on photosynthetic metabolism in transgenic potato plants. *Planta*, **193**, 174-180.

Hendriks, J. H. et al. (2003). ADP-Glucose pyrophosphorylase is activated by posttranslational redox-modification in response to light and to sugars in leaves of *Arabidopsis* and other plant species. *Plant Physiol.*, pp.103.024513.

Huber, S. C. and Huber, J. L. (1992). Role of Sucrose-Phosphate Synthase in Sucrose Metabolism in Leaves. *Plant Physiol.*, **99**, 1275-1278.

Jarvis, P. (2001). Intracellular signalling: The chloroplast talks! *Current Biology*, **11**, R307-R310.

Kandra, G. et al. (1990). Modified branched-chain amino acid pathways give rise to acyl acids of sucrose esters exuded from tobacco leaf trichomes. *Eur. J. Biochem*, **188**, 385-391.

Kempa, S. et al. (2007). A plastid-localized glycogen synthase kinase 3 modulates stress tolerance and carbohydrate metabolism. *The Plant Journal*, **49**, 1076-1090.

Kim, E. J. et al. (1994). Heterologous expression of plant vacuolar pyrophosphatase

in yeast demonstrates sufficiency of the substrate-binding subunit for proton transport. *Proc Natl Acad Sci U S A*, **91**, 6128-6132.

Knight, J. S. and Gray, J. C. (1994). Expression of genes encoding the tobacco chloroplast phosphate translocator is not light-regulated and is repressed by sucrose. *Molecular and General Genetics MGG*, **242**, 586-594.

Kolbe, A. et al. (2005). Trehalose 6-phosphate regulates starch synthesis via posttranslational redox activation of ADP-glucose pyrophosphorylase. *Proceedings of the National Academy of Sciences of the United States of America*, **102**, 11118-11123.

Kötting, O. et al. (2010). Regulation of starch metabolism: the age of enlightenment? *Current Opinion in Plant Biology*, **13**, 320-328.

Koussevitzky, S. et al. (2007). Signals from Chloroplasts Converge to Regulate Nuclear Gene Expression. *Science*, **316**, 715-719.

van der Krogt, G. N. M. et al. (2008). A Comparison of Donor-Acceptor Pairs for Genetically Encoded FRET Sensors: Application to the Epac cAMP Sensor as an Example. *PLoS ONE*, **3**.

Kroumova, A. B. et al. (1994). A pathway for the biosynthesis of straight and branched, odd- and even-length, medium-chain fatty acids in plants. *Proceedings of the National Academy of Sciences of the United States of America*, **91**, 11437 -11441.

- Kühn, C. and Grof, C. P.** (2010). Sucrose transporters of higher plants. *Current Opinion in Plant Biology*, **13**, 287-297.
- Kuzma, M. M. et al.** (1999). The Site of Oxygen Limitation in Soybean Nodules. *Plant Physiol.*, **119**, 399-408.
- Lager, I. et al.** (2003). Development of a fluorescent nanosensor for ribose. *FEBS Lett*, **553**, 85-89.
- Lager, I. et al.** (2006). Conversion of a Putative *Agrobacterium* Sugar-binding Protein into a FRET Sensor with High Selectivity for Sucrose. *Journal of Biological Chemistry*, **281**, 30875 -30883.
- Lalonde, S. et al.** (2005). Shining light on signaling and metabolic networks by genetically encoded biosensors. *Curr. Opin. Plant Biol*, **8**, 574-581.
- Langenkämper, G. et al.** (2002). Sucrose phosphate synthase genes in plants belong to three different families. *J. Mol. Evol*, **54**, 322-332.
- Leigh, R. A.** (1984). The role of the vacuole in the accumulation and mobilization of sucrose. *Plant Growth Regul*, **2**, 339-346.
- Li, L. et al.** (2003). Overexpression of a bacterial branched-chain [alpha]-keto acid dehydrogenase complex in *Arabidopsis* results in accumulation of branched-chain acyl-CoAs and alteration of free amino acid composition in seeds. *Plant*

Science, **165**, 1213-1219.

Lin, T. et al. (1988). Isolation and Characterization of a Starchless Mutant of *Arabidopsis thaliana* (L.) Heynh Lacking ADPglucose Pyrophosphorylase Activity. *Plant Physiol*, **86**, 1131-1135.

Lloyd, J. R. et al. (2005). Leaf starch degradation comes out of the shadows. *Trends in Plant Science*, **10**, 130-137.

Looger, L. L. et al. (2005). Genetically encoded FRET sensors for visualizing metabolites with subcellular resolution in living cells. *Plant Physiol.*, **138**, 555-557.

Lopez-Juez, E. and Pyke, K. A. (2005). Plastids unleashed: their development and their integration in plant development. *Int. J. Dev. Biol.*, **49**, 557-577.

Lou, Y. et al. (2007). PIP5K9, an *Arabidopsis* phosphatidylinositol monophosphate kinase, interacts with a cytosolic invertase to negatively regulate sugar-mediated root growth. *Plant Cell*, **19**, 163-181.

Lu, Y. and Sharkey, T. D. (2004). The role of amylomaltase in maltose metabolism in the cytosol of photosynthetic cells. *Planta*, **218**, 466-473.

Lunn et al (2003). Expression of a *cyanobacterial* sucrose-phosphate synthase from *Synechocystis* sp. PCC 6803 in transgenic plants. *J. Exp. Bot.*, Vol. 54, No. 381, 223-237

Lunn, J. E. et al. (1997). Adenosine-triphosphate-mediated activation of sucrose-phosphate synthase in bundle sheath cells of C 4 plants. *Planta*, **202**, 249-256.

Lunn, J. et al. (2006). Sugar-induced increases in trehalose 6-phosphate are correlated with redox activation of ADPglucose pyrophosphorylase and higher rates of starch synthesis in *Arabidopsis thaliana*. *Biochem J*, **397**, 139-148.

Lütken, H. et al. (2010). Repression of both isoforms of disproportionating enzyme leads to higher malto-oligosaccharide content and reduced growth in potato. *Planta*.

Lytovchenko, A. et al. (2009). Application of GC-MS for the detection of lipophilic compounds in diverse plant tissues. *Plant Methods*, **5**, 4.

Lytovchenko, A. et al. (2002a). Carbon assimilation and metabolism in potato leaves deficient in plastidial phosphoglucomutase. *Planta*, **215**, 802-811.

Lytovchenko, A. et al. (2002b). The influence of cytosolic phosphoglucomutase on photosynthetic carbohydrate metabolism. *Planta*, **215**, 1013-1021.

Lytovchenko, A. et al. (2005). Expression of an Escherichia coli phosphoglucomutase in potato (*Solanum tuberosum* L.) results in minor changes in tuber metabolism and a considerable delay in tuber sprouting. *Planta*, **221**, 915-927.

- MacDougall, A. J. et al.** (1995). The use of nonaqueous fractionation to assess the ionic composition of the apoplast during fruit ripening. *Plant Physiol*, **108**, 1679-1689.
- Maeshima, M.** (2001). Tonoplast transporters: organization and function. *Annu. Rev. Plant. Physiol. Plant. Mol. Biol.*, **52**, 469-497.
- Maloney, G. S. et al.** (2010). Characterization of the Branched-Chain Amino Acid Aminotransferase Enzyme Family in Tomato. *Plant Physiol.*, **153**, 925-936.
- Margulis, L.** (1975). Symbiotic theory of the origin of eukaryotic organelles; criteria for proof. *Symp. Soc. Exp. Biol*, 21-38.
- Marino, D. et al.** (2008). Evidence for transcriptional and post-translational regulation of sucrose synthase in pea nodules by the cellular redox state. *Molecular Plant-Microbe Interactions*, **21**, 622-630.
- Marri, L. et al.** (2009). Prompt and Easy Activation by Specific Thioredoxins of Calvin Cycle Enzymes of *Arabidopsis thaliana* Associated in the GAPDH/CP12/PRK Supramolecular Complex. *Mol Plant*, **2**, 259-269.
- Martin, C. and Smith, A. M.** (1995). Starch biosynthesis. *Plant Cell*, **7**, 971-985.
- Masakapalli, S. K. et al.** (2009). Subcellular flux analysis of central metabolism in a heterotrophic *Arabidopsis thaliana* cell suspension using steady-state stable

isotope labeling. *Plant Physiol.*, pp.109.151316.

Matsuda, F. et al. (2009). MS/MS spectral tag-based annotation of non-targeted profile of plant secondary metabolites. *The Plant Journal*, **57**, 555-577.

Meyer, S. et al. (2004). Wounding Enhances Expression of AtSUC3, a Sucrose Transporter from *Arabidopsis* Sieve Elements and Sink Tissues. *Plant Physiol.*, **134**, 684-693.

Mikkelsen, R. et al. (2004). Functional characterization of alpha-glucan,water dikinase, the starch phosphorylating enzyme. *Biochem J*, **377**, 525-532.

Minet, M. et al. (1992). Complementation of *Saccharomyces cerevisiae* auxotrophic mutants by *Arabidopsis thaliana* cDNAs. *The Plant Journal*, **2**, 417-422.

Moghadam, M. A. and Schleiff, E. (2005). Analysis of expression patterns of translocon subunits of chloroplasts and mitochondria. *Plant Science*, **168**, 1533-1539.

Nakazono, M. et al. (2003). Laser-Capture Microdissection, a tool for the global analysis of gene expression in specific Plant cell types: identification of genes expressed differentially in epidermal cells or vascular tissues of maize. *Plant Cell*, **15**, 583-596.

Nielsen, H. et al. (1997). Identification of prokaryotic and eukaryotic signal peptides and prediction of their cleavage sites. *Protein Eng.*, **10**, 1-6.

- Nielsen, T. H. et al.** (2004). Fructose-2,6-bisphosphate: a traffic signal in plant metabolism. *Trends in Plant Science*, **9**, 556-563.
- Niittyla, T. et al.** (2004). A previously unknown maltose transporter essential for starch degradation in leaves. *Science*, **303**, 87-89.
- Noubhani, A. et al.** (2009). The trehalose pathway regulates mitochondrial respiratory chain content through hexokinase 2 and cAMP in *Saccharomyces cerevisiae*. *Journal of Biological Chemistry*, **284**, 27229 -27234.
- Obel, N. et al.** (2009). Microanalysis of plant cell wall polysaccharides. *Mol Plant*, **2**, 922-932.
- Okar, D. A. and Lange, A. J.** (1999). Fructose-2,6-bisphosphate and control of carbohydrate metabolism in eukaryotes. *BioFactors*, **10**, 1-14.
- Oliver, S. N. et al.** (2008). Decreased expression of plastidial adenylate kinase in potato tubers results in an enhanced rate of respiration and a stimulation of starch synthesis that is attributable to post-translational redox-activation of ADP-glucose pyrophosphorylase. *Journal of Experimental Botany*, **59**, 315 - 325.
- Osuna, D. et al.** (2007). Temporal responses of transcripts, enzyme activities and metabolites after adding sucrose to carbon-deprived *Arabidopsis* seedlings. *The Plant Journal*, **49**, 463-491.

- Patron, N. J. and Keeling, P. J.** (2005). Common evolutionary origin of starch biosynthetic enzymes in green and red algae. *Journal of Phycology*, **41**, 1131-1141.
- Paul, M. J. et al.** (2008). Trehalose Metabolism and Signaling. *Annu. Rev. Plant Biol.*, **59**, 417-441.
- Peltier, J. et al.** (2006). The oligomeric stromal proteome of *Arabidopsis thaliana* chloroplasts. *Molecular & Cellular Proteomics*, **5**, 114-133.
- Perera, I. Y. et al.** (2001). A Role for Inositol 1,4,5-Trisphosphate in Gravitropic Signaling and the Retention of Cold-Perceived Gravitimulation of Oat Shoot Pulvini. *Plant Physiol.*, **125**, 1499-1507.
- Pérez-Castiñeira, J. R. et al.** (2002). Functional complementation of yeast cytosolic pyrophosphatase by bacterial and plant H⁺-translocating pyrophosphatases. *Proceedings of the National Academy of Sciences of the United States of America*, **99**, 15914 -15919.
- Preiss, J. et al.** (1991). Starch biosynthesis and its regulation. *Biochem. Soc. Trans*, **19**, 539-547.
- Preisser, J. and Komor, E.** (1991). Sucrose uptake into vacuoles of sugarcane suspension cells. *Planta*, **186**.

- Pyke, K.** (1997). The genetic control of plastid division in higher plants. *Am. J. Bot.*, **84**, 1017.
- Qi, X. et al.** (2007). AtCYT-INV1, a neutral invertase, is involved in osmotic stress-induced inhibition on lateral root growth in *Arabidopsis*. *Plant Mol Biol*, **64**, 575-587.
- Ratcliffe, R. and Shachar-Hill, Y.** (2006). Measuring multiple fluxes through plant metabolic networks. *The Plant Journal*, **45**, 490-511.
- Ravanel, S. et al.** (1998). The specific features of methionine biosynthesis and metabolism in plants. *Proceedings of the National Academy of Sciences of the United States of America*, **95**, 7805 -7812.
- Reinders, A. et al.** (2008). Functional analysis of LjSUT4, a vacuolar sucrose transporter from *Lotus japonicus*. *Plant Mol. Biol*, **68**, 289-299.
- Riesmeier, J. W. et al.** (1993). Antisense repression of the chloroplast triose phosphate translocator affects carbon partitioning in transgenic potato plants. *Proceedings of the National Academy of Sciences of the United States of America*, **90**, 6160 -6164.
- Riesmeier, J. W. et al.** (1992). Isolation and characterization of a sucrose carrier cDNA from spinach by functional expression in yeast. *EMBO J*, **11**, 4705-4713.

Ritte, G. et al. (2006). Phosphorylation of C6- and C3-positions of glucosyl residues in starch is catalysed by distinct dikinases. *FEBS Letters*, **580**, 4872-4876.

Ritte, G. et al. (2002). The starch-related R1 protein is an α -glucan, water dikinase. *Proceedings of the National Academy of Sciences of the United States of America*, **99**, 7166 -7171.

Roessner, U. et al. (2001a). Metabolic Profiling Allows Comprehensive Phenotyping of Genetically or Environmentally Modified Plant Systems. *Plant Cell*, **13**, 11-29.

Roessner, U. et al. (2001b). Metabolic profiling allows comprehensive phenotyping of genetically or environmentally modified plant systems. *Plant Cell*, **13**, 11-29.

Roitsch, T. et al. (1995). Induction of apoplastic invertase of *Chenopodium rubrum* by D-Glucose and a glucose analog and tissue-specific expression suggest a role in sink-source regulation. *Plant Physiology*, **108**, 285-294.

Rolland F and Sheen J (2005). Sugar sensing and signalling networks in plants.

Rolland, F. et al. (2002). Sugar sensing and signaling in plants. *Plant Cell*, **14**, S185-205.

Ruhlmann, J. M. et al. (2010). CELL wall invertase 4 is required for nectar production in *Arabidopsis*. *J. Exp. Bot.*, **61**, 395-404.

- Saeed, A. I. et al.** (2003). TM4: a free, open-source system for microarray data management and analysis. *BioTechniques*, **34**, 374-378.
- Sauer, N.** (2007). Molecular physiology of higher plant sucrose transporters. *FEBS Letters*, **581**, 2309-2317.
- Sauer, N. et al.** (2004). AtSUC8 and AtSUC9 encode functional sucrose transporters, but the closely related AtSUC6 and AtSUC7 genes encode aberrant proteins in different *Arabidopsis* ecotypes. *The Plant Journal*, **40**, 120-130.
- Scanlon, M. J. et al.** (2009). Laser microdissection-mediated isolation and in vitro transcriptional amplification of plant RNA. *Curr Protoc Mol Biol*, **Chapter 25**, Unit 25A.3.
- Schneider, A. et al.** (2002). An *Arabidopsis thaliana* knock-out mutant of the chloroplast triose phosphate/phosphate translocator is severely compromised only when starch synthesis, but not starch mobilisation is abolished. *The Plant Journal*, **32**, 685-699.
- Schulz, B. et al.** (1993). Expression of the triose phosphate translocator gene from potato is light dependent and restricted to green tissues. *Molecular and General Genetics MGG*, **238**, 357-361.
- Schulze, W. et al.** (2003). Interactions between co-expressed *Arabidopsis* sucrose transporters in the split-ubiquitin system. *BMC Biochemistry*, **4**, 3.

Schünemann, D. et al. (1996). Evidence for the expression of the triosephosphate translocator gene in green and non-green tissues of tomato and potato. *Plant Molecular Biology*, **31**, 101-111.

Scott, P. et al. (2000). Photosynthetic carbon metabolism in leaves of transgenic tobacco (*Nicotiana tabacum* L.) containing decreased amounts of fructose 2,6-bisphosphate. *Planta*, **211**, 864-873.

Sergeeva, L. I. et al. (2006). Vacuolar invertase regulates elongation of *Arabidopsis thaliana* roots as revealed by QTL and mutant analysis. *Proceedings of the National Academy of Sciences of the United States of America*, **103**, 2994 - 2999.

Shannon, J. C. et al. (1998). Brittle-1, an Adenylate Translocator, Facilitates Transfer of Extraplasmidial Synthesized ADP-Glucose into Amyloplasts of Maize Endosperms. *Plant Physiol.*, **117**, 1235-1252.

Smith, A. M. and Stitt, M. (2007). Coordination of carbon supply and plant growth. *Plant, Cell & Environment*, **30**, 1126-1149.

Sowokinos, J. R. (1981). Pyrophosphorylases in *Solanum tuberosum*: II. catalytic properties and regulation of adp-glucose and udp-glucose pyrophosphorylase activities in potatoes. *Plant Physiol.*, **68**, 924-929.

Sowokinos, J. R. and Preiss, J. (1982). Pyrophosphorylases in *Solanum*

- tuberosum*: III. purification, physical, and catalytic properties of adp glucose pyrophosphorylase in potatoes. *Plant Physiol.*, **69**, 1459-1466.
- Sparla, F. et al.** (2005). Regulation of photosynthetic GAPDH dissected by mutants. *Plant Physiol.*, **138**, 2210-2219.
- Stitt, M. et al.** (1983). A role for fructose 2,6-bisphosphate in the regulation of sucrose synthesis in spinach leaves. *Plant Physiol.*, **72**, 1139-1141.
- Stitt, M. and Heldt, H. W.** (1985). Control of Photosynthetic Sucrose Synthesis by Fructose 2,6-Bisphosphate. *Plant Physiol.*, **79**, 599-608.
- Sturm, A. and Chrispeels, M. J.** (1990). cDNA Cloning of carrot extracellular [beta]-fructosidase and its expression in response to wounding and bacterial infection. *Plant Cell*, **2**, 1107-1119.
- Sun, J. et al.** (2006). Glucose inhibits the expression of triose phosphate/phosphate translocator gene in wheat via hexokinase-dependent mechanism. *The International Journal of Biochemistry & Cell Biology*, **38**, 1102-1113.
- Synek, L. et al.** (2006). AtEXO70A1, a member of a family of putative exocyst subunits specifically expanded in land plants, is important for polar growth and plant development. *Plant J*, **48**, 54-72.
- Takaha, T. et al.** (1996). Potato D-enzyme Catalyzes the Cyclization of Amylose to Produce Cycloamylose, a Novel Cyclic Glucan. *Journal of Biological*

Chemistry, **271**, 2902-2908.

Tamoi, M. et al. (2010). Point mutation of a plastidic invertase inhibits development of the photosynthetic apparatus and enhances nitrate assimilation in sugar-treated *Arabidopsis* seedlings. *Journal of Biological Chemistry*, **285**, 15399 - 15407.

Tauberger, E. et al. (2000). Antisense inhibition of plastidial phosphoglucomutase provides compelling evidence that potato tuber amyloplasts import carbon from the cytosol in the form of glucose-6-phosphate. *The Plant Journal*, **23**, 43-53.

Taylor, N. L. et al. (2004). Lipoic Acid-Dependent Oxidative Catabolism of α -Keto Acids in Mitochondria Provides Evidence for Branched-Chain Amino Acid Catabolism in *Arabidopsis*. *Plant Physiol.*, **134**, 838-848.

TerBush, D. R. et al. (1996). The Exocyst is a multiprotein complex required for exocytosis in *Saccharomyces cerevisiae*. *EMBO J*, **15**, 6483-6494.

Tiessen, A. et al. (2003). Evidence that SNF1-related kinase and hexokinase are involved in separate sugar-signalling pathways modulating post-translational redox activation of ADP-glucose pyrophosphorylase in potato tubers. *Plant J*, **35**, 490-500.

Tohge, T. and Fernie, A. R. (2010). Combining genetic diversity, informatics and metabolomics to facilitate annotation of plant gene function. *Nat. Protocols*, **5**,

1210-1227.

Toroser, D. et al. (1998). Site-specific regulatory interaction between spinach leaf sucrose-phosphate synthase and 14-3-3 proteins. *FEBS Letters*, **435**, 110-114.

Toufighi, K. et al. (2005). The botany array resource: e-northern, expression angling, and promoter analyses. *The Plant Journal*, **43**, 153-163.

Tymowska-Lalanne, Z. and Kreis, M. (1998). Expression of the *Arabidopsis thaliana* invertase gene family. *Planta*, **207**, 259-265.

Usadel, B. et al. (2008). Global Transcript Levels Respond to Small Changes of the Carbon Status during Progressive Exhaustion of Carbohydrates in *Arabidopsis* Rosettes. *Plant Physiol.*, **146**, 1834-1861.

van Vaeck, C. et al. (2001). Analysis and modification of trehalose 6-phosphate levels in the yeast *Saccharomyces cerevisiae* with the use of *Bacillus subtilis* phosphotrehalase. *Biochem J*, **353**, 157-162.

Vandesteene, L. et al. (2010). A Single Active Trehalose-6-P Synthase (TPS) and a Family of Putative Regulatory TPS-Like Proteins in *Arabidopsis*. *Mol Plant*, ssp114.

Veyres, N. et al. (2008). The *Arabidopsis* sweetie mutant is affected in carbohydrate metabolism and defective in the control of growth, development and

senescence. *The Plant Journal*, **55**, 665-686.

Walters, R. G. et al. (2004). A mutant of *Arabidopsis* lacking the triose-phosphate/phosphate translocator reveals metabolic regulation of starch breakdown in the light. *Plant Physiol.*, **135**, 891-906.

Wang, Q. et al. (2002). Cloning and expression analysis of triose phosphate/phosphate translocator gene from wheat. *Acta Botanica Sinica*, **44**, 67-71.

Wang, Q. et al. (2002). Molecular cloning and expression analysis of the rice triose phosphate/phosphate translocator gene. *Plant Science*, **162**, 785-790.

Weise, A. et al. (2000). A new subfamily of sucrose transporters, SUT4, with low affinity/high capacity localized in enucleate sieve elements of plants. *The Plant Cell*, **12**, 1345-1355.

Weise, S. et al. (2004). Maltose is the major form of carbon exported from the chloroplast at night. *Planta*, **218**, 474-482.

Weschke, W. et al. (2000). Sucrose transport into barley seeds: molecular characterization of two transporters and implications for seed development and starch accumulation. *Plant J*, **21**, 455-467.

Weston, E. L. and Pyke, K. A. (1999). Developmental Ultrastructure of Cells and Plastids in the Petals of Wallflower (*Erysimum cheiri*). *Annals of Botany*, **84**,

763-769.

Wienkoop, S. et al. (2010). Targeted proteomics for *Chlamydomonas reinhardtii* combined with rapid subcellular protein fractionation, metabolomics and metabolic flux analyses. *Mol Biosyst*, **6**, 1018-1031.

Woll, K. et al. (2005). Isolation, characterization, and pericycle-specific transcriptome analyses of the novel maize lateral and seminal root initiation mutant rum1. *Plant Physiol.*, **139**, 1255-1267.

Wu, L. L. et al. (1993). Kinetic induction of oat shoot pulvinus invertase mRNA by gravistimulation and partial cDNA cloning by the polymerase chain reaction. *Plant Mol. Biol*, **21**, 1175-1179.

Wu, L. and Birch, R. G. (2007). Doubled sugar content in sugarcane plants modified to produce a sucrose isomer. *Plant Biotechnol. J*, **5**, 109-117.

Xiao, W. et al. (2000). The role of hexokinase in plant sugar signal transduction and growth and development. *Plant Molecular Biology*, **44**, 451-461.

Zeeman S et al. (2007). The diurnal metabolism of leaf starch.

Zhang, Y. et al. (2009). Inhibition of SNF1-Related Protein Kinase1 Activity and Regulation of Metabolic Pathways by Trehalose-6-Phosphate. *Plant Physiol.*, **149**, 1860-1871.

Zhou, D. et al. (1994). Complete Nucleotide Sequence of Potato Tuber Acid Invertase cDNA. *Plant Physiology*, **106**, 397-398.

Zrenner, R. et al. (1995). Evidence of the crucial role of sucrose synthase for sink strength using transgenic potato plants (*Solanum tuberosum* L.). *The Plant Journal*, **7**, 97-107.

Zrenner, R. et al. (1996). Soluble acid invertase determines the hexose-to-sucrose ratio in cold-stored potato tubers. *Planta*, **198**.